

Metals Emissions From the Open Detonation Treatment of Energetic Wastes

by

T. L. Boggs, T. M. AtienzaMoore, and O. E. R. Heimdahl
Research Department

M. Pepi, J. E. Hibbs, Jr., K. R. Wells, and M. Martyn
Weapons/Targets Department

D. Wooldridge
Ordnance Systems Department

R. L. Gerber
Sverdrup, Inc., Ridgecrest, California

and

L. A. Zellmer and B. M. Abernathy
Environmental Planning and Management Department
Naval Air Weapons Station, China Lake, California

OCTOBER 2004

**NAVAL AIR WARFARE CENTER WEAPONS DIVISION
CHINA LAKE, CA 93555-6100**

Approved for public release; distribution is
unlimited.

NAVAIR WEAPONS DIVISION

FOREWORD

This report supports the preparation of a science-based human Health Risk Assessment (HRA) of the treatment of energetic wastes by open detonation (OD) at China Lake's Burro Canyon Open Burn/Open Detonation (OB/OD) Facility. The HRA is a significant requirement of the Resource Conservation and Recovery Act (RCRA) Part B permit application and the Clean Air Act Title V permit for OD treatment activities at China Lake.

This report describes the use of metals in munitions and the fate of these metals in OD treatment events. Most of the metals present in munitions are part of the munition casing. The report presents data to prove that the metals from the bomb, warhead, and motor casings produce fragments, and to disprove the assumption that "all casing material vaporizes". In addition, it discusses the fate of metals used as fuels in the explosive/propellant fill and of metals in paints and coatings. This report recommends emission factors for metals from the munition casings, and platings, paints and coatings for various munition types. These emission factors are to be added to the emissions for the various families of propellants, explosives and other energetics that are treated by open detonation.

Allen Lindfors and Steve Finnegan reviewed this paper for technical accuracy.

NAVAIR, China Lake, funded this work.

Approved by
FRANK MARKARIAN, *Head*
Research Department
18 October 2004

Under authority of
W. M. SKINNER,
RDML (sel), U.S. Navy
Commander

Released for publication by
K. L. HIGGINS
Director for Research and Engineering

NAWCWD Technical Publication 8528

Published by..... Technical Information Division
Collation..... Cover, 63 leaves
First printing..... 90 copies, 15 CDs

REPORT DOCUMENTATION PAGE			Form Approved OMB No. 0704-0188	
Public reporting burden for this collection of information is estimated to average 1 hour per response, including the time for reviewing instructions, searching existing data sources, gathering and maintaining the data needed, and completing and reviewing the collection of information. Send comments regarding this burden estimate or any other aspect of this collection of information, including suggestions for reducing this burden, to Washington Headquarters Services, Directorate for Information Operations and Reports, 1215 Jefferson Davis Highway, Suite 1204, Arlington, VA 22202-4302, and to the Office of Management and Budget, Paperwork Reduction Project (0704-0188), Washington, D.C. 20503.				
1. AGENCY USE ONLY (Leave Blank)		2. REPORT DATE	3. REPORT TYPE AND DATES COVERED	
		October 2004	Environmental Status Report; 2002	
4. TITLE AND SUBTITLE			5. FUNDING NUMBERS	
Metals Emissions From the Open Detonation Treatment of Energetic Wastes (U)				
6. AUTHOR(S)				
T. L. Boggs, T. M. AtienzaMoore, O. E. R. Heimdahl, M. Pepi, J. Hibbs, K. Wells, M. Martyn, D. Wooldridge, R. L. Gerber, L. A. Zellmer, and B. M. Abernathy				
7. PERFORMING ORGANIZATION NAME(S) AND ADDRESS(ES)			8. PERFORMING ORGANIZATION REPORT NUMBER	
NAVAIR Weapons Division China Lake, CA 93555-6100			NAWCWD TP 8528	
9. SPONSORING/MONITORING AGENCY NAME(S) AND ADDRESS(ES)			10. SPONSORING/MONITORING AGENCY REPORT NUMBER	
11. SUPPLEMENTARY NOTES				
12a. DISTRIBUTION/AVAILABILITY STATEMENT			12b. DISTRIBUTION CODE	
Approved for public release; distribution is unlimited.				
13. ABSTRACT (Maximum 200 words)				
See reverse.				
14. SUBJECT TERMS			15. NUMBER OF PAGES	
air entrainment, casings, detonation, emissions, metals, munitions, wastes			124	
			16. PRICE CODE	
17. SECURITY CLASSIFICATION OF REPORT	18. SECURITY CLASSIFICATION OF ABSTRACT	19. SECURITY CLASSIFICATION OF THIS PAGE	20. LIMITATION OF ABSTRACT	
UNCLASSIFIED	UNCLASSIFIED	UNCLASSIFIED	SAR	

UNCLASSIFIED

SECURITY CLASSIFICATION OF THIS PAGE (When Data Entered)

Box 13. ABSTRACT

(U) The NAVAIR Weapons Division (NAVAIR WD), China Lake, CA, is the Navy's largest research, development, test, and evaluation (RDT&E) facility. China Lake's mission includes the design, characterization, and qualification of new weapons systems. This RDT&E mission generates sizeable quantities of widely varying energetic wastes. Due to the damaged and/or potentially unstable nature of these wastes, they cannot be transported off-Center and must be treated on-site. The preferred method of treatment is by open detonation (OD).

(U) This report describes the use of metals in munitions and the fate of these metals in OD treatment events. Most of the metals present in munitions are part of the munition casing. The report presents data to prove that the metals from the bomb, warhead, and motor casings produce fragments, and to disprove the assumption that "all casing material vaporizes". In addition, it discusses the fate of metals used as fuels in the explosive/propellant fill and of metals in platings, paints and coatings. This report recommends emission factors for metals from the munition casings, and platings, paints and coatings for various munition types. These emission factors are to be added to the emission factors for the various families of propellants, explosives and other energetics that are treated by open detonation.

CONTENTS

Acknowledgment	4
1.0 Introduction.....	5
1.1 Purpose	5
1.2 Background.....	6
1.3 What Explosive Hazardous Wastes Does China Lake Treat?.....	7
1.4 How Does China Lake Treat Explosive Hazardous Wastes by Open Detonation?	9
2.0 Open Detonation Reactions	10
2.1 Detonation	11
2.2 Afterburning	11
2.3 Air-Entrainment.....	13
2.4 Plume Formation	13
2.5 Plume Dispersion.....	15
2.6 Detonation Versus Incineration.....	15
3.0 Metals in Munitions.....	16
3.1 Ingredients in Propellants, Explosives, and Pyrotechnics	16
3.2 Metals From Munition Casings.....	17
3.3 Metals in Paints and Coatings	17
4.0 Metal Reactions	17
4.1 Metal Vaporization.....	18
4.2 Metal Combustion	22
4.3 Metal Melting.....	23
4.4 Metal Oxidation.....	23
4.5 Non-Reactive Metal.....	23
5.0 What Happens to Metals During Detonation?	23
5.1 Fragmentation of Metal Casings	23
5.2 Test Data.....	26
5.2.1 Results From Fragment Collection of Submunition Detonation	26
5.2.2 Ultra High-Speed Motion Pictures.....	27
5.2.3 Fragments Collected From Deflagration-to-Detonation Tests	28
5.2.4 Results From Shaped Charge Jet Tests.....	29
5.2.5 Results From Arena Tests.....	30
5.2.6 Fragments Recovered From the China Lake OD Treatment Site	33
5.2.7 Results From Explosive-Metal-Explosive Testing	36
5.3 Evidence for Minor Melting of Metals.....	38
5.3.1 Explosive Welding.....	38
5.3.2 Shear Zones.....	39
6.0 The Socorro Fragment	40
6.1 155mm Projectile.....	40

6.0 The Socorro Fragment (Contd.)	
6.2 The Fragment.....	41
6.3 Visual Examination	42
6.4 Samples for Further Examination.....	42
6.5 Results From Metallographic Examination.....	42
6.6 Chemical Analysis.....	43
6.7 Microhardness Testing	44
6.8 Scanning Electron Microscopy.....	44
6.9 Summary of Analyses of Socorro Fragment	47
7.0 So Why Don't Metal Casings Melt or Vaporize During Detonation?.....	47
7.1 Metal Vapor Pressure Compared to Pressures in OD Environment.....	48
7.2 Heat Transfer and Melting of Metal.....	52
7.3 Afterburning and Metal Fragments	54
7.4 Concluding Remarks for Section 7.....	54
8.0 Emission Factors.....	54
8.1 Background.....	54
8.2 How Much Metal Is in a Munition?	55
8.2.1 Metal in Munition Casings.....	55
8.2.2 Metals in Paints/Coatings/Platings on Missile Motors, Missile Warheads, and Bombs.....	56
8.2.3 Metals in Energetic Materials	57
8.3 Emissions Data, Environmental Fate Factors (EFF)	58
8.4 Metal Emission Values Recommended For Use in HRA	59
8.4.1 Approach for Determining Emission Factors	59
8.4.2 Worksheets To Determine Emission Factors.....	60
8.5 Values Recommended For Use in HRA.....	62
9.0 Summary	64
10.0 References.....	66
Appendices:	
A. Plate Testing.....	69
B. Analysis of Socorro Fragment.....	77
C. CCS Metal Emissions Report.....	95
C-1. Description of the Test Conditions and Materials Used To Derive Metal EFF Values.....	107
C-2. Procedure Used to Derive Metal EFF Values Recommended for the HRA	115
C-3. Description of Test Conditions and Materials Used To Derive the Particulate Matter Emission Factors Recommended for the HRA	119

Figures:

1.	China Lake's Land (Shown in Orange) and Airspace (Shown in Blue).....	6
2.	China Lake's Open Detonation Site Location	7
3.	Still Photo Taken From High-Speed Motion Picture of an Open Detonation Event at China Lake	11
4.	Still Photo Taken From High-Speed Motion Picture of an Open Detonation Event at China Lake	12
5.	Still Photo Taken From High-Speed Motion Picture of an Open Detonation Event at China Lake	12
6.	Still Photo Taken From High-Speed Motion Picture of an Open Detonation Event at China Lake	14
7.	Still Photo Taken From High-Speed Motion Picture of an Open Detonation Event at China Lake	14
8.	Still Photo Taken From High-Speed Motion Picture of an Open Detonation Event at China Lake	15
9.	Vapor Pressure vs. 1/Temperature for Aluminum and Aluminum Oxide	20
10.	Vapor Pressure vs. 1/Temperature for Iron	21
11.	Extrapolation of the Data in Table 3 Using the Clausius-Clapeyron Equation.....	21
12.	Still Photo Taken From High-Speed (4000 pps), High-Magnification (4x) Motion Picture of Combustion of Aluminized Propellant	22
13.	Still Photos Taken From Ultra High-Speed Motion (ca. one million pictures per second) Pictures of Detonation of a Grenade.....	24
14.	Compilation of Fragment Mass and Velocity from Many Warheads (Reference 11) .	25
15.	Submunition Fragment Characterization Test Set-Up	27
16.	Submunition Case Fragmentation	27
17.	Rod Warhead Fragmentation.....	28
18.	Deflagration-to-Detonation Transition (DDT) Test Fixture	28
19.	Fragments from DDT Test	29
20.	Shaped Charge Test.....	30
21.	Naturally Fragmenting Warhead Arena	31
22.	Steel Witness Plates from Rod Warhead Arena Test.....	32
23.	Rod Warhead Arena Test	32
24.	Fragments From the OD Treatment of Rod Warhead.....	34
25.	Burro Canyon Fragments	34
26.	Burro Canyon Fragments	35
27.	OD Simulation Test.....	36
28.	Witness Plate	37
29.	OD Simulation Test Showing Test Set-up and Witness Plate.....	37
30.	Explosive Welding	39
31.	The M107 155mm High-Explosive Projectile	41
32.	The Large Fragment Resulting From the Socorro Test.....	41
33.	View of the Bronze Smear Region Where Samples Were Taken.....	42
34.	Scanning Electron Micrograph of the Edge of the Steel Fragment.....	45
35.	Scanning Electron Micrograph at Higher Magnification That Shows the Structure of the Damaged Edge of the Fragment.....	45
36.	Scanning Electron Micrograph of Edge of a Steel Fragment.....	46

37. Scanning Electron Micrograph of Edge of a Second Steel Fragment..... 46

38. Vapor Pressures for Iron (Reference 8) Compared to Expansion Pressure and
Temperatures Beginning at 200 kbar and 5500K, and an Estimated Curve
Using the Clausius-Clapeyron equation for data point at 20 ATM (Table 3)..... 51

39. Vapor Pressures Estimated From Data at 20 ATM (Table 3) by Clausius-
Clapeyron Equation Compared to Expansion Pressure and Temperatures
Beginning at 200 kbar and 5500K..... 52

Tables:

1. Energetic Families..... 8

2. Tabulation of China Lake's Energetic Wastestreams for Tracking Years from
1998 through 2002..... 9

3. Melting and Vaporization Temperatures (°C) at Various Pressures (Reference 6) 19

4. Vapor Pressure for Iron as a Function of Temperature and 1/Temperature
(Reference 7)..... 20

5. Chemical Analysis, Weight Percent..... 44

6. Metal Properties 53

7. Typical Explosive Detonation Properties (Reference 1)..... 53

8. Calculated Metal Melt Depths for Conditions of Detonation Temperatures
and Times 54

9. Ratio of Metal to Explosive for Bomb Casings 55

10. Metals Contained in 20mm Gun Cartridge 56

11. Metals in Munition Paints and Coatings 57

12. Environmental Fate Factors for Metal Emissions 59

13a. Emission Factor Calculations for Emissions From Casings 61

13b. Emission Factor Calculations for Emissions From Platings, Paints, and Coatings62

14. Emission Factors for Metal Emissions From Open Detonation of Energetic
Material Families..... 63

ACKNOWLEDGMENT

The authors would like to acknowledge the help of Jim Hoover, Rodney Robbs, Norm Zwierzchowski, and Lt. Warren Fridley for their efforts in recovering and photographing fragments from the Burro Canyon facility; Alice Atwood and Pat Curran for providing fragmentation data from detonation experiments; and QMC Troy Williams, EOD, for helpful discussions on treatment events at Burro Canyon. Special thanks to John Pearson and Steve Finnegan for coming back from retirement to provide their expert help in understanding the behavior of metals under explosive loading.

1.0 INTRODUCTION

1.1 PURPOSE

This report was prepared in support of the Resource Conservation & Recovery Act (RCRA) Part B permit application and the Clean Air Act Title V permit for treatment of energetic wastes by open detonation (OD) at China Lake's Burro Canyon Open Burn/Open Detonation (OB/OD) Facility. A significant requirement of these two permitting efforts is the preparation of a human Health Risk Assessment (HRA). The HRA addresses health risks to people from the emissions produced by OD of energetic wastes. Preparation of the HRA began in the early 1990s with direction from the California Department of Toxic Substances Control (DTSC) and the Great Basin Unified Air Pollution Control District (GBUAPCD). To compensate for the lack of validated data and the lack of standardized guidance available in the early 1990s, conservative assumptions were used. These conservative assumptions inaccurately inflated the health risks associated with OD emissions.

Since preparation of the preliminary HRA in 1996, additional research and development has provided new data and improved methodologies for analyzing the emissions of OD. Based on these new data and findings, the HRA was reevaluated by scientists and environmental specialists at China Lake. This technical reevaluation determined: (1) The newly available data refutes many of the assumptions used in the 1996 preliminary HRA, and (2) The newly available data should be used in place of those assumptions to provide a more realistic analysis of actual health risks.

The primary concern addressed in this report is the fate of metals in munitions treated by OD. The 1996 HRA assumed that 1.1 pounds of metal casing were treated for every pound of energetic material treated, assumed compositions for these metals, and assumed that all of the metal was vaporized. When, at the request of DTSC, the 1996 HRA was run "backwards" to determine which emissions were responsible for the apparent health risks, metals were determined to be the major cause for acute and chronic non-cancer risks. This is largely because the casing metal was assumed to vaporize upon detonation and persist in the atmosphere as a vapor.

This report describes the reactions that take place in an open detonation, where metals are found in munitions, the various reactions that metals can undergo as well as the necessary conditions, and the fate of metals in the open detonation reactions. More realistic values for emissions from metals are presented.

This report is a companion to the report on emissions produced from the propellants and explosives during the open detonation. That report is in preparation.

1.2 BACKGROUND

China Lake is the Navy's largest Research, Development, Test, and Evaluation (RDT&E) facility for weapons development and testing. It consists of 1.1 million acres of land in California's remote and sparsely populated Mojave Desert (Figure 1). Much of the surrounding land is either owned or controlled by the United States government.



FIGURE 1. China Lake's Land (Shown in Orange) and Airspace (Shown in Blue).

A diverse energetic wastestream is generated from activities associated with China Lake's RDT&E mission. Department of Transportation, Department of Defense (DoD), and Navy regulations prohibit the transport of most of this RDT&E energetic wastestream on public roadways, either because the wastes are research-and-development (R&D) materials that have not been fully classified with respect to explosive safety, or because they have been altered or damaged during testing. Therefore, most of this RDT&E energetic wastestream must be treated at China Lake.

Energetic wastes generated at other facilities are not treated at China Lake. China Lake is not a designated demilitarization facility. Only wastes generated from China Lake's RDT&E mission are treated. Currently, OD is the primary method of treating these energetic wastes. Two permits are required to conduct OD treatment activities: (1) a Resource Conservation & Recovery Act Part B permit; and (2) a Clean Air Act Title V permit.

China Lake operates one site for the OD treatment events (Figure 2). It is seven miles from the nearest base boundary, which is to the east. The nearest base boundary in the dominant wind direction is 17 miles to the northeast, while the nearest town (Trona) is located 9 miles to the southeast. A monitoring well at the site indicates that groundwater (nonpotable) is more than 400 feet below the surface. The nearest surface water is on the base and is 4 miles to the west. Mountains surround the OD site, 1,400 feet higher than the site to the north and 700 feet higher

to the south, creating a natural amphitheater. The mountainous terrain mitigates the noise and blast from the OD. Additionally, the site is located in rocky terrain well outside the habitats of the desert tortoise and other sensitive species.

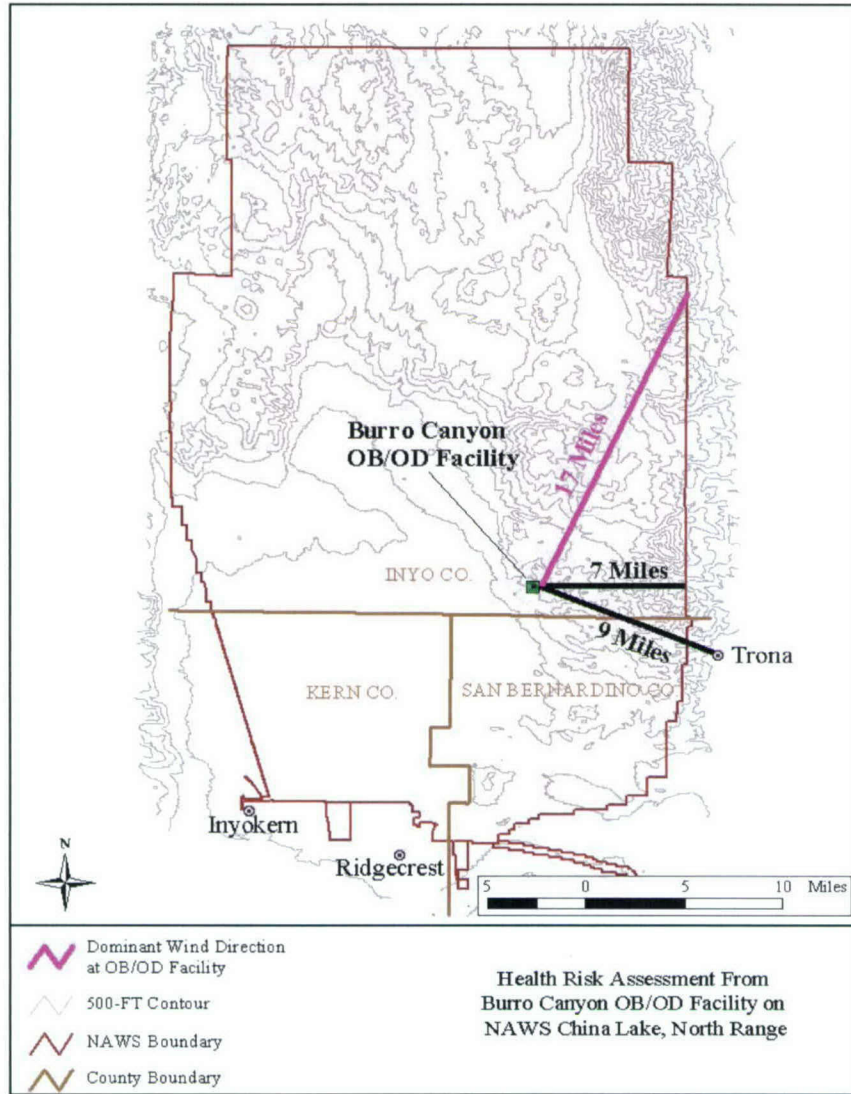


FIGURE 2. China Lake's Open Detonation Site Location.

1.3 WHAT EXPLOSIVE HAZARDOUS WASTES DOES CHINA LAKE TREAT?

Activities at China Lake generate a diverse energetic wastestream. The wastestream may be described chemically, physically, and by amount and type. First, China Lake's energetic wastestream may be described by its chemical diversity. The wastestream can be grouped into nine families of propellants, and six families of explosives. A list of these families is included as Table 1. Energetic-contaminated wastes (rags, gloves, plastic, etc.), and pyrotechnics may be considered as two additional groups.

TABLE 1. Energetic Families.

Explosives		Propellants	
<i>Melt Cast Explosives</i>		<i>Gun Propellant</i>	
A1	TNT Based (Comp-B, Cyclotol, Octol)	IA	Single Base (NC)
A2	TNT / Aluminum (H-6)	IA	Double Base (NC / NG)
<i>Plastic Bonded Explosives (PBXs)</i>		IA	Triple Base (NC / NG / NQ)
B1	Nitramine / binder	<i>Rocket/Missile Propellant</i>	
B2	Nitramine / binder / aluminum	IIA	Double base with lead
B3	Nitramine / binder / aluminum / AP	IIB	Double base without lead
<i>Other Explosives</i>		IIC	AP / binder / aluminum
C1	e.g., PbN3, ammonium picrate	IID	AP / binder / aluminum / nitramines (>50% AP)
Miscellaneous		IIE	AP / Binder Reduced Smoke
P	Pyrotechnics	IIF	Nitramine / energetic binder / Al / <20% AP
W	Energetic contaminated wastes (ECW)		

AP - ammonium perchlorate

NC - nitrocellulose

NG - nitroglycerin

NQ - nitroguanidene

TNT - trinitrotoluene

Second, the China Lake energetic wastes can be grouped into four categories based on their physical forms, even though the chemical compositions within a category vary considerably. The four energetic waste categories are described below.

Bulk energetics. This category includes "unconfined" energetic wastes, such as blocks, pellets, chunks, powders, or liquids; energetic-contaminated wastes, such as cotton rags, gloves, plastic (primarily polyethylene); and energetic-contaminated containers, such as wood crates, cardboard boxes, velostat bags, and cellulose drums.

Small cased munitions. These items have confined energetics and contain less than 0.5 lb. of energetic material in each item. This category includes cartridge-actuated devices (CADs), propellant-actuated devices (PADs), exploding bolts, fuzes, small projectiles, ammunition, and numerous other small items. The casings for the items in this category are typically thin metal casings, such as in a ammunition cartridge. In addition to the hazards of and the potential damage from the confined energetic materials, the metal casing fragments may create some additional hazards and damage.

Medium cased munitions. These items have confined energetics and contain between 0.5 lb. to 100 lb. of energetic materials in each item. This category includes bomblets, warheads, rocket motors, projectiles, sectioned munitions, all-up missiles, and numerous other types of items. The casings for the items in this category are usually thick. In addition to the hazards of and the potential damage from the confined energetic materials, the metal casing fragments may create significant additional hazards and damage.

Large cased munitions. These items have confined energetics and contain more than 100 lb. of energetic materials in each item. This category includes bombs, rocket motors, warheads, sectioned munitions, and all-up missiles. The casings for the items in this category are usually

thick. In addition to the hazards of and the potential damage from the confined energetic materials, the metal casings will create significant additional hazards and damage during a detonation. Thick metal casings are typical in warheads and bombs and if the energetic material is detonated, a significant quantity of both large and small fragments are created.

Using categories previously described, China Lake's energetic wastestream may be described by its amount. A tabulation of the China Lake energetic wastes, grouped into categories based on physical form previously described, for tracking years 1998 through 2002 is summarized in Table 2. The amount and type of energetic hazardous wastes treated in any given year varies considerably. Therefore, no conclusions should be made in a trend toward reduction in wastes.

TABLE 2. Tabulation of China Lake's Energetic Wastestreams for Tracking Years from 1998 through 2002.

Wastestream category	Tracking year (July to July)				Average lb. ^a (% waste)
	1998/1999 lb. ^a	1999/2000 lb. ^a	2000/2001 lb. ^a	2001/2002 lb. ^a	
Bulk Energetics ^b (% of waste)	12,000 (22%)	8,000 (22%)	12,000 (47%)	27,000 (64%)	15,000 (37%)
Small Cased Munitions ^c (% of waste)	2,000 (4%)	2,000 (5%)	1,000 (4%)	1,000 (2%)	2,000 (5%)
Medium Cased Munitions ^c (% of waste)	7,000 (13%)	3,000 (8%)	5,000 (18%)	3,000 (7%)	5,000 (12%)
Large Cased Munitions ^c (% of waste)	33,000 (61%)	23,000 (65%)	8,000 (31%)	11,000 (26%)	19,000 (46%)
Subtotal of Waste Only	54,000	36,000	26,000	42,000	41,000
Donor (% of total treated)	84,000 (61%)	39,000 (52%)	10,000 (28%)	12,000 (22%)	36,000 (47%)
TOTAL treated by OD at China Lake	138,000	75,000	36,000	54,000	77,000

^aRounded to the nearest 1000 lb.

^bIncludes bulk energetic and waste contaminated with energetics.

^cIncludes the explosive weight of the items.

1.4 HOW DOES CHINA LAKE TREAT EXPLOSIVE HAZARDOUS WASTES BY OPEN DETONATION?

A treatment event can treat up to 15,000 pounds of explosive material. As mentioned above, the wastes are widely varied. There is no typical treatment event. Each one is different, and the waste items for a treatment event are tailored to maximize the efficiency of treatment. Some items are very easy to initiate, and quickly and thoroughly react, while some items are harder to initiate.

Treatment of warheads, bombs and hazard class 1.1 motors (i.e., those with detonable propellants) is very easy. A very small amount of donor explosive (e.g., less than one pound of

C-4 explosive) packed in fuze wells and nozzles, and a small-scale initiator on a few rounds is all that is required for complete reaction. The detonation of one round will set off the adjacent rounds (often called sympathetic detonation). Examples of easily initiated munitions that were treated at Burro Canyon include: (1) pallets of four Mk 84 (2000-lb.) bombs, and (2) 200 rounds of 81 mm mortar rounds stacked with every tenth or twelfth round having a small amount of C-4 and a blasting cap. The adjacent rounds were quickly consumed by sympathetic detonation.

Some items are more difficult to treat, such as explosively contaminated wastes, and hazard class 1.3 and 1.4 motors.

Within the 15,000-pound limit for an individual treatment, the operators try to mix and match the items with easily initiated materials together with harder to initiate materials. At times the easily initiated waste items that are designated for treatment, such as warheads, bombs, hazard class 1.1 motors, rolls of DETAsheet, and explosive cast into ice cream cartons (1 and 5 gallons), serve as the donor explosives for the harder to initiate materials. In other events re-claimed explosives are used as the donor, such as multiple steel ammo boxes containing 65 lbs. of re-claimed A-3 flake explosive in each box.

Arrangement of waste items is equally important as choosing the mix-match of items to be treated. Bombs are placed so that the fragments from the base plates, lugs and strongbacks will go in a desired direction. The initiation of the pile is usually from the ends and top to minimize the "kick out" of munitions from the pile before they have time to initiate. This arrangement is especially important when treating submunition weapons. Once a weapon is detonated the metal fragments that are produced will travel a great distance from the detonation site, in some instances over a mile. Care is also taken with hazard class 1.3 and 1.4 motors. If not treated properly, these motors can ignite, go propulsive, and leave the treatment site. Obviously this presents a safety concern, because some missiles have a long flight range. This potential problem is solved by placing the motors at the bottom of the pile and using lots of donor explosives.

2.0 OPEN DETONATION REACTIONS

The open detonation of propellants, explosives, and munitions involves several reactions and processes including detonation, afterburning, air-entrainment, plume formation, and plume dispersion. Each of these reactions is described below in terms of temperature, reaction speeds, typical reaction products, and other products (such as dirt).

2.1 DETONATION

Detonation is a chemical reaction(s) propagating into the unreacted material at supersonic speeds. The detonation of explosives and propellants does not require air; it can occur in a vacuum, in an inert atmosphere, or under water. The temperatures associated with detonations range from about 2500°C to 5600°C (Reference 1). The pressures associated with detonations are in hundreds of kilobars (hundreds of thousands of atmospheres). The reactions are very rapid, progressing at rates on the order of 5 to 9 mm/microsecond (approximately 25,000 feet/second). The reactions are over in microseconds (1 microsecond = one millionth of a second). Figure 3 is a still photo from high-speed motion pictures taken of an open detonation treatment event. It shows the initiation at the ends of the pile being treated. The next frame on the film (not shown here) showed the “white-out” of the detonation. Typical gaseous reaction products include carbon monoxide, hydrogen, methane, ethane, formaldehyde, nitrogen, carbon dioxide, and water vapor. If the explosive or propellant contains aluminum fuel, then aluminum oxide may be a product, although much of the aluminum does not react in the detonation. If the explosive or propellant contains ammonium perchlorate (a common oxidizer), then hydrogen chloride (HCl) will be produced. If the explosive or propellant is contained in a metal case, then fragments of the metal case are formed when the energetic material detonates. (This process will be discussed in more detail in later sections.) If the explosive is sitting on dirt, the detonation forms a crater and dirt will be blown into the air. If the explosive is sitting on a metal plate, then the metal plate will be fractured and form fragments.



FIGURE 3. Still Photo Taken From High-Speed Motion Picture of an Open Detonation Event at China Lake. The flash at either end of the detonation pile is the initial initiation.

2.2 AFTERBURNING

Afterburning immediately follows detonation and is seen as the fireball. Figures 4 and 5 are still photos from high-speed motion pictures of the same OD treatment event at China Lake as shown in Figure 3. They show the afterburning reactions. Afterburning requires an air atmosphere (see also air-entrainment). During afterburning the incomplete reaction products produced in the detonation reaction (e.g., carbon monoxide, methane, ethane, formaldehyde, and

hydrogen) react to final reaction products at subsonic rates. The afterburning reactions take several seconds to complete. The temperatures are on the order of 700°C to 1700°C. Obviously, the stable reaction products already produced in the detonation reaction will be present in the afterburning reaction volume, but the afterburning will produce additional carbon dioxide from the reaction of carbon monoxide and air, and additional water vapor will be produced from oxidation of the hydrogen gas. The intermediate hydrocarbon products will also be oxidized primarily to water and carbon dioxide.



FIGURE 4. Still Photo Taken From High-Speed Motion Picture of an Open Detonation Event at China Lake. The fireball is the afterburning reaction of the intermediate products from the detonation reaction reacting with air.



FIGURE 5. Still Photo Taken From High-Speed Motion Picture of an Open Detonation Event at China Lake. The fireball is the afterburning reaction of the intermediate products from the detonation reaction reacting with air.

As will be discussed later, by this time most of the metal fragments from the metal cases will have been accelerated to high velocities and will be far outside the fireball.

Suppression of afterburning, sometimes done at other facilities to reduce blast and noise, reduces the amount of intermediate reaction products converted to final, stable reaction products and increases the health risk. One of the advantages of OD is that the afterburning converts the intermediate reaction products such as carbon monoxide, hydrogen, and hydrocarbons, forming stable reaction products such as carbon dioxide and water. Stable reaction products are less of a health risk than intermediate products.

2.3 AIR-ENTRAINMENT

Detonation is extremely violent. The solid explosive or propellant reacts to gases in microseconds. These gases rapidly expand and mix with the surrounding air. As the incomplete gaseous products from the detonation react with the air in the afterburning, the reaction volume continues to expand and rise. As the hot gases rise, they entrain additional air, and this entrained air allows further combustion reactions to take place. The air-entrainment and afterburning occur almost simultaneously and are highly coupled.

2.4 PLUME FORMATION

As the gases rise and air is entrained, it also entrains surrounding dirt from the surface as well. Figure 6 shows the entrained dirt. This entrained dirt, along with the dirt produced from the crater, forms a highly visible plume (Figure 7). In fact, what you see as a plume is primarily dirt. The gaseous products produced by the detonation and the afterburning (e.g., carbon dioxide, water vapor, nitrogen) are not visible to the eye. Some researchers (Reference 2) believe that some of the species (e.g., HCl) nucleate on the dirt particles, become adsorbed, and "rain out" of the plume, hence explaining lack of HCl found in the plume in some large-scale tests. Plume formation takes seconds to hundreds of seconds.



FIGURE 6. Still Photo Taken From High-Speed Motion Picture of an Open Detonation Event at China Lake. As the plume rises, it entrains dirt from the desert floor.



FIGURE 7. Still Photo Taken From High-Speed Motion Picture of an Open Detonation Event at China Lake. The highly visible plume is dirt from the initial crater and entrained dirt.

2.5 PLUME DISPERSION

The visible plume, Figure 8, is clearly seen for many minutes after the reactions have occurred. If there is any wind, the plume will move in the direction of the wind. Terrain also plays a role. Obviously the heavier particles in the plume may settle out. The plume as it moves also continues to expand, further diluting the concentration of emissions within the plume.



FIGURE 8. Still Photo Taken From High-Speed Motion Picture of an Open Detonation Event at China Lake. The highly visible dirt plume exists for minutes over the treatment site.

These reactions are clearly shown in an edited video produced at NAVAIR China Lake. The video contains real-time, slow motion, and stop-action framing taken from high-speed motion pictures of an open detonation treatment event. The still photos presented above were taken from the video. This video is available on loan.

2.6 DETONATION VERSUS INCINERATION

Because OD and incinerators both involve combustion processes, one might assume that studies performed on incinerators may be applicable to open detonation. This is not the case. There are fundamental differences between open detonation and incineration. As discussed above the open detonation process does involve combustion in the afterburning reactions, but these reactions occur after the initial detonation. Obviously, detonations don't routinely occur in incinerators. There are other significant differences in operation, temperatures, pressures, reaction rates, and residence times. Among the differences are:

- Solid hazardous waste incinerators are used to burn fuel-rich materials with air passed over the combusting materials to enhance oxidation. OD treats propellants and explosives that are intimate mixtures (at the micron to hundred of microns scale - a human hair is approximately 75 microns in diameter) of fuel and oxidizers in stoichiometric proportions - external sources of oxygen are not needed to support reaction.

- The temperatures of detonation (2500°C to 5600°C) and its afterburning (700°C to 1700°C) are significantly higher than the temperatures associated with hazardous waste incinerators (500°C to 1200°C) (References 3 through 5).
- The pressures involved in the detonation reactions are in the hundreds of kilobars. Incinerators essentially run at one atmosphere. This is an especially critical difference when the vapor pressure-temperatures of metals are concerned. (See discussion in Section 4.1.)
- Incinerators tend to confine the reactions and have long residence times, when compared to the rapid, unrestrained expansion of gases present in OD.

Special incinerators (e.g., the APE 1236 incinerator at Tooele, Utah) are used to demilitarize some military munitions; primarily small caliber ammunition, cartridges, and disassembled fuzes. These incinerators cannot treat items that contain significant amounts of propellants and explosives. For example, some incinerators can handle approximately one pound per flight (a flight is the spacing between turns on the feed auger that feeds the furnace). Typically the incinerators treat materials that contain about 30 grams of energetic material per item. As discussed later, a 20 mm cartridge has 38 grams of gun propellant. The temperatures of the incinerator range from 350°F to 1200°F (177°C to 649°C) at the entry to the furnace to 1200°F (649°C). These temperatures are much lower than the temperatures found in the detonation and afterburning reactions of open detonation. The metals from the casings are recovered after the energetic material cooks off in the incinerator, and is sold for scrap.

One of the concerns with incinerators is the production of dioxins and furans. This subject is addressed in the companion paper on treatment of propellants and explosives.

3.0 METALS IN MUNITIONS

Munitions include ammunition, projectiles, bombs, warheads, submunitions (small warheads), rocket motors, and their components. Metals may be present in munitions as:

- Ingredients in explosives, propellants, and pyrotechnics
- Metal casings
- Platings, paints and coatings

The following sections briefly describe these three topics. Chapter 8 presents a much more detailed description.

3.1 INGREDIENTS IN PROPELLANTS, EXPLOSIVES, AND PYROTECHNICS

Examples include:

- Aluminum (or other metal) powder (approximately 1 to 100 microns in diameter) in propellants or explosives to increase performance
- Burn rate modifiers in propellants, i.e., iron oxide
- Primary explosives, i.e., lead azide

Metal powders are typically incorporated in propellants and explosives to enhance performance or to increase burn rates. These metals may be present in milligram quantities (e.g., lead azide) in primary explosives to several thousand pounds (e.g., aluminum) in propellants of large rocket motors. These metal additives are mainly oxidized in combustion and detonation reactions.

3.2 METALS FROM MUNITION CASINGS

Casings are usually one of three types:

- Very thin cartridge cases for ammunition- and cartridge-actuated devices
- Rocket motor cases
- Thicker projectiles, warhead and bomb cases

Rocket motor and warhead cases are typically steel. Aluminum is sometimes used for rocket motor cases. Casings range in weight from ounces to hundreds of pounds. In addition, the cases of special design warheads may include titanium, tungsten, zirconium, or copper. The casing metal of a rocket motor or warhead does not participate in the detonation reaction, rather it fractures and forms fragments. Warheads and bombs are designed to produce fragments as discussed later.

3.3 METALS IN PAINTS AND COATINGS

Examples include:

- Protective paints and paints to designate ordnance type and explosive fill
- Anodization
- Zinc plating

Paints and coatings are very thin and in very small quantities.

4.0 METAL REACTIONS

Metals, in general, can react in several ways. In most instances metals are inert, but in certain circumstances they can melt, vaporize or burn. The reactions that occur depend on the metal properties (melting and vaporization parameters), the temperature, the thickness of the

sample, the pressure, and the environment (e.g., whether oxidizing species are present or not). The reactions will be discussed from the most complex to the simplest, i.e., from vaporization to non-reactive fragmentation.

4.1 METAL VAPORIZATION

Metals can vaporize under the right conditions. Vaporization of a metal is dependent on both temperature and pressure and the sample configuration. While metals can go directly from solid to vapor (sublime), very special conditions are required. Sublimation requires conditions below the triple point of pressure and temperature (Reference 6) (the triple point is the point where gas, liquid, and solid phases of the metal can occur). This requires extremely low pressures; pressures much lower than atmospheric. Most metal vaporization occurs at conditions above the triple point requiring that the solid metal liquefy (melt) before evaporating. If melting is not evident, then vaporization is extremely unlikely.

If vaporization is to occur, the vapor pressure of the metal must be higher than the surrounding pressure. From a practical standpoint, this often means that a vacuum is required. Coating samples with gold for scanning electron microscopy provides an excellent example. First, fine gold wires are placed on high resistance electric filaments. The sample to be coated and the wire/filament apparatus are placed in a bell jar that is then evacuated. Passing current through the filaments heats the thin gold wires above the vaporization temperature and the gold vaporizes. When the gold vapor touches the cooler sample, the vapor condenses and a gold coating results on the sample.

Examples of the temperature and pressure parameters required for melting and vaporization of a variety of metals are given in Table 3. As indicated, metals have a high boiling point, even at very low pressures. As pressure increases, so does the temperature required for the metal to vaporize. The table lists the melting points for various metals and the vaporization temperature, °C, at the specified pressure. Unfortunately the data are only for modest pressures, up to 20 atmospheres. These pressures are much, much lower than the pressures associated with detonations (hundreds of thousands atmospheres).

In later discussion we will present what happens when metals are subject to the conditions of detonation and afterburning. This table will be used in those discussions.

The data in Table 3 can be extrapolated to higher pressures and temperatures using the Clausius-Clapeyron equation.

$$\ln p = -\frac{\Delta H_{\text{vap}}}{RT} + C \quad (1)$$

where

p = vapor pressure
 ΔH_{vap} = enthalpy of vaporization
 R = gas constant

T = temperature
C = integration constant

TABLE 3. Melting and Vaporization Temperatures ($^{\circ}\text{C}$) at Various Pressures (Reference 6).

Material	Melting point	Vaporization temperature at pressure				
		1mm Hg	100mm Hg	1 ATM ^a	10 ATM	20 ATM
Aluminum	660	1540	2080	2467	3050	3270
Chromium	1890	1610	2140	2480	3010	3180
Copper	1083		2190	2600	3500	3460
Gold	1064	1880	2520	2940	3630	3890
Iron	1535	1780	2370	2750	3360	3570
Lead	327	970	1420	1740	2320	2620
Manganese	1244		1810	2100	2850	
Mercury	-39		260	357	517	581
Nickel	1455	1800	2370	2730	3300	3310
Zinc	420		730	907	1180	1290

^a760mm Hg = 1 ATM, which is the nominal barometric pressure at sea level.

Often the data are plotted as p vs $1/T$ in semi-logarithmic coordinates as shown in Figure 9, for aluminum and aluminum oxide.

Data for iron (Reference 7) are presented in Table 4 and Figure 10 over the range of temperatures 1800 K to 9000 K (Temperature $^{\circ}\text{C} + 273 =$ Temperature, K).

Figure 10 also presents the data points for iron from Table 3 and the extrapolation of these data using the Clausius-Clapeyron equation, equation (1). The agreement between the data from Reference 7 and the extrapolation of the data from Table 3 is quite good. Figure 11 presents similar extrapolations of the data in Table 3 for the other metals, again using the Clausius-Clapeyron equation. These data will be used in Section 7.1.

Configuration is also an important consideration. For example the thickness of the sample is extremely important as will be discussed later in transient heat conduction calculations. Because it takes time for heat to "soak" into a sample, the response of a very thin foil will be dramatically different than for a thick warhead casing.

In the gold coating example previously presented, the atmosphere was inert and evacuated. If metal vapors, such as aluminum, are exposed to oxidizing species, they are converted almost immediately to metal oxides such as aluminum oxide. This is what happens during combustion of metal powders found in propellants and explosives (see Section 4.2).

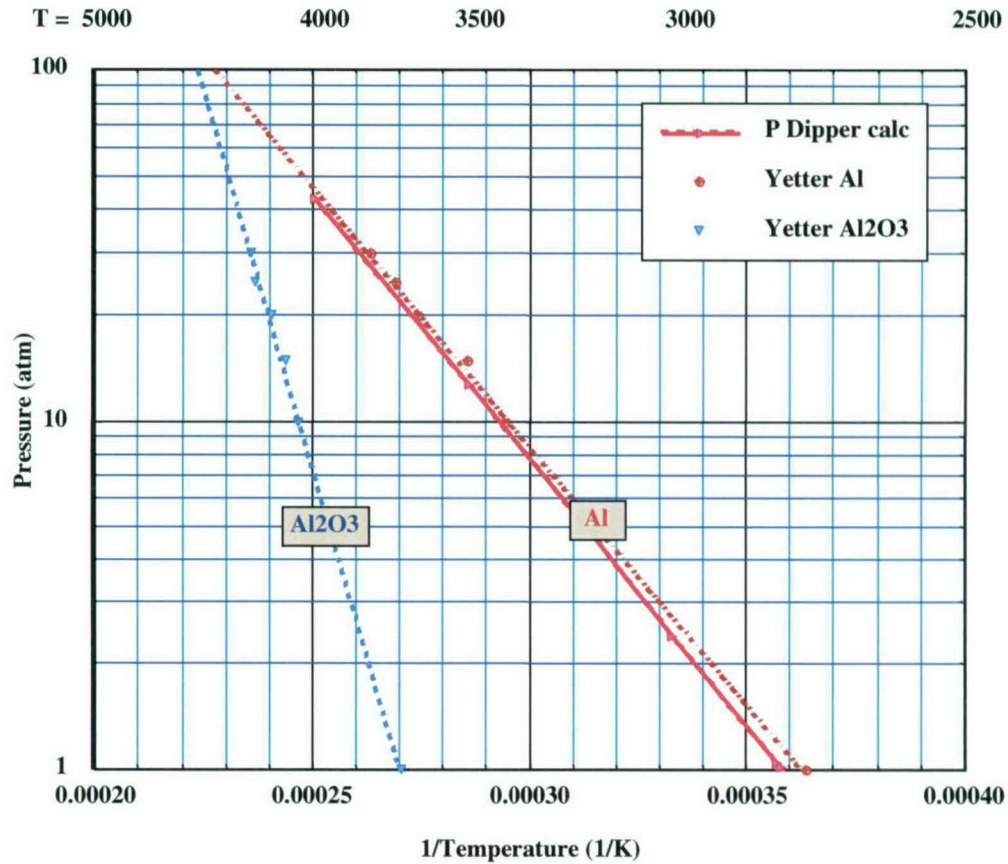


FIGURE 9. Vapor Pressure vs. 1/Temperature for Aluminum and Aluminum Oxide (courtesy of Professor M. W. Beckstead, Brigham Young University, Provo, Utah).

TABLE 4. Vapor Pressure for Iron as a Function of Temperature and 1/Temperature (Reference 7).

T (K)	P Pascals	P atm	1/T
1800	3.11E+00	3.07E-05	0.000556
2000	3.85E+01	3.80E-04	0.000500
2500	3.21E+03	3.17E-02	0.000400
3000	5.61E+04	5.54E-01	0.000333
3500	4.14E+05	4.08E+00	0.000286
4000	1.81E+06	1.79E+01	0.000250
4500	5.67E+06	5.60E+01	0.000222
5000	1.42E+07	1.40E+02	0.000200
5500	3.02E+07	2.98E+02	0.000182
6000	5.74E+07	5.66E+02	0.000167
6500	1.00E+08	9.90E+02	0.000154
7000	1.65E+08	1.62E+03	0.000143
7500	2.57E+08	2.54E+03	0.000133
8000	3.87E+08	3.82E+03	0.000125
8500	5.66E+08	5.59E+03	0.000118
9000	8.08E+08	7.98E+03	0.000111

Vapor Pressure of Iron

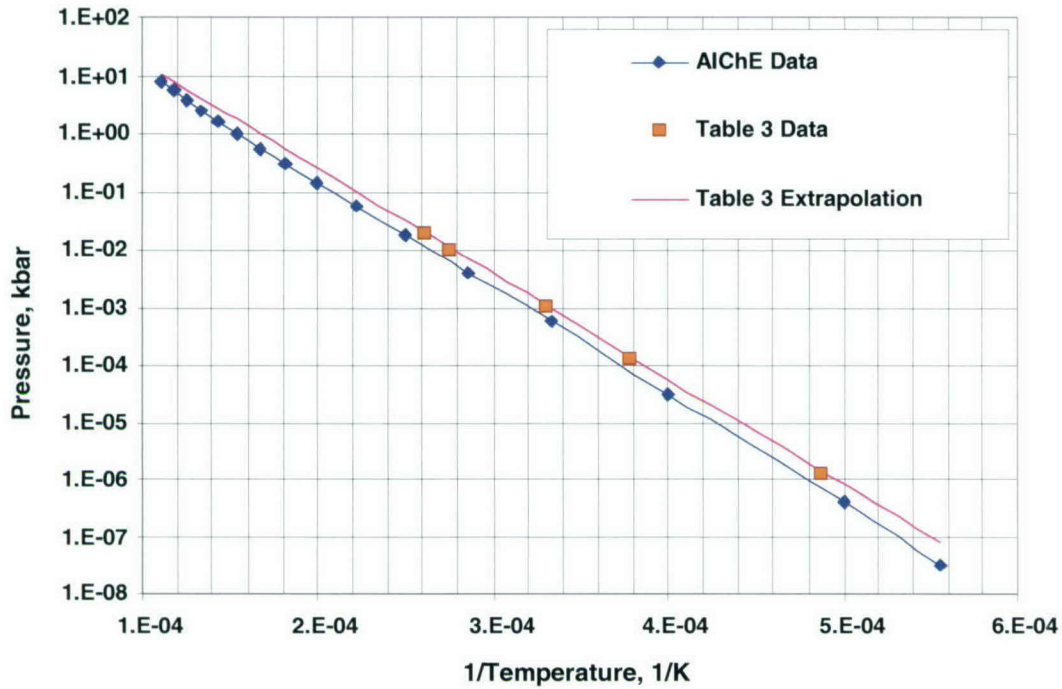


FIGURE 10. Vapor Pressure vs. 1/Temperature for Iron. AIChE data from Reference 7, data from Table 3, and extrapolation of Table 3 data using Clausius-Clapeyron Equation.

Extrapolated Vapor Pressures

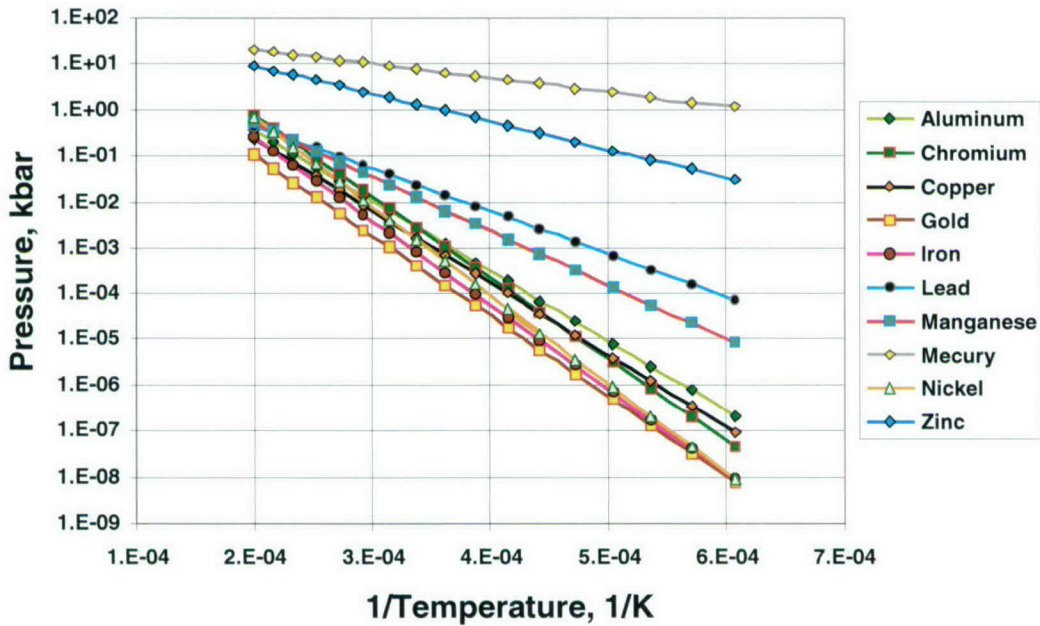


FIGURE 11. Extrapolation of the Data in Table 3 Using the Clausius-Clapeyron Equation.

4.2 METAL COMBUSTION

During metal combustion, metal evaporates from the molten metal and is oxidized by the oxidizing species. Combustion of metals contained in propellants and explosives provides a good example of this reaction. The metal, usually finely divided aluminum powder (approximately 10s of microns in diameter), and its associated protective oxide coating, are intimately mixed with the other ingredients to form the propellant. The amount of aluminum in propellants is usually 20% by weight (20 weight percent) or less. When the propellant burns, the oxide-encased metal comes to the propellant surface as the propellant recedes. The metals accumulate on the surface soaking up heat. As the temperature increases, the aluminum melts, but does not react because it is still encased in the protective aluminum oxide skin. When the temperature finally reaches the melting temperature of the aluminum oxide ($T = 2050^{\circ}\text{C}$), the oxide melts and retracts to form a liquid oxide cap on the molten aluminum particle. The now-exposed molten aluminum evaporates. This metal vapor then reacts with oxidizing species from the ammonium perchlorate to form micron-sized aluminum oxide smoke, liberating energy to sustain the burning of the propellant. These can be seen in Figure 12, a still picture taken from high-speed, high-magnification motion pictures of the combustion of an aluminized propellant. The particles in the photo clearly show the molten aluminum (the shiny metallic looking sphere), the residual aluminum oxide (the orange cap), and the aluminum oxide smoke produced by the oxidation of the aluminum vapor (the white "tail"). The residual oxide from the molten cap is often greater than 15 microns in diameter. The particle size distribution of aluminum oxide ranges from about 40 weight percent diameters less than 2 microns, about 50% between 2 microns and 37 microns, and about 10% greater than 37 microns, to instances where about 80% of the oxide is fine smoke particles less than 2 microns. For a more complete description of metal combustion, please refer to Reference 8.



FIGURE 12. Still Photo Taken From High-Speed (4000 pps), High-Magnification (4x) Motion Picture of Combustion of Aluminized Propellant.

Emission factors for aluminum in propellants and explosives are contained in a validated database (Reference 9), and will be discussed in the companion report.

4.3 METAL MELTING

Metals can melt without vaporizing, if the temperatures are above the melt temperature but below the evaporation conditions. We are all aware of examples in industry (steel manufacture), the arts (metal casting), and nature.

4.4 METAL OXIDATION

Metals can also oxidize without melting or vaporizing. For example, iron forms iron oxide (rust) and aluminum dulls by the formation of aluminum oxide (tarnish).

4.5 NON-REACTIVE METAL

Lastly, metal can remain inert. In these instances, the temperatures of the metal are below the melting temperature, and/or the temperature and pressure conditions for evaporation are not met.

5.0 WHAT HAPPENS TO METALS DURING DETONATION?

The metal powders in the propellant and explosives react to metal oxide particles as discussed above. Some of the metal present in paints and coatings can vaporize and react. The metals in the motor, warhead, and bomb casings fracture and produce high-velocity fragments. These fragments can travel considerable distances.

5.1 FRAGMENTATION OF METAL CASINGS

When the explosive or propellant in a munition is detonated, the solid is converted to high-pressure (hundreds of kilobars, hundreds of thousands of atmospheres), high-temperature gases. The pressures inside the casing exceed the yield strength of the metal casing by more than an order of magnitude, so the case yields and expands. The case fractures or ruptures producing discrete fragments. As the case ruptures, the gaseous detonation products flow through the cracks and around the fragments. The fragments are accelerated to considerable velocity (thousands of feet per second). The rapid expansion of the gaseous detonation products compresses the surrounding air. The pressures and velocities produced in the compressed air are high enough to produce a blast wave. The blast wave pressures are on the order of 100 atmospheres at a distance of about 4 to 5 charge diameters from the detonated charge. As the blast wave expands it decreases in maximum pressure (down to 25 atmospheres at approximately 10 charge diameters

and 4.5 atmospheres at approximately 25 charge diameters), and decreases in speed. The gaseous detonation products continue to expand and slow until about 16 charge diameters from detonated charge, at which point they cease to expand. While the blast wave continues traveling outward, at a point behind the blast wave the pressure decreases until it reaches one atmosphere: after which there is a slight negative (about 0.7 atmospheres) phase with a reversed blast wind.

As the gaseous reaction products and blast wave expand, they slow due to the attenuating effect of expansion. The fragments also slow due to drag forces, but the deceleration of drag is much less than the attenuating effects of expansion. As a result the fragments very quickly overtake and then lead the blast wave and the detonation reaction product gases. A more thorough description of the fragmentation processes can be found in Reference 10. Because the reaction products from the detonation are usually fuel rich, they react with the air in the after-burning reactions, but by the time these reactions occur the fragments are well outside this after-burning reaction zone. These effects can clearly be illustrated in arena tests discussed later.

Figure 13, ultra high-speed motion pictures taken of an exploding hand grenade, clearly shows the early steps: cracking of the case and fragment formation, and gaseous products escaping through the cracks. While this series does not show the acceleration or trajectory of the fragments, grenades produce lethal fragments over a significant distance.



FIGURE 13. Still Photos Taken From Ultra High-Speed Motion (ca. one million pictures per second) Pictures of Detonation of a Grenade.

The number of fragments and their sizes, velocities, and trajectories are functions of many variables including the explosive or propellant type, the weight of the explosive or propellant, the metal casing material, the mass of the metal case, and the shape of the case. In some instances the case is scored or notched to produce fragments of a desired size.

The number, size, and velocities of fragments produced by a munition are sensitive information because such data are used to determine the lethality of a given weapon. As will be discussed below, fragment recovery tests have been performed to determine the number and size/weight of fragments as part of determining a weapon's lethality. To avoid compromising security, we present fragment mass and velocity data for a range of weapons in the composite plot of Figure 14. The axes give the individual fragment masses and velocities. As can be seen, the data range from very small to very large fragments (a 1/2-inch steel cube weighs about 250 grains, 1 pound = 7000 grains) with a wide range of velocities. The star on the figure gives the mass and velocity of the standard fragment used in testing to determine Insensitive Munition status. If the munition detonates or violently explodes when hit with this standard fragment, then it fails the Insensitive Munitions fragment impact test.

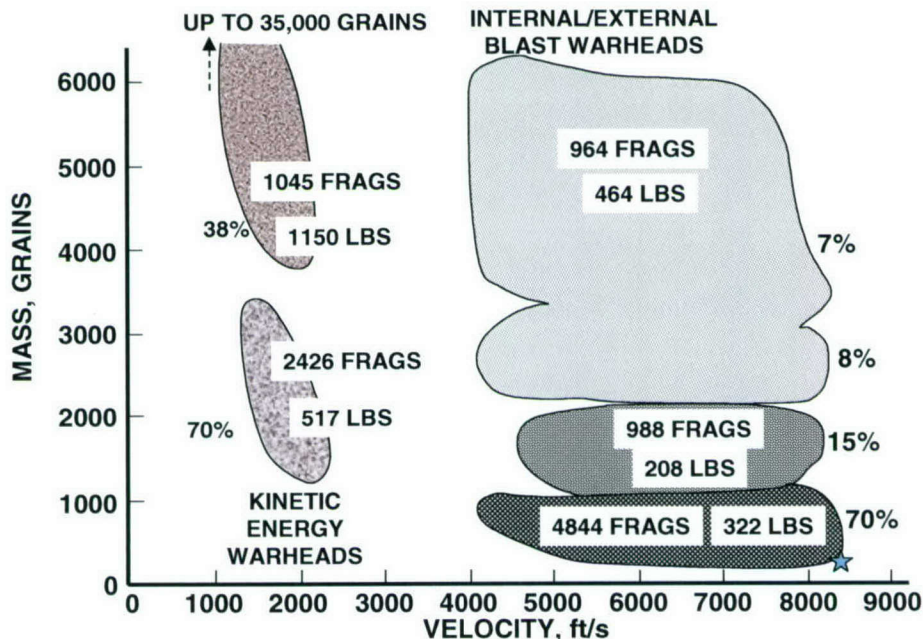


FIGURE 14. Compilation of Fragment Mass and Velocity from Many Warheads (Reference 11). [Note: The percentages indicated on the plot are by number, not by weight, for the two types of warheads: blast warheads and kinetic energy warheads. There is an error in the percentages listed on the figure, though: the larger fragments for the kinetic energy warheads should be 30%, not 38% as indicated on the plot]]

The velocities shown in Figure 14 were measured close to the warhead initiation. The velocities decrease with distance due to drag. Obviously at some point the velocities decay to zero and the fragment hits the ground (or hits something in its path). The distance traveled can be significant (several hundred feet). Because the fragments travel in many directions, the fragments may be spread over acres. (For example a 700-foot radius is slightly more than 35 acres.) Trying

to recover all or even a majority of fragments over such a wide area is prohibitively expensive. At China Lake's OD treatment site we only remove the fragments when the amount of metal makes collection of residue economically feasible in terms of manpower (often quarterly or yearly) and/or when the fragments pose a safety and/or handling problem (e.g., sharp fragments on the ground that can puncture tires). The fragment collection is limited to picking up the large (several inches or greater) fragments.

5.2 TEST DATA

Much testing involving detonation of munitions and explosives and propellants has been performed at China Lake. Usually this testing is performed to understand how munitions perform so that improvements can be made in their design. The following sections are examples of results from this testing. The results presented include:

- (1) fragment collection from detonating submunitions;
- (2) ultra high-speed motion pictures taken of detonating submunitions and rod warheads;
- (3) fragment collection from deflagration-to-detonation tests;
- (4) steel plates showing the penetration of a copper jet from a shaped-charge jet munition;
- (5) arena tests;
- (6) actual fragments from the China Lake OD treatment facility; and
- (7) results from explosive-metal-explosive OD simulation tests.

The literature also indicates that minor melting of metals may be associated with explosive welding and high shear due to high rate failure of metals. In Section 5.3 we will explain these two processes and their relative applicability to OD.

5.2.1 Results From Fragment Collection of Submunition Detonation

These tests were designed to recover fragments so that their sizes and masses could be determined for use in lethality studies (Reference 12). As depicted in Figure 15, the submunition is placed inside an air-filled balloon, which is then lowered into a 12 foot by 12 foot water tank, with a 5 foot conical section on the bottom. The balloon ensures the submunition casing can expand in air as designed. The water is used to stop the fragments without causing damage to the tank or to the fragments. The water volume was 1545 cubic feet or 11,563 gallons.

The submunition was placed inside of an air-filled balloon and then placed underwater in a 12 ft. by 12 ft. tank with a 5 ft. conical section on the bottom.

The tank used in these fragment characterization tests is approximately 60 times larger in volume than the munitions being tested, limiting this technique to relatively small munitions. In the test, the submunition is initiated and the fragments are collected by draining the tank. In 12 fragment recovery tests, 94.47 to 99.03% of the original metal mass was recovered as fragments. Very small fragment sizes (less than 0.32 gram or about 1/8 cubic inch) are very difficult to recover, do not influence lethality so they are of little concern, and thus contribute to less than complete recovery rates.

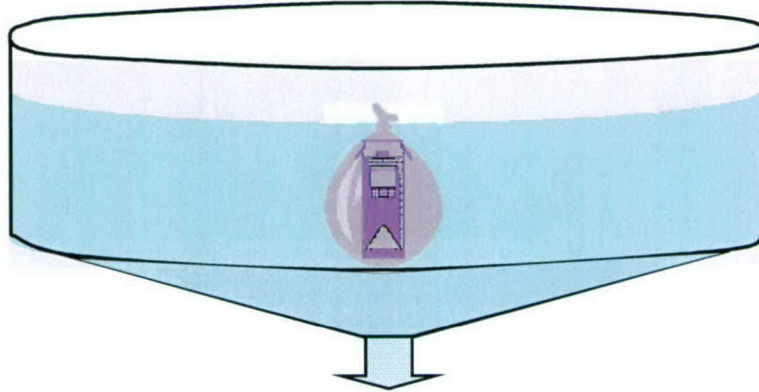


FIGURE 15. Submunition Fragment Characterization Test Set-Up.

5.2.2 Ultra High-Speed Motion Pictures

Figure 16 presents stop-action photos taken at a million frames per second of the submunition (discussed in Section 5.2.1) metal case breaking up. The photographs show metal case expansion at 1, 4, and 6 microseconds after initiation.

Looking closely at Figure 16, particularly pictures 2 and 3, you can see that the casing is breaking up in a pattern of small diamond shapes. The center section had thinner wall resulting in this section rupturing before the rest of the casing. This pattern is a result of controlling the fragmentation by pre-scoring the case. In addition to controlled fragmenting warheads, naturally fragmenting warheads (in which the case is allowed to freely break up) are also used. In the instance of the naturally fragmenting warhead, capture of the fragments is even more difficult since the fragments do not follow a well-defined trajectory as they move away from the point of initiation and the different sizes and masses determine how far fragments travel.

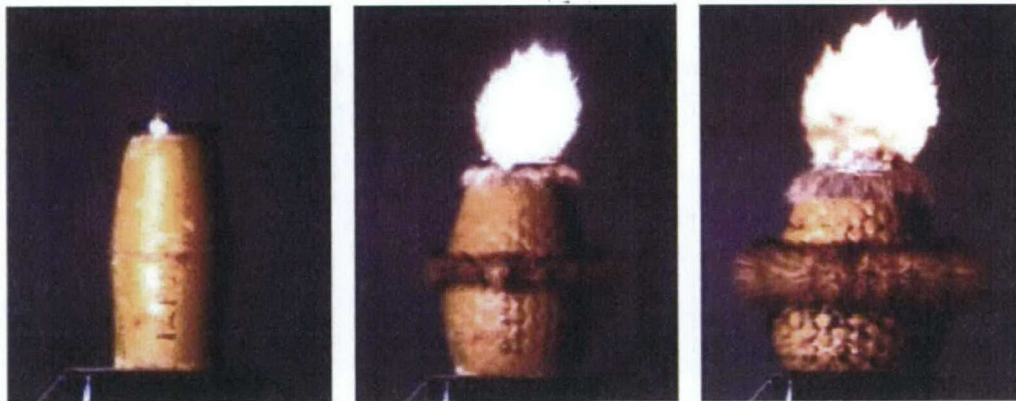


FIGURE 16. Submunition Case Fragmentation.

Figure 17 presents stop-action photos taken at one million frames per second showing early time initiation at both ends and fragmentation of a rod warhead. Rods run vertically and can be seen just breaking out of the protective thin metal skin in the last picture frame. This warhead is another example of controlled fragmentation.

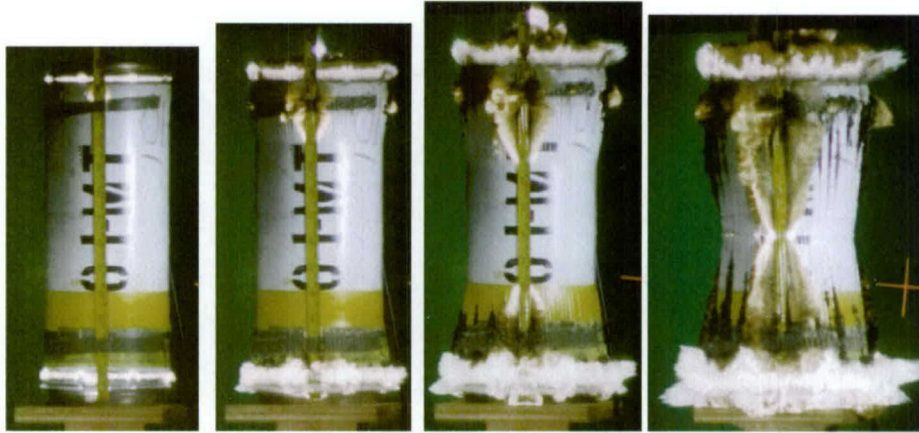


FIGURE 17. Rod Warhead Fragmentation.

5.2.3 Fragments Collected From Deflagration-to-Detonation Tests

In these tests, granular explosives (e.g., HMX or CL-20) are loaded into a hollow Lexan cylinder, Figure 18. The explosive is then ignited. The reaction transitions from a deflagration (burning) to a detonation. The detonation shatters the Lexan tube and the bottom plate. The pieces from the plate were recovered, and reassembled as shown in Figure 19. In these tests typically 99.8% of the plate is recovered. As expected the Lexan tube was shattered into many fragments that were recovered. Examination of the Lexan fragments showed sharp jagged edges and no evidence of melting/softening. [Note: Lexan is polycarbonate, an amorphous material, and does not have a melt temperature. It does have a glass transition temperature of 150°C (300°F). The glass transition temperature is where the material goes from rigid solid to soft and rubbery.]

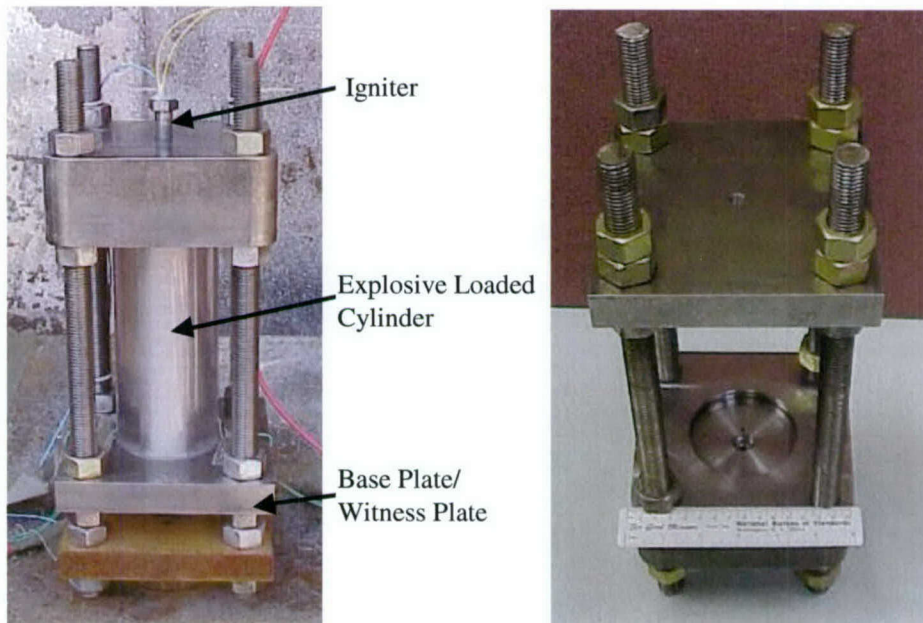


FIGURE 18. Deflagration-to-Detonation Transition (DDT) Test Fixture. The picture on the left shows the DDT test set-up; the picture on the right shows the details of the lower witness plate.



(a) The bottom plate, looking from bottom up through hole.



(b) Fragments produced from hole in bottom plate, looking from top down.



(c) Fragments from (b) re-assembled in hole in bottom plate shown in (a).

FIGURE 19. Fragments from DDT Test.

5.2.4 Results From Shaped Charge Jet Tests

A Shaped Charge Jet (SCJ) or Explosively Formed Projectile (EFP) is a munition designed to give a jet or a very fast, large primary fragment. A SCJ consists of a metal cone (often copper) surrounded by explosive contained in a tube. When the explosive detonates, the cone collapses and a metal jet is formed. This fast moving metal (copper in this instance) can penetrate through the steel target. SCJs are often used to penetrate through metal armor.

In these tests, an M47/77 shaped charge grenade was used. It has 30 grams of explosive, typically Comp A-5 explosive and a 23 gram copper cone. The copper shaped charge is placed above steel witness plates (the shaped charge jet is placed some distance above the witness plates to improve performance assessment: the distance above the plates is described as standoff) and the SCJ is initiated (see Figure 20). The copper jet penetrates the steel witness plates and copper is deposited in the resulting bore. The state of the copper (i.e., molten or otherwise) then becomes the question.

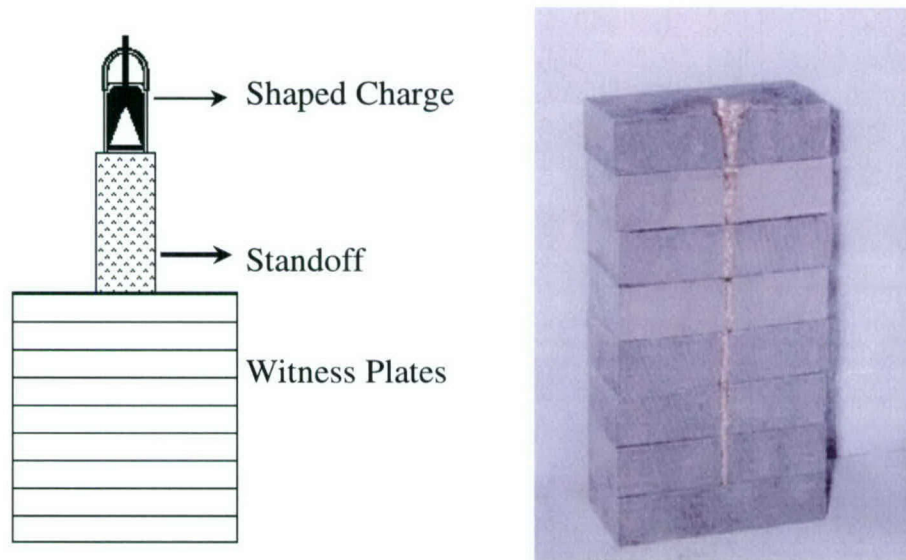


FIGURE 20. Shaped Charge Test. Drawing at left shows test set-up; picture on right shows sectioned steel witness plates and shaped charge jet penetration.

Tests done at the Army's Ballistic Research Laboratories (Reference 13) have shown that the temperature of the copper shaped charge jet was below the melting point of copper indicating that the metal in the jet remains as a solid instead of melting or vaporizing. The jet is formed via plastic flow of the metal, not from melting. Plastic flow is associated with a large load applied to a body. The material first starts to undergo elastic deformation, followed by plastic yielding, which may lead to fragmentation. Stopping short of fragmentation, the body that has undergone plastic yielding will have permanently changed its shape when the load is removed, but will remain a continuous body. A familiar example is metallic gaskets that deform when a load is applied. In the case of the shaped charge jet, the load is applied very quickly by the explosive detonation, and the metal liner deforms plastically to form the jet.

Other literature suggests that very minor amounts of melting during jet formation and during plate penetration may occur. But as shown on the right in Figure 20, copper is deposited as smaller solid metal fragments along the entire length of the penetration.

5.2.5 Results From Arena Tests

Most of the examples presented above were for relatively small scale tests. Larger scale tests are performed in arenas. Figure 21 shows an arena test in process, and the post-test appearance.

These tests are very violent and fragment recovery is more difficult than in the small scale tests. In these tests, Celotex fragment catching bundles, metal witness plates, and ultra high-speed motion pictures are used. The Celotex fragment catching bundles are simply many large sheets of Celotex insulation material bundled together. These Celotex bundles are arranged in a semi-circle near the munition to be detonated. In Figure 21, the Celotex bundles are shown on the left of the upper photo and are still standing in the lower photo. The detonation produces fragments that are then "caught" by the Celotex bundles. The fragments are sharp-edged. The fragments are later extracted from the Celotex bundles for analysis of size, shape, and mass. This process is time consuming and expensive and is not often used. Because lethality studies are only concerned with the fragments between 2 and 40 grams, no effort was made to try to recover all fragments. It is mentioned here only to show that a warhead produces fragments, and these fragments are cool enough (well below the melting or vaporization temperatures of metals) to be captured in Celotex.



FIGURE 21. Naturally Fragmenting Warhead Arena.

The metal witness plates are suspended in a semi-circle around the arena. When the munition detonates, the resulting fragments penetrate the witness plates and give an indication of the fragment trajectory, the fragment sizes, and the resultant damage inflicted. Witness plates are shown in Figure 21. You can see the holes that the fragment penetration produced. The two photos shown in Figure 21 clearly illustrate the earlier discussions of fragment location vs. blast wave and afterburning reaction location. In the upper photo the fragments have clearly

penetrated the steel plates on the right, with some of the fragments kicking up dust on impact with the dirt. The fireball is clearly shown on the inside of the plate array, well behind the fragments. The blast wave is also inside the plate array because the plates are still standing. The bottom photo shows that when the blast wave hits the plates, it knocks them down. Figure 22 shows examples of witness plates after the detonation of the rod warhead. The holes in the plate clearly show the results of fragment penetration through the plate.



FIGURE 22. Steel Witness Plates from Rod Warhead Arena Test.

Figure 23 shows another example of witness plates being perforated by fragments produced by the detonation of a rod warhead. Once again, at the time that the photo of Figure 23 was taken, the fragments had penetrated the witness plates, the fireball and the blast wave were still inside the plate array.



FIGURE 23. Rod Warhead Arena Test.

The ultra high-speed motion pictures (framing rates of one million frames per second) give indication of the fragments, the penetration through witness plates, and the fragments trajectory. Figures 13, 16, 17, 21, and 23 are stills taken from the ultra high-speed motion pictures.

Clearly the results from arena tests show that the metal casings of munitions fracture when the energetic fill detonates and solid fragments are formed. These fragments are thrown at very high velocities (approximately 1100 to 8500 feet per second) and travel some distance from the detonation (in rare cases fragments have even whizzed over the observation bunker a mile away from the Burro Canyon treatment site). This wide area presents obvious practical problems in recovery of the fragments.

5.2.6 Fragments Recovered From the China Lake OD Treatment Site

So what happens when there are explosives on both sides of the metal casings, such as might be found in an OD treatment? This section will show that the metal casings still fragment, not vaporize. [Note: As mentioned in Chapter 1, donor explosive is often placed adjacent to hard to initiate materials such as hazard class 1.3 or 1.4 rocket motors. Even in these instances, the donor charge does not completely surround the hard to initiate materials. In contrast, easy-to-initiate materials such as bombs, warheads and hazard class 1.1 require a very small amount of donor explosive (less than one pound) in the fuze well or nozzle. These in turn will initiate adjacent rounds by sympathetic detonation.]

Many fragments found in and around the OD site are from years of OD treatment events. The fragments are found throughout the site, with many found several hundred yards from the actual OD area. Examination of these fragments indicates no evidence of melting. Evidence of melting would include rounded edges. Fragments from the OB/OD site reveal sharp edges or edges that may be blunted as a result of impact. Since melting would occur at a lower temperature than the temperature required for vaporization, any appreciable vaporization of case metals is not possible because there is no evidence of melting. Examples of some of these fragments are depicted and discussed in the figures below.

An earlier version of the rod warhead depicted in Figures 17, 22, and 23, results in fragments as shown in the four photographs of Figure 24, when treated by OD. Having donor explosive on the outside of the warhead does alter the fragmentation. Instead of the rod warhead breaking up as designed, the donor explosive on the outside results in the case breaking up into chunks instead of the rod design.

A recent OD treatment event at the China Lake OD Facility resulted in the fragments shown in Figure 25. These photographs show fragments with sharp edges, and no indication of rounded edges from melting. In particular, the last photograph shows a fragment from a thin aluminum-cased munition with no signs of melting (i.e., the edges are all sharp).

The fragments depicted in Figure 26 show that fragment collection can be quite a challenge. Fragments can be found at elevations several hundred feet above the OD Facility. Fragments have been thrown over a mile. One-mile radius corresponds to over 3 square miles over which fragments could be distributed. Some become buried in the sand upon impact, while others "skip"/ricochet.



FIGURE 24. Fragments From the OD Treatment of Rod Warhead. Fragments were found at varying distances in the hills surrounding the China Lake OD site. The left photo shows a rod warhead that did not initiate in design mode, while the other photos show the rod fragments more typical of design mode.



Top right photograph shows thin aluminum case. The edges are all sharp, so there is no sign of melting.

FIGURE 25. Burro Canyon Fragments. Fragments from a recent OD treatment event.



(a)



(b)

(a) For an indication of the distance from the OD site, note the truck in the distance.

(b) This fragment is a thin steel case not unlike what might be found on a tactical rocket motor



(c)

(c) The photograph on left shows a number of fragments among the rocks and sand.



(d)

(d) and (e) Another collection of fragments high above the canyon floor. The rust indicates that the fragments were generated many years ago.



(e)

FIGURE 26. Burro Canyon Fragments. Evidence of previous OD treatment events can be found at elevations several hundred feet above the OB/OD facility. These fragments show sharp edges that indicate the lack of melting.

5.2.7 Results From Explosive-Metal-Explosive Testing

Sections 5.2.1 through 5.2.5 describe results from testing where the explosive is present on only one side of the metal casing. Section 5.2.6 presents fragments from OD treatment of munitions. In treatment events, donor explosive is sometimes placed on the outside of the munition to ensure complete reaction of the energetic waste. Some people may speculate that explosive on both sides of the metal might alter the fragmentation process. And in fact, it does. This can be seen in Figure 24. In this instance, the rod bundles did not separate as designed. While the presence of explosive on the outside of the munition alters the fragmentation, the metal casings still exist as solid metal. They do not melt or vaporize. To answer the argument that explosive on both sides of the metal might cause melting or vaporization, tests were conducted in one of China Lake's enclosed bombproof chambers. The purpose of the series of experiments was to simulate the behavior of metals under worse case conditions. These experiments were conducted under partially controlled laboratory conditions to maximize the recovery of metal fragments. A mild steel metal witness plate was weighed and an equal weight of sheet explosive was applied, half on each side of the metal plate (Figure 27). Both sides were initiated simultaneously to ensure that the maximum amount of heat/energy was deposited into the plate at the same time.

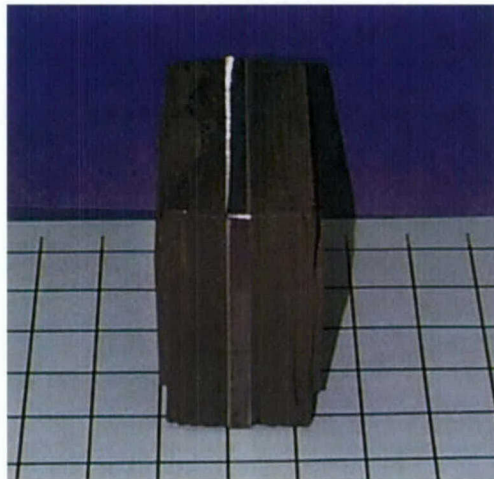


FIGURE 27. OD Simulation Test. Pre-test picture showing sheet explosive on both sides of a metal witness plate.

A large portion of the witness plate, approximately 70%, was recovered. Further collection of smaller fragments was not possible since they could not be distinguished from fragments deposited from previous testing in the chamber. In this OD simulation test, detonation of the explosive sent shock waves into the witness plate. As these waves collided, they produced very intense shear deformations along the edges of the plate, shearing off approximately 1/8-inch around the entire steel plate (Figure 28). The edges of this witness plate are sharp and jagged indicating a lack of melting. The corner of the witness plate located at the bottom of the photograph was flattened due to an impact with one of the test bay walls.

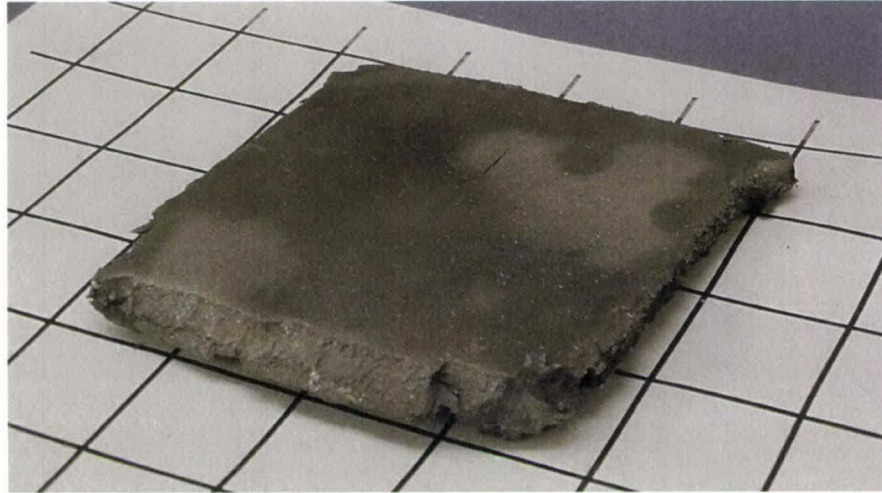


FIGURE 28. Witness Plate. Photograph reveals jagged edges from shearing of the outer rim of the witness plate.

After the initial test shown in Figures 27 and 28, two additional tests were conducted using steel witness plates. Fragments were removed from the test chamber between the tests. As shown in Figure 29, these two tests used sheet explosives with a surface area smaller than the surface area of the metal plate. The purpose of this configuration was to keep the witness plate from breaking up into small fragments so that any change in mass could be accurately measured. The total explosive weight was equivalent to the weight of 1 square inch of the metal plate. Half of the explosive was placed on one side of the metal plate with the other half on the other side of the metal plate. As indicated in the right photograph of Figure 29, the witness plate was still fragmented even with this variation in the test set-up. The average recovery for the two additional tests was 94.04%. The remaining fragments are on the order of 1/8 inch and are difficult to collect.

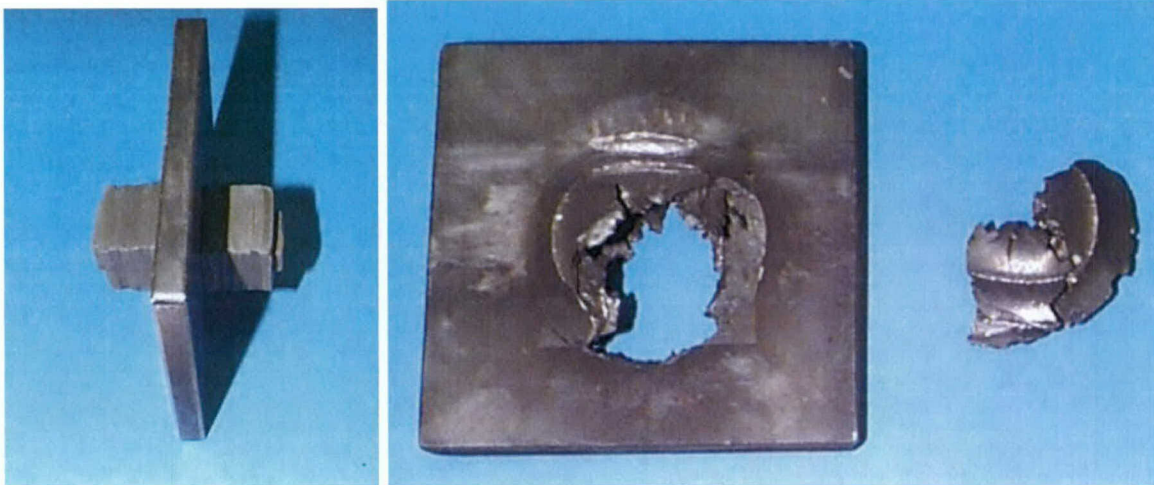


FIGURE 29. OD Simulation Test Showing Test Set-up and Witness Plate. The area of the witness plate involved in the test was reduced to decrease edge effects and to increase fragment recovery.

A fourth test was conducted using an aluminum witness plate. An aluminum plate was used to help separate fragments from this fourth test with fragments from previous tests conducted in the test bay. As in the previous test configuration (Figure 25), 1 square inch of the plate weight was matched with explosive weight. Again, half of this explosive was placed on one side of the plate with the other half on the other side of the plate. Recovery for this test was 94.70%. More material was recovered in the bay from this test, but the very fine (about 1/8-inch) particles of fragments could not easily be separated from the dirt and other foreign debris.

The test report documenting this entire test series is available in Appendix A. Recovery of fragments from all four tests was less than expected due to the difficulties collecting fragments as described earlier in the various fragment recovery tests.

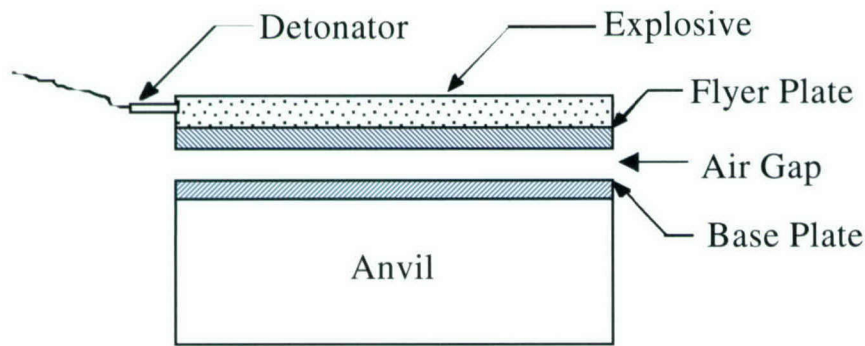
The laboratory experiments simulating OD treatment demonstrate that even with explosives on both sides of the metal, the metal remains as a solid rather than vaporizing. Additionally, fragments recovered from the China Lake OD treatment facility provide evidence of fragmentation from OD treatments. For a more complete description of metal behavior under explosive loads, please see Reference 14.

5.3 EVIDENCE FOR MINOR MELTING OF METALS

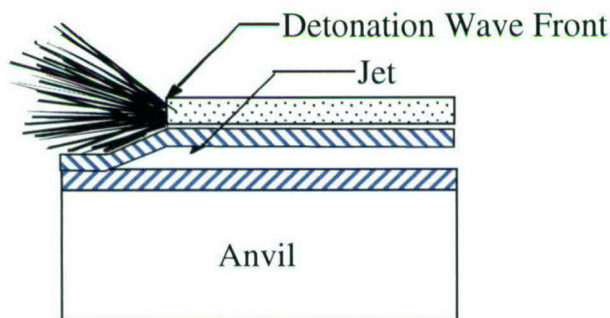
A literature search was performed to determine if others found evidence of metal melting or vaporization. Two areas indicated some evidence of melting: (1) explosive welding and (2) localized melting during high rate crack formation of metals.

5.3.1 Explosive Welding

Explosive welding is a technique that is used to join two or more materials together (see Reference 15). This process is capable of joining materials with vastly different characteristics such as lead and steel (Reference 16). The process in its simplest form joins two parallel metal plates that are initially separated by an air gap (Figure 30). One plate, referred to as the "base plate," rests on a rigid body or anvil. A second plate called the "flyer plate" is suspended above it and covered with an explosive on the side opposite the air gap. The explosive is initiated along one edge of the upper sheet, such that a planar detonation wave moves across it. The upper plate area ahead of the detonation wave is not affected until the detonation wave passes over it. As the detonation wave moves across the upper plate, it is driven into the lower plate at high velocity. The force under which the two plates collide exceeds their shear strength resulting in plastic flow in the collision area. Metal flow is restricted in the direction of the joined metals and can only take place in the direction of the unaffected air gap (see frame 2 of Figure 30). The plastic flow produces a jet in the gap, which is similar to that of a shape charge. The jet material includes the plate surface contaminants that are ejected from the weld zone. The resulting clean metal surfaces, joined under enormous pressure, with intimate contact, are welded together.



The process of explosive welding shown here is to join two metal plates, base and flyer plates, separated by an air gap.



The explosive is initiated along one edge of the upper sheet. As the flyer plate is propelled into the base plate they are welded together.

FIGURE 30. Explosive Welding.

Examination of the weld joint microstructure gives evidence of melting only in the impact zone (Reference 17). The melting is primarily the result of heat generated in producing the plastic flow. Heating that results from the adiabatic compression of the air gap gas is a minor contributor. The weld area melt zone varies from less than 1 micron to several microns in thickness. Cooling rates of $10^{\circ}\text{C}/\text{second}$ have been calculated for the melt zone. The impact affected deformation zone is about 30 to 50 microns wide. So while melting is evident, it is in a very restricted and very small zone.

5.3.2 Shear Zones

The rate at which heat is added and lost from a metal, the method in which it is added, the metal thermal mass, alloying elements, heat capacity, heat of fusion, and electrical and thermal conductivity are all factors affecting the state of a metal in thermal transient. In explosive events the timeframe of interest is very short, because forces are high and temperatures are extreme. In a detonation the explosive energy is almost instantly converted into heat and work. Some small amount (as we will see in a later section) of the heat is conducted into the warhead case. The work is expended in deforming the metal case, fragmenting it, accelerating the fragments, and expanding the gaseous products of reaction.

The detonation energy plastically deforms the metal case as it expands before rupture. A plastic deformation process is one in which no energy is stored and all energy input to the deformed body is converted to heat. This heat raises the warhead case temperature. As the case

continues to expand, it begins to fail in shear. Shear failure onset forms along bands at very high rates (Reference 18). The formation of the shear band is so rapid that heat cannot escape from it. The shear band heating softens the shear zone metal further concentrating the shear slip to a narrower band. Post-test scanning electron microscope examination of fragment surfaces resulting from such shear bands has revealed evidence of minute melt zones. The melting only occurs at extremely high shear rates such as experienced in explosive deformation and in metals with poor to moderate heat transfer coefficient (such as steel). Shear band melting is not normally seen in metals such as copper and aluminum that conduct the heat away from the shear zone too fast for melting to occur. The shear band melting is localized at the crack tip and is about one micron thick and a few microns wide. (A human hair is about 75 microns in diameter.) This is consistent with earlier discussions of fragmentation. Even with this microscopic investigation, a few microns at most would even melt and vaporization is not a possibility.

So while there appears to be evidence of some melting in explosive welding and shear zones, it is very, very localized and represents an almost insignificant amount of the total metal.

6.0 THE SOCORRO FRAGMENT

The information and conclusions in Section 5 that metal casings fragment, and the information in Section 7 that metal casings do not melt or vaporize, have been presented at various technical meetings. At these meetings we have appealed to audience members to provide data or samples that might lead to a different conclusion.

As a result, the Army Defense Ammunition Center, McAlister, Oklahoma, offered a large fragment that was produced from an open detonation of multiple 155mm projectiles. The test was conducted at the New Mexico Institute of Mining and Technology, Socorro, New Mexico on 11 September 2001. This particular fragment was of interest because there was smear of bronze on the steel sample. The smear could be evidence that the bronze melted.

This section describes the evaluation of this approximately 19-inch long fragment. The techniques included: visual observation, metallographic examination, chemical analysis, microhardness testing, and scanning electron microscopy. More detailed discussion can be found in Appendix B.

6.1 155MM PROJECTILE

The 155mm high explosive (HE) M107 is the Army's standard high-explosive projectile used primarily for fragmentation and blast effects. Its maximum diameter is 155mm and it is 27 inches long. It weighs 92 pounds and has 14 pounds of TNT-based Comp B explosive. It is depicted in Figure 31. The steel casing is either AISI 1045, 1046, or 1050 steel and weighs 76 pounds. A C22000 bronze-rotating band that weighs 2 pounds is at the base of the projectile. The composition of the bronze is 90% Cu, 9.90 % Zn, 0.05% Fe, and 0.05% Pb.

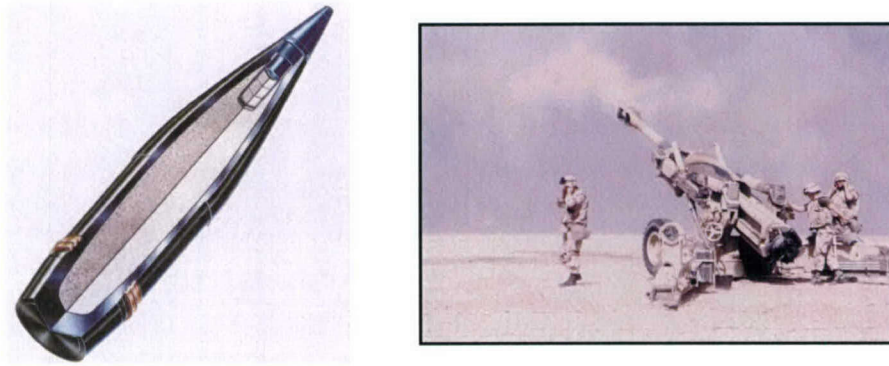
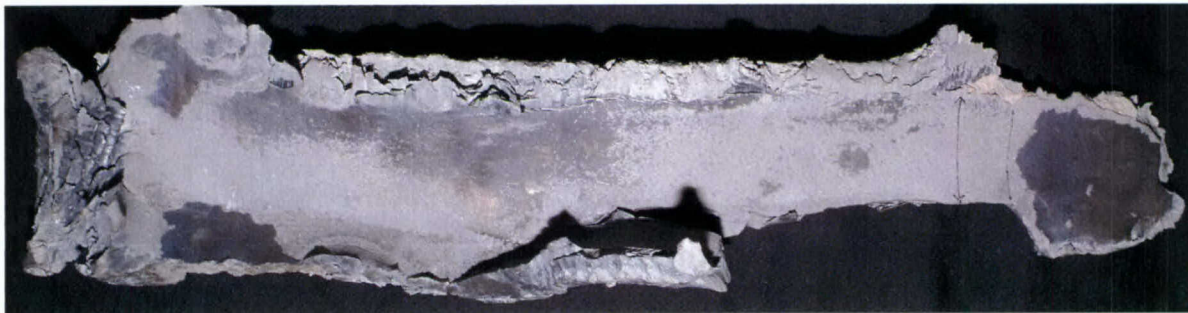


FIGURE 31. The M107 155mm High-Explosive Projectile.

6.2 THE FRAGMENT

The fragment was found after the open detonation of 98 155mm projectiles stacked in a pyramid configuration. The test was initiated by the detonation of 22 one-half blocks of M-112 explosive charge. The M-112 blocks are 1.25 lbs. of C-4 explosive. These donor charges (0.625 pounds each) were placed in the fuze wells of 22 of the 98 155mm projectiles. The other 76 rounds detonated via sympathetic detonation.

The fragment is shown in Figure 32. It was approximately 19 inches long and weighed approximately 20 pounds. As shown in Figure 32, there was evidence of what appeared to be bronze metal on the steel fragment.



(a) View of the fragment as seen from the interior portion.



(b) Outer portion in the region of the bronze smear.

FIGURE 32. The Large Fragment Resulting From the Socorro Test.

6.3 VISUAL EXAMINATION

The edges of the fragment appear sharp and jagged indicating shear and tensile failure. There is no visual evidence of steel melting. The inner surface of the fragment appeared unaffected, contained original machining marks, and had a scale appearance. The outer surface does have some wavy appearance and evidence of flow. A flattened area indicates possible contact with other projectiles or other hard surface.

6.4 SAMPLES FOR FURTHER EXAMINATION

Three metallographic samples were sectioned from the bronze smear region as shown in Figure 33. These samples were polished and etched.

In addition, three samples were taken from the steel near what was the fuze well. These samples were also polished and etched to determine the effects of the detonation on the steel and determine the approximate temperature experienced by the steel during the detonation. In the following sections, summaries of the results will be presented. The details and detailed discussions may be found in Appendix B.

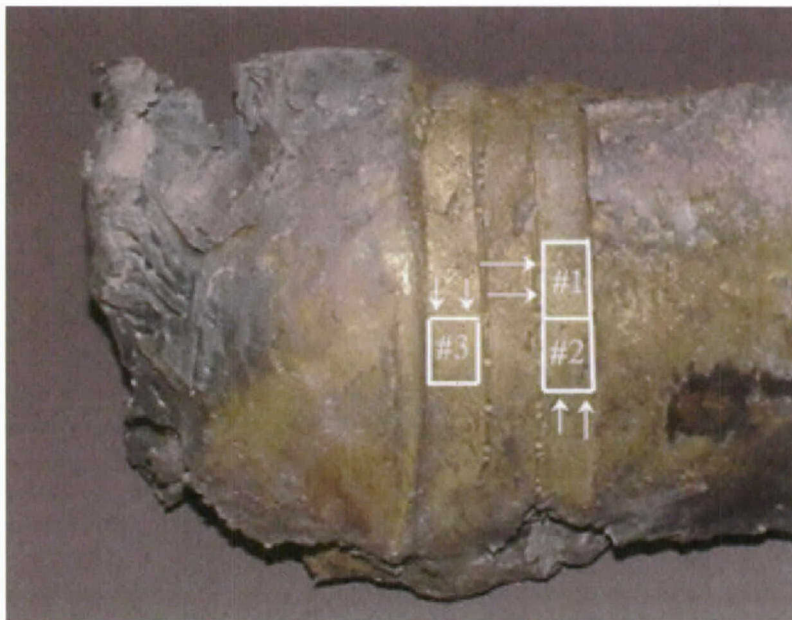


FIGURE 33. View of the Bronze Smear Region Where Samples Were Taken. Arrows indicate direction of subsequent examination.

6.5 RESULTS FROM METALLOGRAPHIC EXAMINATION

The bronze on steel samples showed evidence of recrystallization of the bronze. Recrystallization generally occurs as a result of annealing this alloy between temperatures of

800°F to 1450°F. The grains were fairly equiaxed. Grain distortion and twinning was also evident.

These results indicate a distorted bronze produced by plastic flow, rather than melted bronze. Melting and subsequent solidification upon cooling would have produced a needle-like dendritic structure that was not observed. The very close proximity of the bronze on the steel suggests that similar peak temperatures would have been experienced by both bronze and steel. The conclusion from this part of the investigation is that the bronze did not melt and the smearing of bronze on the steel was the result of cold plastic flow.

The steel samples 1 and 2 showed six distinct features noted after etching. (1) As-produced "original" structure of pearlite/ferrite (this was the bulk of the material), and (2) deformed "original" as-produced structure. At the outer portion of the fragment a relatively uniform layer of (3) untempered martensite was evident, interrupted by shear bands (4) extending from the outer surface into the sample (about 1/8 of the fragment thickness). A decarburized ferrite layer (5) at the interior surface with adjacent forging lines (6) was observed. Discussions with Chamberlain Manufacturing, a producer of 155mm projectiles, confirmed:

- (a) The predominant structure of the fragment is consistent with the as-produced structure indicating no fundamental change.
- (b) Untempered martensite on the outer surface most likely resulted from machining during production.
- (c) Decarburization on the interior surface is as-produced.

Other conclusions made from the metallographic studies of steel samples 1 and 2 are:

- Shear banding and elongated grains near the exterior surface are common with cylindrical warhead fragments formed during the detonation process.
- Forging flow lines were created during production of the projectile.

Steel sample 3 was taken from the steel in the region of highest deformation. This sample also showed the untempered martensite on the exterior, as well as a transition from untempered to tempered martensite. Transition from untempered martensite to tempered martensite occurs between 750°F to 1100°F, indicating that this portion of the fragment experienced temperatures in that range. In contrast to the steel samples 1 and 2, this fragment had significant, deep penetrating shear bands at the edge and interior surfaces, and intermittent decarburization on one of the fractured edges. Overall there was increased deformation of the original structure. Even with the violence experienced by this portion of the fragment, there was no indication of temperatures approaching the melting temperature of steel.

6.6 CHEMICAL ANALYSIS

The results from the chemical analysis of the steel is presented, and compared to various steels used in producing 155 mm projectiles, in Table 5. The results compare well with the AISI 1046 used by Chamberlain Manufacturing, a major manufacturer of 155mm projectiles.

TABLE 5. Chemical Analysis, Weight Percent.

Element	Fragment	AISI 1045	AISI 1046	AISI 1050
Carbon	0.47	0.43 – 0.50	0.43 – 0.50	0.48 – 0.55
Manganese	0.86	0.60 – 0.90	0.70 – 1.00	0.60 – 0.90
Phosphorus	0.009	0.040 max. typ.	0.040 max. typ.	0.040 max. typ.
Sulfur	0.022	0.050 max. typ.	0.050 max. typ.	0.050 max. typ.
Chromium	0.01	N/A	N/A	N/A
Copper	0.02	N/A	N/A	N/A
Molybdenum	<0.01	N/A	N/A	N/A
Nickel	0.01	N/A	N/A	N/A
Silicon	0.25	N/A	N/A	N/A
Iron	balance	balance	balance	balance

6.7 MICROHARDNESS TESTING

Microhardness testing was conducted on (1) exterior surface, untempered martensite, (2) “original” structure bulk pearlite/ferrite, (3) deformed “original” structure, (4) interior surface decarburized ferrite, and (5) exterior surface tempered martensite from steel sample 3. The detailed results are presented in Appendix B and will not be presented here. Here we present only the following conclusions:

- The “original” structure of pearlite/ferrite was modified by passage of an intense shock wave.
- Work hardened “flattened” pearlite/ferrite adjacent to the shear banding and deformation was observed.
- The readings from the exterior surface confirm existence of untempered martensite due to machining in the production of the 155mm projectile.
- The decarburized ferrite grains at the interior are consistent with the manufacturers claim of no machining of the interior surface subsequent to heat treating.
- The results are consistent with the detonation causing fragmentation of the original projectile casing and no melting/vaporization.

6.8 SCANNING ELECTRON MICROSCOPY

Typical results are shown in Figures 34 through 37. These micrographs, taken of the fractured edges, show structure indicative of plastic flow and deformation due to the detonation, but do not show evidence of melting that would have produced a rounded featureless edge.

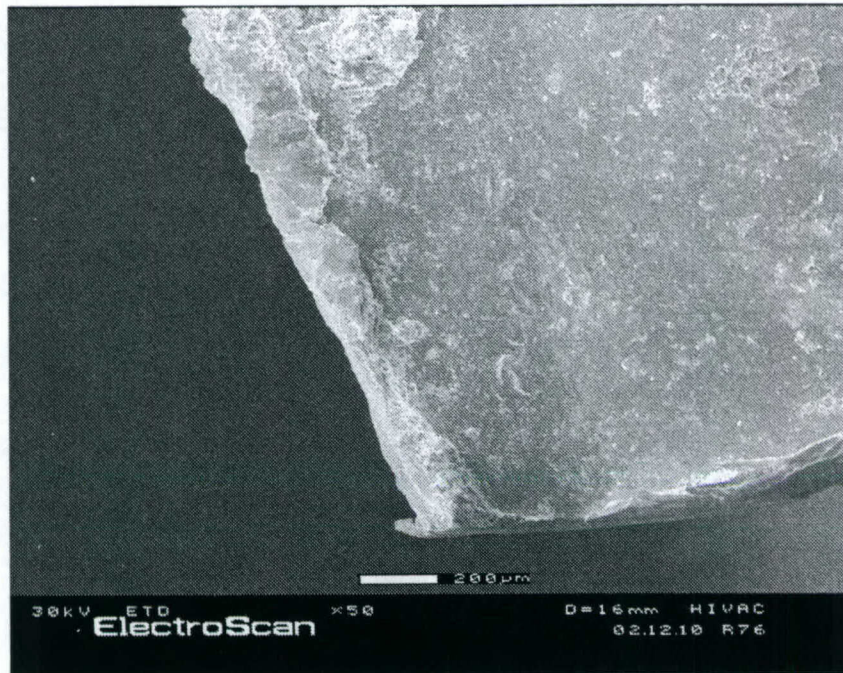


FIGURE 34. Scanning Electron Micrograph of the Edge of the Steel Fragment. Magnification 50x.

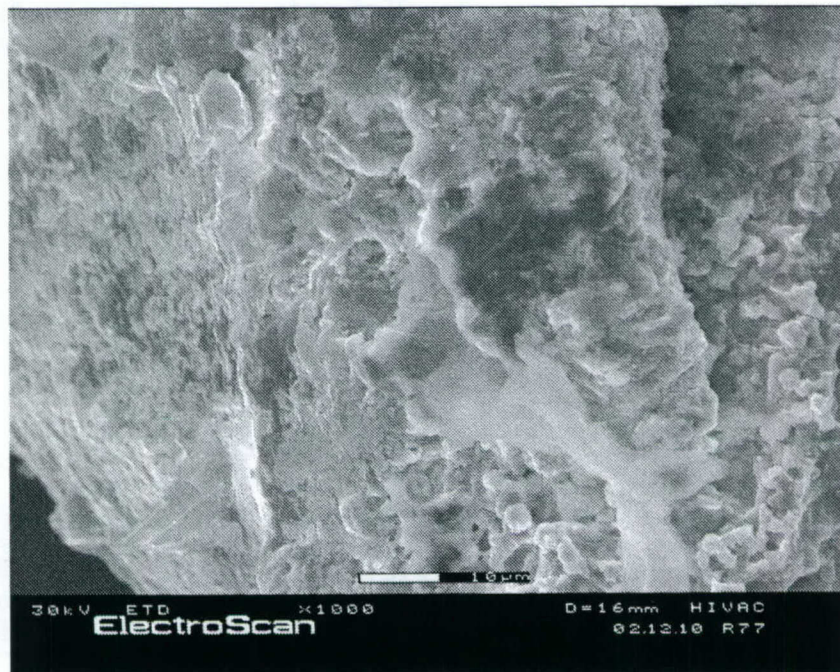


FIGURE 35. Scanning Electron Micrograph at Higher Magnification That Shows the Structure of the Damaged Edge of the Fragment. Magnification 1000x.



FIGURE 36. Scanning Electron Micrograph of Edge of a Steel Fragment. Magnification 1000x.

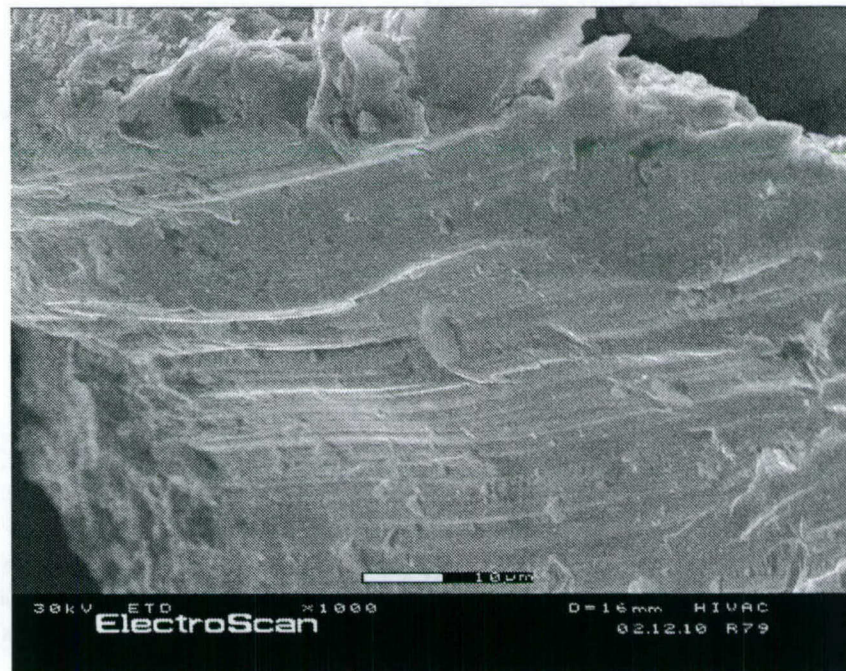


FIGURE 37. Scanning Electron Micrograph of Edge of a Second Steel Fragment. Magnification 1000x.

6.9 SUMMARY OF ANALYSES OF SOCORRO FRAGMENT

Based on visual observations, metallographic examinations, chemical analysis, microhardness measurements, and scanning electron microscopy the following conclusions are made:

- The fragment is the result of a detonation causing fragmentation of the original projectile and work hardening of the original steel.
- There is no evidence of melting of the bronze rotating band nor the steel case.
- The temperatures experienced by the fragment during the detonation process ranged from 800°F to 1450°F depending on location within the fragment. This is below the 1910°F melting point of bronze.
- Softening and plastic flow of the bronze rotating band produced the bronze smear that was observed on the steel fragment.

7.0 SO WHY DON'T METAL CASINGS MELT OR VAPORIZE DURING DETONATION?

Section 5.2 and Section 6 provides evidence that the metals of munition casings do not vaporize during detonation. Section 5.3 described melting of metal in only very specialized instances. Reviewing previous discussions, the temperatures of the detonation can range from about 2500°C to 5600°C. The temperatures associated with afterburning are on the order of 1700°C, comparing those temperatures to the data from Table 3 (reproduced here for ease of discussion), causes one to wonder why there is no evidence of melting or vaporization.

TABLE 3. Melting and Vaporization Temperatures (Reference 6). The table lists the melting points for various metals and the vaporization temperature, °C, at the specified pressure.

Material	Melting point	Vaporization temperature at pressure				
		1mm Hg	100mm Hg	1 ATM ^a	10 ATM	20 ATM
Aluminum	660	1540	2080	2467	3050	3270
Chromium	1890	1610	2140	2480	3010	3180
Copper	1083		2190	2600	3500	3460
Gold	1064	1880	2520	2940	3630	3890
Iron	1535	1780	2370	2750	3360	3570
Lead	327	970	1420	1740	2320	2620
Manganese	1244		1810	2100	2850	
Mercury	-39		260	357	517	581
Nickel	1455	1800	2370	2730	3300	3310
Zinc	420		730	907	1180	1290

^a760mm Hg = 1 ATM, which is the nominal barometric pressure at sea level.

7.1 METAL VAPOR PRESSURE COMPARED TO PRESSURES IN OD ENVIRONMENT

Discussion of metal vaporization during open detonation will be made before discussing why there is no evidence of melting. The data of Table 3 is only marginally pertinent because it is only to 20 atmospheres. It has been extrapolated to higher pressures and temperatures using the Clausius-Clapeyron equation as discussed in Section 4.1. The data for iron, also presented in Section 4.1 and reproduced here, is very pertinent because:

- 1) Most of the warhead, bomb, and missile motor casings are steels having very high iron content, and
- 2) The data for iron in Table 4 and Figure 10 (reproduced here) spans the temperature range 1800 to 9000K, encompassing the detonation temperatures of explosives.

For example, the vapor pressure of iron at 6000K (above the detonation temperature of the "hottest" explosive) is 566 atmospheres, or less than 1 kilobar. The vapor pressure at 2500K (the lowest detonation temperature) is much less than 1 atmosphere. The pressures of detonation are over 200 kilobars. Thus, the vapor pressures are much lower than the detonation pressure, and the iron would not vaporize during detonation.

TABLE 4. Vapor Pressure for Iron as a Function of Temperature and 1/Temperature (Reference 7).

T (K)	P Pascals	P atm	1/T
1800	3.11E+00	3.07E-05	0.000556
2000	3.85E+01	3.80E-04	0.000500
2500	3.21E+03	3.17E-02	0.000400
3000	5.61E+04	5.54E-01	0.000333
3500	4.14E+05	4.08E+00	0.000286
4000	1.81E+06	1.79E+01	0.000250
4500	5.67E+06	5.60E+01	0.000222
5000	1.42E+07	1.40E+02	0.000200
5500	3.02E+07	2.98E+02	0.000182
6000	5.74E+07	5.66E+02	0.000167
6500	1.00E+08	9.90E+02	0.000154
7000	1.65E+08	1.62E+03	0.000143
7500	2.57E+08	2.54E+03	0.000133
8000	3.87E+08	3.82E+03	0.000125
8500	5.66E+08	5.59E+03	0.000118
9000	8.08E+08	7.98E+03	0.000111

Vapor Pressure of Iron

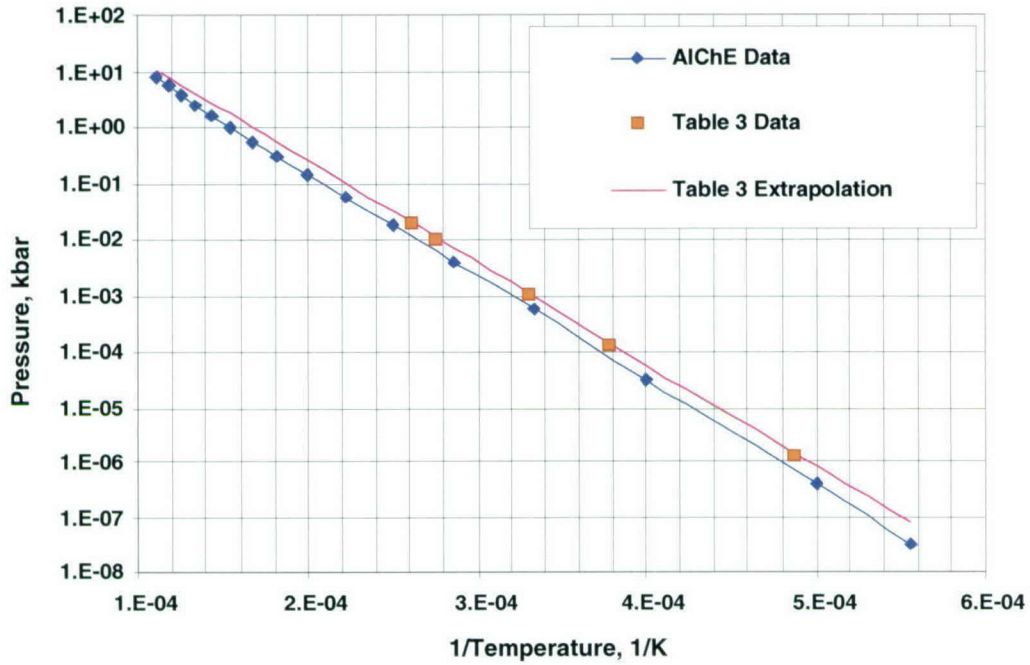


FIGURE 10. Vapor Pressure vs. 1/Temperature for Iron. AICHe data from Reference 7, data from Table 3, and extrapolation of Table 3 data using Clausius-Clapeyron Equation.

The extrapolation for the other metals of Table 3, shown in Figure 11 is also presented here.

Extrapolated Vapor Pressures

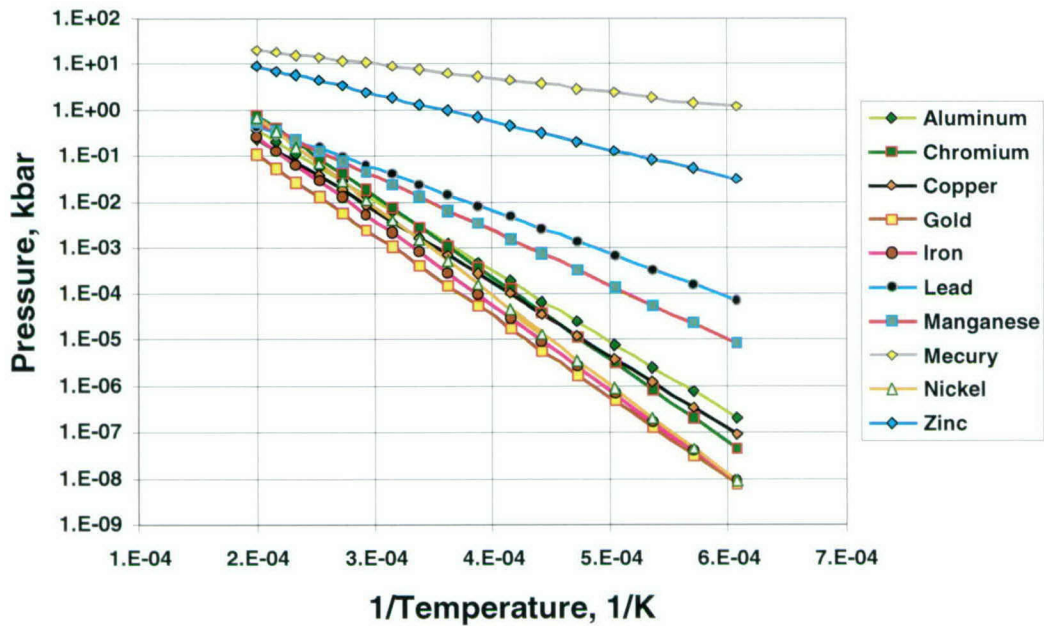


FIGURE 11. Extrapolation of the Data in Table 3 Using the Clausius-Clapeyron Equation.

Again, as seen for iron, the vapor pressure for all of the metals over the temperature range is less than 100 kilobars, with most data below 1 kilobar.

During the fragmentation of the metal casings and expansion of detonation products, the conditions of pressure and temperatures during expansion can be calculated and compared to the vapor pressure data. In order to determine the pressures and temperatures during the expansion, two equations are required:

(1) The internal explosive pressure, P , exerted on the inner surface of a case is related to the cavity volume through the perfect gas law,

$$P \cdot V = n \cdot R \cdot T \quad (2)$$

where V is the volume and T is the Temperature (K), assuming the pressure is uniform throughout the cavity.

(2) For adiabatic, reversible flow, an isentropic expansion of detonation product gases results in (Reference 19)

$$P \cdot (m_e / V)^{\gamma} = \text{constant} \quad (3)$$

where γ is the expansion coefficient, and m_e the mass of the gas. For our purposes γ taken to have a constant value of three although it may vary in an actual expansion starting at five and falling to smaller values. For a cylindrical expansion V will increase as the square of the radius. For a spherical expansion V will increase as the cube of the radius.

Equation (3) may be re-written as

$$P = P_o \cdot (V_o / V)^3 \quad (4)$$

where the subscript "o" designates an initial or original condition. Combining equations (2) and (4) gives

$$T = T_o \cdot (V_o / V)^2 \quad (5)$$

For temperatures from 1811 to 9340K, an equation for the vapor pressure of iron is (Reference 7)

$$\ln P = 75.649 - 5431.5 / T - 6.0834 \ln T + 0.000698 T \quad (6)$$

where P has units of Pascals (see Table 4).

Taking representative initial values of pressure and temperature of 200 kbar and 5500K gives a graph, shown in Figure 38, comparing the gas pressure applied to the case with the vapor pressure of iron during a case expansion as a function of volume expansion ratio over a range of

temperatures for which equation (6) was determined. Also shown in Figure 38 is the equivalent point for this expansion to a 20 bar vapor pressure temperature of 3843K from Table 3. Additionally, on Figure 38 is the vapor pressure iron as a function of volume ratio, calculated using the Clausius-Clapeyron equation using the 20 bar data from Table 3. The agreement between the extrapolation using the Clausius-Clapeyron and the actual data from Reference 7 is excellent.

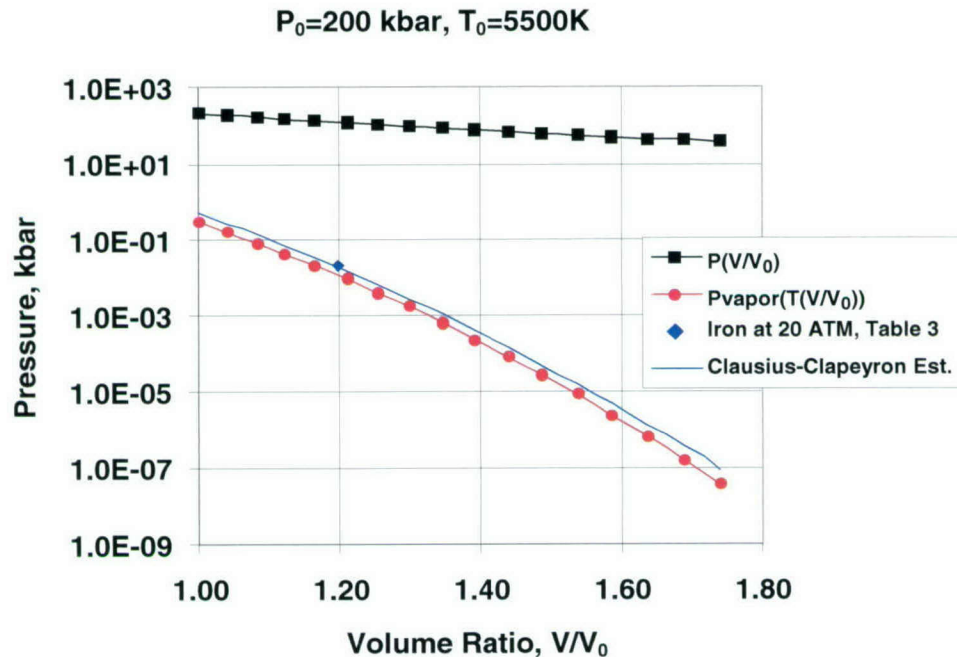


FIGURE 38. Vapor Pressures for Iron (Reference 8) Compared to Expansion Pressure and Temperatures Beginning at 200 kbar and 5500K, and an Estimated Curve Using the Clausius-Clapeyron equation for data point at 20 ATM (Table 3).

The results clearly show that the pressures for the expanding detonation products are orders of magnitude higher than the vapor pressure for iron, indicating that there would be no vaporization of iron during the expansion of detonation products. But would there be melting of iron? That will be discussed in Section 7.2.

Figure 39 presents the same analysis using the data from Figure 11. Again, these results show that the pressures for the expanding detonation products are significantly above the vapor pressures of all metals, including zinc and lead.

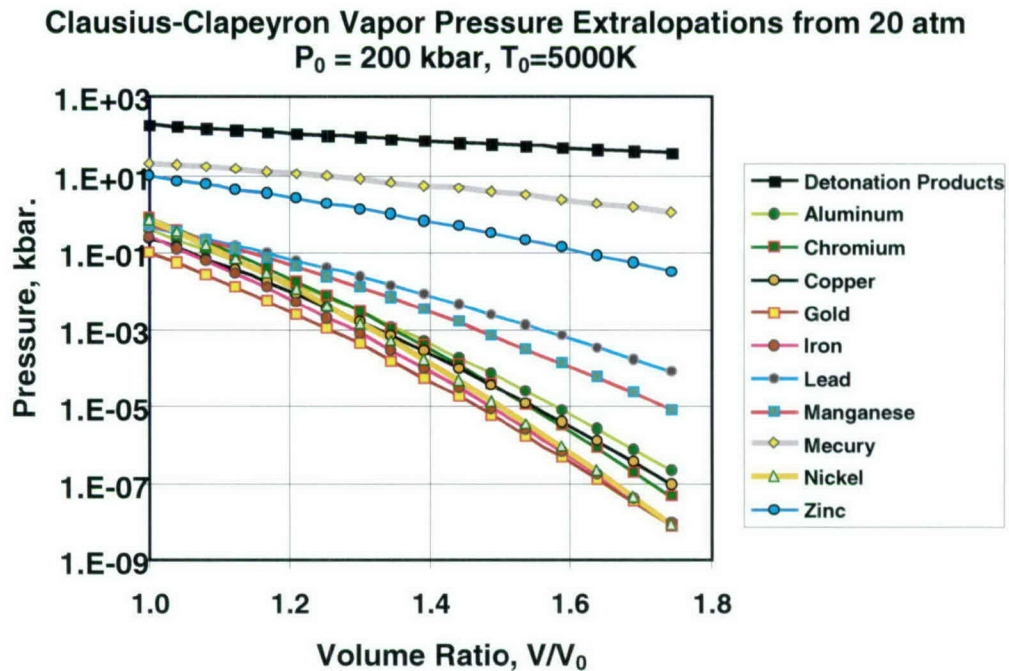


FIGURE 39. Vapor Pressures Estimated From Data at 20 ATM (Table 3) by Clausius-Clapeyron Equation Compared to Expansion Pressure and Temperatures Beginning at 200 kbar and 5500K.

7.2 HEAT TRANSFER AND MELTING OF METAL

The preceding calculations assumed infinitely fast heat transfer, e.g., the metal was at the same temperature as the detonation products; however, it takes time to transfer heat from the detonation products into the fragments, and to raise the temperatures in the fragments. The change in temperature distribution in the fragment can be estimated using the transient heat transfer equation (see Reference 18):

$$\frac{T(x, t) - T_s}{T_i - T_s} = \text{erf} \left(\frac{x}{2\sqrt{\alpha t}} \right), \text{ where } \alpha = k / \rho C \quad (7)$$

- Where,
- T_i = initial temperature of the metal case, °C
 - T_s = applied surface temperature, °C
 - k = thermal conductivity of the metal case, cal/cm-s-°C
 - C = specific heat of the metal case, cal/gm-°C
 - ρ = density of the metal case, gm/cm³
 - $T(x, t)_{\text{melt}}$ = temperature distribution that is above the melt temperature as a function of distance at time t , °C
 - t = time after detonation, sec.
 - x = distance into solid
 - erf = error function, the right hand term of equation 7 is the Gaussian error integral

Values for the metal properties needed to solve the equation are provided in Table 6.

TABLE 6. Metal Properties.
Note value marked with "*" are for iron.

	4130 Steel, (Reference 20)	Aluminum, (Reference 21)
Thermal conductivity, k (cal/cm-s-°C)	0.072	0.291
Specific heat, C (cal/gm-°C)	0.12	0.281
Density, ρ (gm/cm ³)	7.85	2.80
Jump temperature, T (°C)	526	177
Melting point, T_{melt} (°C)	1371*	582

Typical properties of an explosive detonation are provided in Table 7. Temperatures of the detonation reactions are well in excess of what is required to melt these metals.

TABLE 7. Typical Explosive Detonation Properties (Reference 1).

Property	Metalized explosive	Non-metalized explosive
Detonation temperature, T_s (°C)	5,600	2,500
Detonation pressure (ATM)	190,000	340,000
Duration/case breakup (μsec) ^a	6 - 30	

^aBased on design mode initiation for a range of weapons.

For the purposes of making a very conservative calculation, the following assumptions were used. The initial temperature (T_i) of the metal was taken to be the jump temperature. The jump temperature is the temperature in the metal that results from passage of the shock wave associated with the detonation of the explosive. The applied surface temperature (T_s) was taken to be the detonation temperature for a metalized explosive (see Table 6). This is very conservative for the donor explosive because aluminized explosives are not usually used as donor explosive. The time (t) that these temperature conditions are assumed to exist is on the order of 0.001 seconds (1000 μsec). This estimate is very conservative given that the detonation portion of an OD event is complete in a few tens of microseconds. So, for the surface to be at 5600°C for 1000 microseconds is extremely conservative. The depth to which the metal melts can be calculated by setting $T(x, t)$ to the melt temperature and solving for x in Equation 7. For these conditions, the melt depth for steel would be 210 microns and 530 microns for aluminum.

If we apply more realistic values of temperatures and time (e.g., the 5600°C detonation temperature applied for only 10 microseconds), the depth of melting is only 17 microns for the steel and 69 microns for the aluminum. If the detonation temperature is 2500°C and applied for 10 microseconds the melt depth is 9.8 microns for steel and 21.8 microns for aluminum. The calculated melting depths are compiled in Table 8.

TABLE 8. Calculated Metal Melt Depths for Conditions of Detonation Temperatures and Times. These depths are based on explosive detonation temperatures.

Detonation Temperature	Contact Time	Melt Depth, microns	
		Steel	Aluminum
5600°C	1000 μ sec	210	530
5600°C	10 μ sec	17	69
2500°C	10 μ sec	9.8	21.8

7.3 AFTERBURNING AND METAL FRAGMENTS

The previous calculations showed that even with the unrealistic input parameters to the transient heat conduction analysis, there was almost no calculated melting of metal casings associated with detonation. But what about afterburning? Why is there almost no evidence of melting? One reason is that the fragments formed during the detonation are accelerated to high velocity and travel great distances—they quickly pass through the fireball and are deposited well outside the fireball. The high-speed motion pictures clearly show this, as shown in the still frames of Figures 19 and 21. You can see the fragments passing through the witness plates, and the witness plates are outside the afterburning fireball. You can clearly see puffs of dirt where fragments have impacted. Again, these puffs of dirt occur well outside the fireball.

7.4 CONCLUDING REMARKS FOR SECTION 7

The calculations in this section show why there is no vaporization during the detonation and expansion of detonation products: the detonation pressures are orders of magnitude higher than the vapor pressures for iron and other metals over the range of the detonation temperatures. Melting is almost non-existent as well because the metals are not in contact with the hot products of the detonation long enough to allow significant heat transfer, and are accelerated out of the region of afterburning, ending up several hundred to a thousand feet from the detonation site.

8.0 EMISSION FACTORS

8.1 BACKGROUND

The previous sections present experimental and analytical results that show that metal casings fragment and do not melt or vaporize. The results clearly show that the metal vaporization assumptions used in the 1996 Health Risk Assessment are unrealistic and grossly conservative and do not reflect the real fate of the metal casings during OD. However, even though the data are convincing, we cannot state that absolutely no particulate metal emissions occur.

Chemical Compliance Systems, Inc., has collected emissions data in a database. These data were published on the Government Cooperative Group on Demilitarization Quickplace website for peer review and feedback (Reference 19). Chemical Compliance Systems, Inc. (CCS) incorporated the suggested changes into a modified database. China Lake is using the modified database to determine the emissions from the various families of propellants and explosives as the first step of its Health Risk Assessment of treating explosive hazardous wastes by open detonation/open burn. China Lake has also tasked CCS to focus on the metal issue and provide data that can be used to determine the emissions from the metals casings; from the paints, coatings, and platings, and from the energetic materials. The report from CCS is included as Appendix C. Our use of the data is reported in following sections.

It must be noted that the data of Appendix C is limited in the number of tests, reflecting the difficulty in obtaining these types of data.

8.2 HOW MUCH METAL IS IN A MUNITION?

As discussed previously, metals are found in munition casings; in the paints, platings and coatings, and in the energetics. Before discussing how much metal might be emitted, we must know how much metal and what types are present in munitions.

8.2.1 Metal in Munition Casings

Before discussing the quantity of metal emitted from a casing, in a form other than fragments, the weight of the munition casing compared to the energetic fill must be discussed.

Rocket motors have steel or aluminum casings. Some rocket motors have organic/fiber composite casings but they are not addressed in this report on metal emissions. The ratio of metal to propellant ranges from 0.157 to 0.569 lb. metal casing/lb. propellant. Performance considerations force motor designers to try to minimize the inert weight of the case compared to the propellants. Most motors that contain un-metallized propellant have an average of 0.357 lb. of metal casing/lb. of propellant, and propulsion systems that use metallized systems have an average of 0.397 lb. metal casing/lb. of propellant. Thus, a factor of 0.40 lb. of metal casing/lb. of propellant to describe all rockets motor casings is representative and slightly conservative. The steel most commonly used in missile motor casings is 4130 Steel. This steel contains 0.28-0.33% C, 0.6% Mn, 1.1% Cr, and 0.25% Mo (maximum levels) with the rest being iron.

For bombs, the amount of metal casing to amount of explosive varies by bomb size and is given in Table 9.

TABLE 9. Ratio of Metal to Explosive for Bomb Casings.

Bomb size	Metal/explosive ratio
250-lb. bomb	1.5
500-lb. bomb	1.6-1.9
1000-lb. bomb	1.3-1.5
2000-lb. bomb	1.1

A value of 1.5 lbs. of metal casing per lb. of explosive will be used to characterize the bomb family. Most bombs use 1000 series steels, with 1035 being the most common. This steel contains up to 0.9% Mn, 0.32-0.38% C, and the rest is iron.

For warheads, the amount of metal casing to explosive ratio varies by the type of warhead. An air-to-surface penetrator warhead typically has 4 lbs. metal casing/lb. of explosive, while an air-to-air warhead typically has 0.82 lbs. of metal casing/lb. of explosive. Warheads are typically 4300 series steel with 4340 being common. This steel contains 0.38-0.43% C, 0.8% Mn, 2% Ni, 0.9% Cr, and 0.3% Mo (maximum levels) with the rest being iron.

In the following calculations the small amount of carbon in the steels will be ignored and only metallic elements considered.

Gun cartridges are also treated by open detonation at China Lake. A review of the cartridges treated over the past several years, shows that most of the cartridges were 20mm ammunition (over 50%), with 25mm, 30 cal, and impulse cartridges comprising about 15% each. While 20mm cartridges are relatively small they are complex. There is metal in the casing, there is metal in the projectile body and nose tip and there are metal powders within the projectile. There is also lead styphnate, barium nitrate, antimony sulfide and aluminum in the primer. The amounts and types of metals are shown in Table 10. [Note: The 20mm data will be used for all gun cartridges as a conservative assumption. The bases for the assumption include: (1) 20mm has been the most widely treated gun cartridge at China Lake, (2) the 20mm incendiary round described is the most complex, (3) the 25mm cartridges have a steel casing and a unitary steel projectile, and (4) the 30-cal ammunition was a one-time single treatment event.]

TABLE 10. Metals Contained in 20mm Gun Cartridge.

Item	lbs. metal/lb. gun propellant	Composition
Cartridge casing	3.16 lb. brass/lb. gun propellant	70% Cu, 30% Zn
Primer	0.00678 lb. primer/lb. gun propellant	Pb, Ba, Sb, Al salts
Projectile casing	2.21 lbs. steel/lb. gun propellant	1043 steel
Projectile tip	0.21 lbs./lb. gun propellant	Aluminum
Projectile fill	0.11 lbs./lb. gun propellant	50/50 Mg/Al powders
Projectile pad	0.0021 lbs./lb. gun propellant	Zr
Projectile rotating band	0.063 lbs. brass/lb. gun propellant	70% Cu, 30% Zn

If the above amounts of metal seem large, remember that the numbers are lbs. of metal/lb. of gunpowder. There are only 38 grams of gunpowder per gun cartridge.

8.2.2 Metals in Paints/Coatings/Platings on Missile Motors, Missile Warheads, and Bombs

Missiles and bombs often have coatings/platings to protect the ordnance from the corrosive effects of the maritime environment. For example steel components often have a cadmium plating, a chromated chemical conversion coating, and a chromated epoxy primer. Aluminum motor casings do not have the cadmium plating but are coated with a chrome-containing chemical conversion coating and a chromated epoxy primer.

To estimate the amounts of metal contained in coatings and platings found on missiles, the AIM-7 Sparrow was chosen because it is an older, mid-size missile that has higher cadmium and chromium levels than currently-manufactured missiles. The Sparrow dates from the 1970s and is about the same size as the current AMRAAM and HARM missiles, and is larger than the Sidewinder missile. Since the 1970s, the Navy has employed thinner and more "environmentally friendly" paints and coatings. For example, the Navy is substituting aluminum and zinc instead of cadmium plating. The aluminum is ion vapor deposited. Similarly, the Navy is using non-chromate-based primers instead of the old chromate-based primer paint. Using the Sparrow missile motor and warhead values will be on the conservative side because of its size, type of coating, and thicker coatings.

The Mk 82 (500 lb.), Mk 83 (1000 lb.), and Mk 84 (2000 lb.) series bombs were also examined. The cadmium and chromate on the bombs is all on the fuze well and suspension lugs. The fuze well is the same size for all three bombs and the suspension lugs are close to the same size for all three bombs, so there is essentially no difference in the cadmium and chromate amounts for all three bombs. The amount of zinc will change because the surface areas of the bombs change. The 2000-lb. bomb has about 1.6 times the surface as the 1000-lb. bomb and the 500-lb. bomb has about 0.63 times the coating of the 1000-lb. bomb. But the 2000-lb. bomb has almost twice as much explosive as the 1000-lb. bomb, while the 500-lb. bomb has about half the explosive of the 1000-lb. Since all of the emission calculations involve pounds of coating per pound of explosives, the differences in surface areas almost wash with the differences in explosive weights. The values for the 1000-lb. bomb were chosen to be representative of the bomb family.

The representative values for metals in paints, platings, and coatings are presented in Table 11.

TABLE 11. Metals in Munition Paints and Coatings.

Type of munition	Zinc grams	Zinc lbs.	Cadmium grams	Cadmium lbs.	Strontium grams	Strontium lbs.	Chromium grams	Chromium lbs.
Warhead	0	0	24	0.0528	1.1	0.00242	1.1	0.00242
Motor	0	0	88	0.1936	3.9	0.00858	3.4	0.00748
Bombs (Mk 83)	550	1.21	12	0.0264	0	0	0.15	0.00033

8.2.3 Metals in Energetic Materials

Propellants and explosives often contain metal powders, usually aluminum, for fuel. When the aluminum burns to aluminum oxide much energy is liberated. The aluminum oxide that is formed also plays a role in suppressing combustion oscillations in the motor. The amount of aluminum added to a propellant is on the order of 20%. Some plastic bonded explosives (PBX) contain 17-20% aluminum.

Propellants often include small concentrations (approximately 1% to 2%) of metal compounds for burn rate control. Examples of burn rate modifiers include iron oxide, oxides of

copper and chromium for ammonium perchlorate composite propellants, and lead salts for double base propellants.

In addition, propellants, especially minimum signature propellants (family IIE) sometimes contain a small amount (approximately 1%) of combustion instability suppressants such as aluminum oxide or zirconium carbide.

This report does not present an analysis for emission factors for the metals contained in the propellants and explosives, because these emissions are already contained in the validated database (Reference 22) and will be input into the Health Risk Assessment from that database.

8.3 EMISSIONS DATA, ENVIRONMENTAL FATE FACTORS (EFF)

The CCS report, presented in Appendix C, provides EFF for metals in:

- Propellants and explosives
- Thick wall steel casings and rotating bands
- Thin wall casings such as cartridge casings
- Protective coatings such as paints and platings.

An EFF is defined as the amount of metal emitted as a fraction of the amount of metal originally present. Table C.7 of Appendix C gives recommended EFFs for the above configurations in open detonation and open burning.

We have accepted the recommended EFFs with two exceptions: (1) open detonation of munitions having thick wall steel casings and bronze/brass rotating bands, and (2) open burning of propellants or explosives containing aluminum fuel. The rationale for the exceptions and the accepted values are presented in the next paragraphs.

Rather than using the single value for both thick wall steel casing and the projectile rotating band as presented in Table C.7 of Appendix C, we describe the steel case and the rotating band separately, assigning an EFF for each. Almost all of the metal casings of munitions treated by open detonation at China Lake are classed as heavy wall steel since the thickness of the steel is large compared to the heat transfer calculations presented in Section 7. We treat very few projectiles having rotating bands. So instead of the single value of Table C.7 we instead use the data from Table C.4 of Appendix C to determine the EFFs for the steel casing and the bronze rotating band. For the steel casing, the 0.0067% for manganese (Mn) and the 0.0026% for iron have been averaged to give an EFF of 0.00465% for steel. The Mn and Fe values are averaged to reflect that the emission is particulate steel, not individual emissions of manganese and iron. This average EFF will be used for all steels. Similarly, the two EFFs for the rotating band, 0.015% for copper (Cu) and 0.061% for zinc (Zn), were averaged to give 0.038% for all brass and bronze rotating bands. [Note: Some confusion may arise later. The Health Risk Assessment uses toxicity based on elemental considerations not molecular species. While the Environmental Fate Factors reflect particulate steel and brass emissions, the emission factors used in the HRA must be expressed in terms of weight of a given element emitted.]

The emissions from propellants and explosives containing aluminum powder as fuel have been measured in BangBox tests. The emission factors for the metal oxide products from these metallized propellants and explosives will be presented with the emission factors for the other products for the propellants and explosives and will not be presented in this report. The emission factors in this report are for emissions from the metal casings; the metals from paints, coatings, or platings; and from metal gun projectiles.

The EFFs that are used in this report are given in Table 12.

TABLE 12. Environmental Fate Factors for Metal Emissions.

Treatment	Metal configuration	EFF value
OD	Thin wall casing	1.6%
OD	Thick wall steel casing	0.00465%
OD	Brass/bronze rotating band	0.038%
OD	Painted, coated, plated surface	10%

The EFF values shown in Table 12 are very conservative in determining emission factors for health risk assessment because they were based on results for all air-borne particulates regardless of particle size. The health risk is due to the fine particulates (PM10, PM2.5), not the larger particulates. Because the EFF is based on mass emitted, large particles significantly bias the results in a conservative direction. For example, a 100-micron particle has 1000 times the mass of a 10-micron particle, or it takes 1000 ten-micron particles to have the mass of a 100-micron particle.

8.4 METAL EMISSION VALUES RECOMMENDED FOR USE IN HRA

8.4.1 Approach for Determining Emission Factors

Metal emission factors, encompassing emissions from the metal casings and paints, coatings and platings, will be defined for each family of energetic materials (see Table 1, reproduced here for ease of discussion), using the following approach.

- (1) Identify the family, e.g., family IIC AP/binder/aluminum.
- (2) **To determine the emission factor (lb. of metal emission/lb. of energetic material) resulting from metal casing**, use the following steps.
- (3) Determine the type of munition this energetic material is used in, e.g., rocket motors.
- (4) Determine the typical amount of metal casing for the application identified above, e.g., for rocket motors typically there is 0.4 lbs. of metal/lb. of propellant.
- (5) Determine the EFF for the casing material, e.g., for a steel case use 0.00465%.
- (6) Determine the amount of the element in question in the metal casing, e.g., how many lbs. of Mn in steel/lbs. of steel. For example for 4130 Steel there is 0.4-0.6% Mn or up to 0.006 lbs. Mn/lb. 4130 Steel. There is also 0.80-1.10 % Cr, and 0.15-0.25% Mo. [Note: 4130 Steel is the most common steel used in missile motor casings.]

- (7) Determine the emission factor by multiplying the answers for steps (4), (5), and (6), e.g., the emission factor for Mn in this example is 0.4 lbs. of steel casing/lb. of AP/binder/aluminum propellant x 0.0000465 lbs. Mn emitted/lb. of Mn in steel motor case x 0.006 lbs. Mn/lb. 4130 Steel = 1.12×10^{-7} lbs. Mn emitted/lb. of AP/binder/aluminum propellant. There would also be up to $0.4 \times 0.0000465 \times 0.011 = 2.05 \times 10^{-7}$ lbs. of Cr/lb. propellant, and up to $0.4 \times 0.0000465 \times 0.0025 = 4.65 \times 10^{-8}$ lbs. of Mo/lb. of propellant.

[Note: These values will be used for all steel rocket and missile motors.]

To determine the emissions from paints and plating use the following steps.

- (8) For a bomb, multiply the amount of metals in the coatings, Table 11, by EFF of 10% to get the metals emitted from the coating/bomb. The 1000-pound bomb has approximately 400 pounds of explosive. To obtain emission factors based on pounds of explosive, divide the amount emitted/bomb by 400.
- (9) For a missile warhead, multiply the amount of metals emitted for warhead coatings by 10% to get emissions from coatings/warhead. The Sparrow warhead has 169.5 pounds of explosive, so divide by 169.5. For a missile motor, multiply the amounts of metals emitted from motor coatings by 10%. The Sparrow motor has 90 pounds of propellant.

TABLE 1. Energetic Families.

Explosives		Propellants	
<i>Melt Cast Explosives</i>		<i>Gun Propellants</i>	
A1	TNT based (Comp-B, Cyclotol, Octol)	IA	Single base (NC)
A2	TNT / Aluminum (H-6)	IB	Double base (NC / NG)
<i>Plastic Bonded Explosives (PBXs)</i>		IC	Triple base (NC / NG / NQ)
B1	Nitramine / binder	<i>Rocket/Missile Propellant</i>	
B2	Nitramine / binder / aluminum	IIA	Double base with lead
B3	Nitramine / binder / aluminum / AP	IIB	Double base w/o lead
<i>Other Explosives</i>		IIC	AP / binder / Al
C1	e.g., PbN3, ammonium picrate	IID	AP / binder / Al / nitramines (>50% AP)
Miscellaneous		IIE	AP / binder reduced smoke
P	Pyrotechnics	IIF	Nitramine/energetic binder/Al/ <20% AP
W	Energetic contaminated wastes (ECW)		

8.4.2 Worksheets To Determine Emission Factors

The values presented and discussed in earlier sections have been entered into the spreadsheets of Table 13a and b. The data have been used to calculate the emission factors from metals emitted from the metal casings and from the metals in the platings, paints and coatings. Because there are emission factors for the metals in the propellants and explosives in the validated database (Reference 22), those data will be used in the health risk assessment and are not presented in this report.

TABLE 13a. Emission Factor Calculations for Emissions From Casings.

Family	Application	Emission factor calculation						
		(a)	(b)			(c)	(d)	
		Casing metal/ energetic (lb./lb.)	Composition of metal (percent)			Metal emitted/ metal in case (lb./lb.) (EFF)	Emission factor (lb. metal/lb. energetic)	
	Section 8.2.1	Section 8.2.1 & 8.4.2			Section 8.3	(a)x(b)x.01x(c)		
A1, A2, B2	Bomb	1.5	1035 Steel					
				Fe	99.1	0.0000465	6.91E-05	
				Mn	0.9	0.0000465	6.28E-07	
B1	A-A warhead	0.82	4340 Steel					
				Fe	96	0.0000465	3.66E-05	
				Mn	0.8	0.0000465	3.05E-07	
				Ni	2	0.0000465	7.63E-07	
				Cr	0.9	0.0000465	3.43E-07	
				Mo	0.3	0.0000465	1.14E-07	
B3	A-S warhead	4	4340 Steel					
				Fe	96	0.0000465	1.79E-04	
				Mn	0.8	0.0000465	1.49E-06	
				Ni	2	0.0000465	3.72E-06	
				Cr	0.9	0.0000465	1.67E-06	
				Mo	0.3	0.0000465	5.58E-07	
C1	none							
IA-IC	gun cartridge	3.16	brass					
				Cu	70	0.016	3.54E-02	
				Zn	30	0.016	1.52E-02	
	Primer	0.00678	Lead styph	Pb	0.1848	0.011	1.375E-07	
				Barium nitra	Ba	0.1946	0.011	1.45E-07
				Antimony su	Sb	0.12172	0.011	9.08E-08
				Aluminum	Al	0.08	0.048	2.60E-07
				projectile	2.21	1043 steel	Fe	99
				Mn	1	0.0000465	1.03E-06	
		0.21	Al		100	0.0000465	9.77E-06	
		0.11	powder					
				Mg	50	0.048	2.64E-03	
			Al	50	0.048	2.64E-03		
	0.0021	Zr		100	0.016	3.36E-05		
rotating band	0.063	brass						
			Cu	70	0.00038	1.68E-05		
			Zn	30	0.00038	7.18E-06		
IIA-IIIE	missile motor	0.4	4130 Steel					
				Fe	98.05	0.0000465	1.82E-05	
				Mn	0.6	0.0000465	1.12E-07	
				Cr	1.1	0.0000465	2.05E-07	
				Mo	0.25	0.0000465	4.65E-08	
IIF	none							

TABLE 13b. Emission Factor Calculations for Emissions From Platings, Paints, and Coatings.

Family	Application	Emission factor calculation					
		(a) Energetic per item (lb.)	(b) Metal in coating per item (lb.)		(c) Metal in coating/ energetic (lb./lb.)	(d) Metal emitted/ metal in coating (lb./lb.) (EFF)	(e) Emission factor (lb. metal/lb. energetic)
		Section 8.4.1	Section 8.2.2		(b)/(a)	Section 8.3	(c)x(d)
A1, A2, B2	bomb	400					
			Zn	1.21	0.003025	0.1	3.03E-04
			Cd	0.0264	0.000066	0.1	6.60E-06
			Cr	0.00033	0.00000825	0.1	8.25E-08
B1, B3	warhead	169.5					
			Cd	0.0528	0.000311504	0.1	3.12E-05
			Sr	0.00242	1.42773E-05	0.1	1.43E-06
			Cr	0.00242	1.42773E-05	0.1	1.43E-06
C1	none						
IA-IC	none						
IIA-IIIE	missile motor	90					
			Cd	0.1936	0.002151111	0.1	2.15E-04
			Sr	0.00858	9.53333E-05	0.1	9.53E-06
			Cr	0.00748	8.31111E-05	0.1	8.31E-06
IIF	none						

8.5 VALUES RECOMMENDED FOR USE IN HRA

Table 14 presents the results of the calculations in Section 8.4 metal emission values recommended for use in the HRA for each family.

TABLE 14. Emission Factors for Metal Emissions From Open Detonation of Energetic Material Families.

Family	Application	Emission from case, lbs. X/lb. energetic								Emission from coating						
		Mn	Ni	Cr	Mo	Fe	Zn	Cd	Sr	Cr	Zn	Mg	Al	Pb	Sb	Al
A1	Bomb	6.28x10-7	NA	NA	NA	6.91x10-5	3.03x10-4	6.60x10-6	0	8.25x10-8						
A2	Bomb	6.28x10-7	NA	NA	NA	6.91x10-5	3.03x10-4	6.60x10-6	0	8.25x10-8						
B1	Air-to-air warhead	3.05x10-7	7.63x10-7	3.43x10-7	1.14x10-7	3.66x10-5	0	3.12x10-5	1.43x10-6	1.43x10-6						
B2	Bomb	6.28x10-7	NA	NA	NA	6.91x10-5	3.03x10-4	6.60x10-6	0	8.25x10-8						
B3	Air-to-surface whd	1.49x10-6	3.72x10-6	1.67x10-6	5.58x10-7	1.79x10-4	0	3.12x10-5	1.43x10-6	1.43x10-6						
C1	Primary explosive	NA	NA	NA	NA	NA	NA	NA	NA	NA						
IIA	Missile motor	1.12x10-7	NA	2.05x10-7	4.65x10-8	1.82x10-5	0	2.15x10-4	9.53x10-6	8.31x10-6						
IIB	Missile motor	1.12x10-7	NA	2.05x10-7	4.65x10-8	1.82x10-5	0	2.15x10-4	9.53x10-6	8.31x10-6						
IIC	Missile motor	1.12x10-7	NA	2.05x10-7	4.65x10-8	1.82x10-5	0	2.15x10-4	9.53x10-6	8.31x10-6						
IID	Missile motor	1.12x10-7	NA	2.05x10-7	4.65x10-8	1.82x10-5	0	2.15x10-4	9.53x10-6	8.31x10-6						
IIE	Missile motor	1.12x10-7	NA	2.05x10-7	4.65x10-8	1.82x10-5	0	2.15x10-4	9.53x10-6	8.31x10-6						
IIF	Missile motor	NA	NA	NA	NA	NA	NA	NA	NA	NA						

Family	Application	Emission from cartridge case			Emission from projectile				Emission from rotating band			Emission from projectile fill			Emission from primer			
		Cu	Zn	Mn	Mn	Fe	Al	Zr	Cu	Zn	Mg	Al	Pb	Sb	Al	Ba	Sb	Al
IA	Gun cartridge	3.54x10-2	1.52x10-2	1.03x10-6	1.02x10-6	9.77x10-4	3.36x10-5	1.68x10-5	7.18x10-5	2.64x10-3	2.64x10-3	1.375x10-7	1.45x10-7	9.08x10-8	2.60x10-7			
IB	Gun cartridge	3.54x10-2	1.52x10-2	1.03x10-6	1.02x10-6	9.77x10-4	3.36x10-5	1.68x10-5	7.18x10-5	2.64x10-3	2.64x10-3	1.375x10-7	1.45x10-7	9.08x10-8	2.60x10-7			
IC	Gun cartridge	3.54x10-2	1.52x10-2	1.03x10-6	1.02x10-6	9.77x10-4	3.36x10-5	1.68x10-5	7.18x10-5	2.64x10-3	2.64x10-3	1.375x10-7	1.45x10-7	9.08x10-8	2.60x10-7			

9.0 SUMMARY

China Lake is the US Navy's largest research, development, test and evaluation (RDT&E) facility. In performing its weapons RDT&E mission, China Lake produces significant amounts of explosive hazardous wastes. These explosive hazardous wastes range from small amounts of new energetic molecules to ordnance damaged during testing. For safety reasons these items cannot be shipped off-Center. They are treated on-Center by open detonation (OD) because OD is safe, environmentally clean, capable of treating large amounts in a timely manner, and relatively inexpensive.

Open detonation does result in emissions, and must be permitted under provisions of the Resource Conservation and Recovery Act (RCRA) and the Clean Air Act. The permit processes require a human Health Risk Assessment (HRA) to ensure that the open detonation is performed in a safe, health conscious manner. The HRA considers the emissions produced at the detonation site and the subsequent dispersal to the Center's boundaries, and the health risks at the boundaries. The health risks considered include cancer, acute non-cancer, and chronic non-cancer risks. The China Lake HRA considers (1) emissions from the propellants, explosives, and other energetic materials, (2) emissions from the inert components, and (3) emissions, such as dirt, from the environment.

This reports considers emissions resulting from the metal components; specifically the (1) casings and projectiles, and (2) platings, paints and coatings used to protect the munitions from the harsh marine environment. While the report discusses metallic ingredients present in propellants and explosives, the emissions data for these metals is presented in a separate report describing emissions from propellants and explosives.

Munitions considered include bombs, air-to-air warheads, air-to-surface warheads, missile motors and gun ammunition. For each munition group the amounts, types and composition of the metals in the munition are presented.

The metals can react in various ways and this report discusses the conditions necessary for the various reactions to occur. The open detonation treatment process involves two types of reactions, as discussed in the report: the detonation that is over in microseconds, and the subsequent afterburning that takes seconds.

During the detonation process, the explosive rapidly goes from a solid to high temperature and high pressure gases. These gases cause the casing to expand and fracture forming fragments. These fragments are accelerated and travel at high speeds for several hundreds of feet from the detonation site. Although they are in contact with the hot gases produced by the detonation they are not in contact long enough for significant heat transfer to occur. As a result, the fragments do not reach their melt temperature, and certainly do not reach conditions necessary for vaporization. Results from various detonation tests are presented in the report to illustrate that the casings fragment. Transient heat conduction calculations show that the fragments do not reach the temperatures necessary for significant melting. Analysis of a large fragment from an open detonation test conducted at Socorro, New Mexico showed that the fragment did not reach

the temperatures necessary for melting or vaporization. Very nearly all of the metals in the casing end up as fragments, although very small amount of particulates may be formed.

In order to perform the HRA, emission factors have to be determined. The emission factors reflect the various possible reactions and the various munitions. For each munition group, the emission factor determination considered the amount of metal originally present compared to the amount of energetic material, the type and composition of the various metals, and the amount of metal emitted compared to the amount of metal originally present in the munition. The amount of metal emitted compared to the amount of metal originally present, called the Environmental Fate Factor, was determined for thin-walled casings; thick-walled casings; rotating bands; and platings, paints, and coatings. The results of these analyses are presented in the report, and recommended emission factors presented. The emission factors are very conservative as discussed in the report.

10.0 REFERENCES

1. C. L. Mader. *Numerical Modeling of Detonations*, University of California Press, 1979. 483 pp.
2. M. L. Lindsay and R. McMorris, CH2M Hill, E. E. Baroody, J. W. Watkins, and T. Olsen. "Use of Blimps to Collect In-situ Reaction Products from Detonation Plumes," presented at the 7th Global Demil Symposium & Exhibition, Tulsa, Oklahoma, May 1999.
3. Richard Prober. *Handbook of Environmental Control – Air Pollution*. Boca Raton, FL, CRC Press, Inc., 1980.
4. J. P. Reynolds, R. Dupont, and L. Theodore, *Hazardous Waste Incineration Calculations: Problems and Software*. New York, NY, John Wiley & Sons, Inc., 1991.
5. Eco Services, International. <http://eco-web.com/cgilocal/sfc?a=/editorial/index.html&b=/editorial/01234.html>
6. *CRC Handbook of Chemistry and Physics*, 63rd edition. Boca Raton, FL, CRC Press, Inc., 1982-1983.
7. Brigham Young University. *DIPPR Database*, "Data Compilation of Pure Compound Properties," Design Institute for Physical Property Data, American Institute of Chemical Engineers (AIChE), New York, NY, 2000, <http://dippr.byu.edu>
8. Naval Weapons Center. *Behavior of Aluminum in Solid Propellant Combustion*, by E. W. Price, K. J. Kraeutle, J. L. Prentice, T. L. Boggs, J. E. Crump, and D. E. Zurn. China Lake, Calif., NWC, March 1982. 180 pp. (NWC TP 6120, publication UNCLASSIFIED.)
9. U.S. Environmental Protection Agency. *Emission Factors for the Disposal of Energetic Materials by Open Burning and Open Detonation (OB/OD)*, by William J. Mitchell and Jack C. Suggs. Triangle Park, North Carolina, US EPA, August 1998. (EPA/600/R-98/103, publication UNCLASSIFIED.)
10. Naval Weapons Center. *Terminal Ballistics*, by M. E. Backman. China Lake, Calif., NWC, February 1976. (NWC TP 5780, publication UNCLASSIFIED).
11. M. R. Wagenhals, E. A. Lundstrom, and R. Heimdahl. "Which Threat? Which Response? Or Determining Vulnerability of Weapons to Real World Ballistic Impact Hazards," 1988 *JANNAF Propulsion Systems Hazards Subcommittee Meeting, CPIA Publication 477, Vol. I*, March 1988. p. 139.
12. Naval Air Warfare Center Weapons Division. "Fragment Breakup Testing of BLU-97 Bomblets with PBXN-107 Explosive Fill," by Steve Davis. China Lake, Calif., NAWCWPNS, January 1996. (NAWCWPNS TM 7954, publication UNCLASSIFIED.)

13. W. G. Von Hole and J. J. Trimble. "Shaped Charge Temperature Measurement," *Proceedings Sixth Symposium (International) on Detonation, August 1976, Aberdeen Proving Ground, Maryland, 1976*. Pp. 691-699.
14. J. S. Rinehart and J. Pearson. *Behavior of Metals under Impulsive Loads*, New York, Dover Publications, 1954. 256 pp.
15. J. S. Pearson. "The Working of Metals with Explosives," *Steel, International Review for Development of Uses of Steel*, No. 9 (September 1962).
See also J. S. Pearson. "Metal Working with Explosives," *Journal of Metals*, Vol. 12, No. 9, (September 1960) pp. 673-681.
16. H. E. Otto and S. H. Carpenter. "Explosive Cladding of Large Steel Plates with Lead," *Metals and Materials*, February 1973.
17. B. Crossland and J. D. Williams. "Explosive Welding," *Metallurgical Review*, 1970.
18. M. Stilly and R. Domical. "Adiabatic Shearing," in *Metallurgical Applications of Shock-Wave and High Strain Rate Phenomena*, Chapter 32, 1968.
19. J. E. Kennedy. "Explosive Output for Driving Metal," *Proceedings of the 12th Annual Behavior and Utilization of Explosives in Engineering Design Symposium*, published by New Mexico American Society of Mechanic Engineers, Albuquerque, NM, March 1972, pp. 109-124.
20. Frank Kreith and Mark S. Bohn, eds. *Principles of Heat Transfer*. 4th ed. Harper & Row Publishers, Inc., 1986. 700 pp. (See Reference 8 for a more complete discussion.)
21. "Properties of Iron and Steel," in *Metals Handbook*, ed. by Bruce P. Bardes, et. al. Ninth edition, Vol. 1, American Society for Metals, 1976.
22. Chemical Compliance Systems, Inc. validated database published on Government Cooperative Demilitarization Group Quickplace website, <https://sierra-xb.ran.sandia.gov/gov-co-op>.

**Appendix A
PLATE TESTING**

8010
478300D/
13 Feb 02

MEMORANDUM

From: Fuze Development Branch (D. Wooldridge Code 478300D)
To: Scientific Staff, Engineering Sciences Division (T. AtienzaMoore, Code 4T43A0D)
Subj: PLATE TESTING

1. Plate Testing has been completed for the Open Burn Open Detonation Metals Effort being undertaken by Terry AtienzaMoore. The purpose for this testing was to show that metals are not vaporized in a detonation. Testing was conducted using both mild steel and aluminum. All mild steel witness plates had the sharp edges ground off in an attempt to minimize spalling.
2. The first test was conducted using a 4-inch X 4-inch X 3/8-inch thick mild steel witness plate. The explosive used was an RDX based sheet explosive, Primasheet 2000, which is 0.125-inch thick. The witness plate was weighed and an equal amount of the sheet explosive was cut into 4-inch squares and stacked together. Half the explosive was placed on either side of the witness plate, Figure A.1, and both sides were initiated simultaneously using two Reynolds RP-501 Exploding Bridgewire (EBW) detonators. This test resulted in approximately 1/8-inch to 3/16-inch of material being lost off each of the edges of the witness plate or approximately 39% weight loss (see Figure A.2).

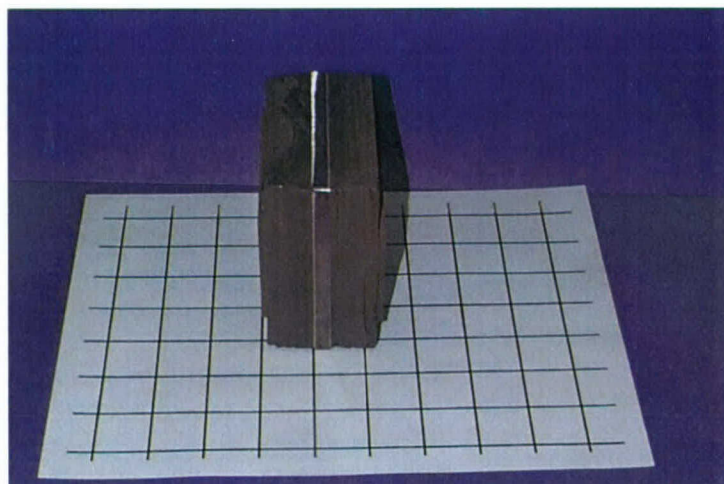


FIGURE A.1. Test #1 Test Item.

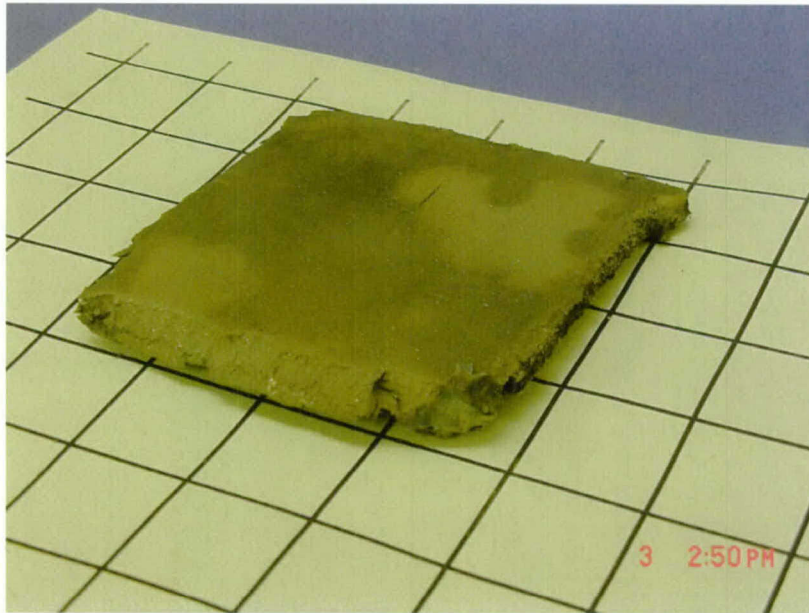


FIGURE A.2. Post-Test Witness Plate (Note Fractured Edges).

3. The second and third tests were conducted using the same mild steel witness plates as the first test. The plates were weighed and that weight was divided by 16 to determine the weight of one square inch of the plate. This weight was then matched by an equal weight of Primasheet 2000 cut into 1-inch squares and stacked together, half centered on either side of the witness plate as shown in Figure A.3. Both sides were initiated simultaneously using two Reynolds RP-501 Exploding Bridgewire detonators as shown in Figure A.4.

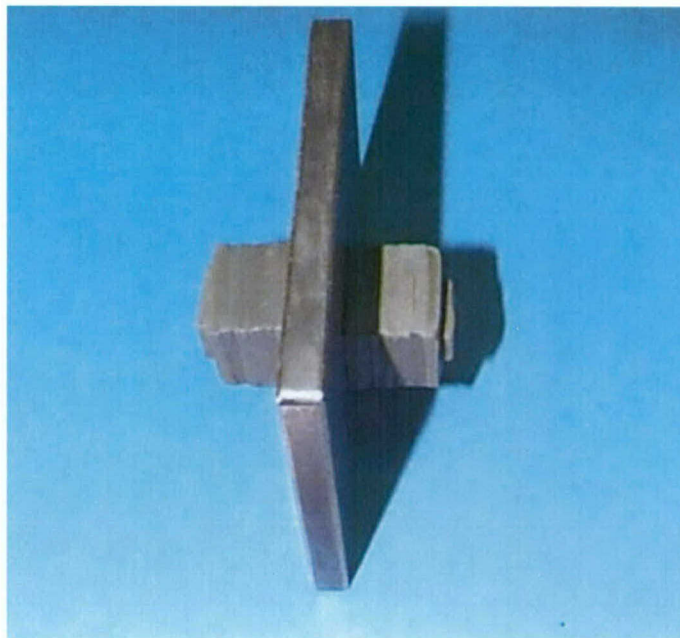


FIGURE A.3. Test Item Tests #2 and #3.

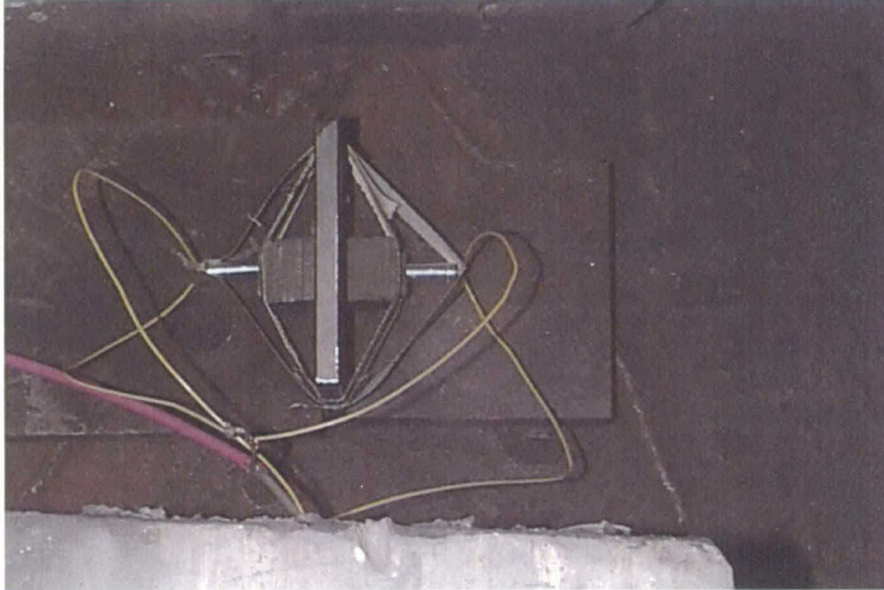


FIGURE A.4. Test Set-up Showing Detonator Placement.

4. For test number 2, the witness plate weighed 750.4 grams or 46.9 grams/in². Half this amount of Primasheet 2000 was placed on either side of the witness plate. The witness plate is shown in Figures A.5 and A.6. The weight of material recovered was 741.6 grams; 8.8 grams were not recovered. The amount of material lost equals 18.76% of the one-inch square we were testing against making the amount recovered 81.24%.

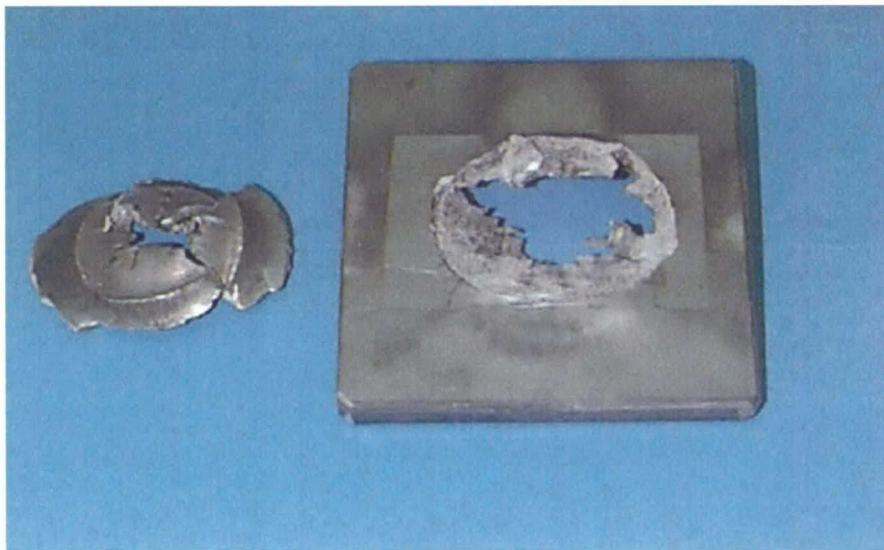


FIGURE A.5. Test #2 Witness Plate Side "A".

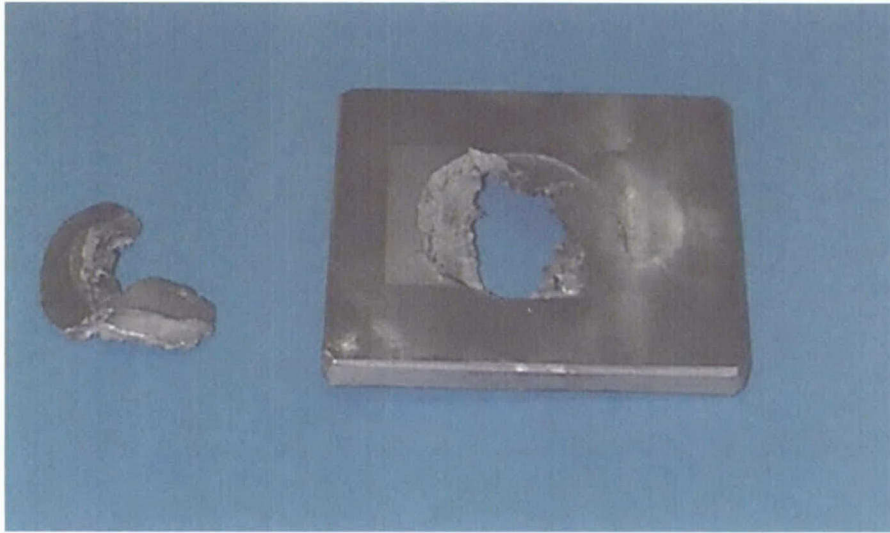


FIGURE A.6. Test #2 Witness Plate Side "B".

5. For test number 3, the witness plate weighed 742.2 grams or 46.4 grams/in². Half this amount of Primasheet 2000 was placed on either side of the witness plate. The witness plate is shown in Figures A.7 and A.8. The weight of material recovered was 743.0 grams or 0.8 gram more than we started with. One reason for this extra material might be that fragments from the previous test had been lodged in the wall of the bay and then dislodged by the shock from this test.

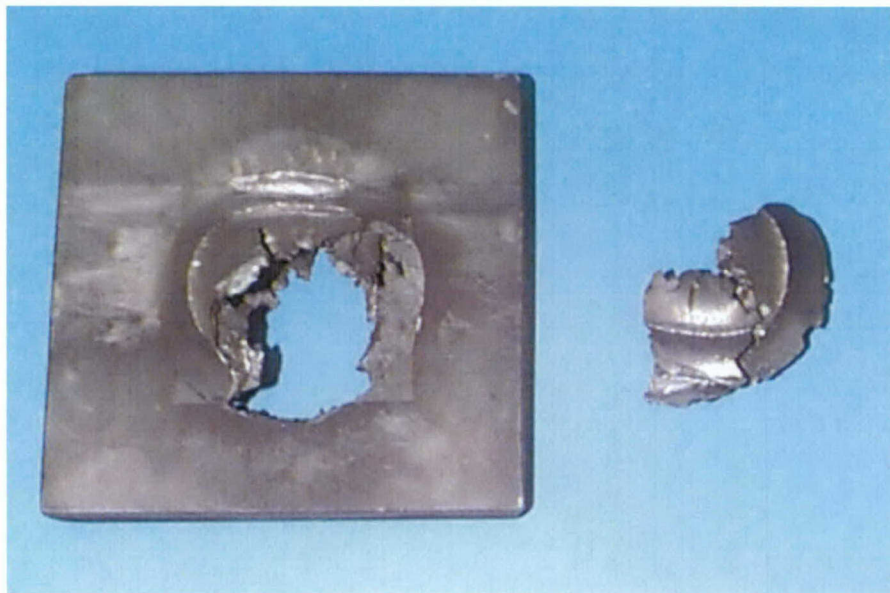


FIGURE A.7. Test #3 Witness Plate Side "A".

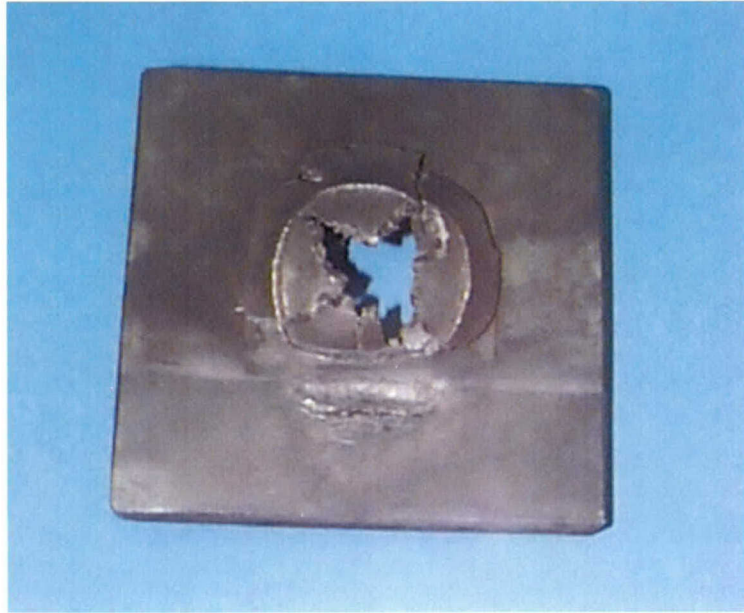


FIGURE A.8. Test #3 Witness Plate Side "B".

6. The fourth test was conducted using a 3-inch X 6-inch X 7/16-inch aluminum witness plate. An aluminum plate was used for this test to eliminate fragments from one test being mistaken for fragments from another. Once again, one square inch of the plate weight was matched by the weight of Primasheet 2000 cut into 1-inch squares and stacked together, half centered on either side of the plate. Both sides were initiated simultaneously using two Reynolds RP-501 Exploding Bridgewire detonators. The test set-up is shown in Figures A.9 and A.10.

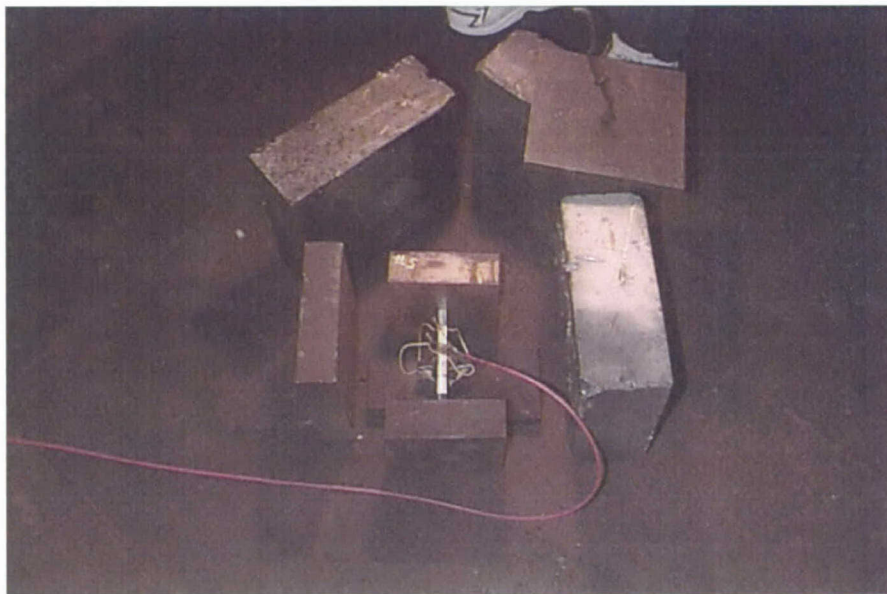


FIGURE A.9. Test #4 Set-up.



FIGURE A.10. Test #4 Set-up with Cover Plate in Place.



FIGURE A.11. Test #4 Witness Plate Side "A".



FIGURE A.12. Test #4 Witness Plate Side "B".

7. For test number 4, the witness plate weighed 383.47 grams or 21.3 grams/in². Half this amount of Primasheet 2000 was placed on either side of the witness plate. The witness plate is shown in Figures A.11 and A.12. The weight of material recovered was 381.56 grams; 1.91 grams were not recovered. The amount of material lost equals 8.97% of the one-inch square we were testing against making the amount recovered 91.03%. There was more material recovered from the bay but the very fine particles could not be separated from the dirt and other contaminants.

8. The fourth test conducted provided the most reliable results since materials recovered from this test and those from other tests could be separated out with the greatest amount of reliability. It is obvious that material from test #2 was recovered after test #3. If we look at tests #2 and #3 combined we are better able to determine the percentage of material actually recovered. If we were to combine the weights of material not recovered in both tests, (8.8 - 0.8 = 8 grams), and divide that by the combined weights of one square inch of both witness plates (46.9 + 46.4 = 93.3 grams) we end up with 91.5% recovered weight. Not only are these results more accurate than when the data from each is considered separately, but they also better track the results obtained in test #4.

9. Further testing of very small amounts of metal and explosives could be done inside a small test chamber of some kind eliminating the possibility of lost material. This would make the results more accurate and reliable in my opinion. If you have any questions about the results of this testing, contact Danny Wooldridge at (760) 939-7588 or e-mail: daniel.wooldridge@navy.mil.

DANNY WOOLDRIDGE

Copy to:
478300D (Wooldridge, files)

Written by: D. Wooldridge, Code 478300D, 939-7588
Typist: J. Beck, 939-7618, 13 Feb 02

Appendix B
ANALYSIS OF SOCORRO FRAGMENT

8800
476500D/XXX
11 June 03

MEMORANDUM

From: Marc Pepi, Joe Hibbs, Katie Wells, Materials Engineering Branch (Code 476500D)
To: Terry Atienzamoore, Engineering Sciences Division (Code 4T43A0D)
Via: Head, Materials Engineering Branch (Code 476500D)

EXECUTIVE SUMMARY. A fragment of steel from a detonated M107 projectile was examined in order to determine whether the temperature produced by the explosion was extreme enough to melt the bronze rotating band. There was an environmental concern that the detonation temperature may have been high enough to melt and/or vaporize the bronze alloy. Extensive metallographic analysis, hardness testing and scanning electron microscopy were conducted in an attempt to determine the temperature imparted on the projectile. Based on the results of this testing and examination, as well as information provided by the probable manufacturer of this ordnance, it was determined that the temperature reached most likely did not approach the melting point of the bronze rotating band.

INTRODUCTION. A fragment from an M107 155mm high explosive (HE) projectile steel casing was examined utilizing metallographic examination, microhardness testing and scanning electron microscopy. The purpose of this analysis was to determine, if possible, the maximum temperature attained during explosion, and whether this temperature was high enough to melt the bronze rotating band associated with the projectile case. The original fragment was approximately 19-inches long and is shown in Figure B.1. Evidence of the smeared bronze is shown in Figure B.2. This fragment of steel was sectioned into six separate samples (three through the bronze smear and three away from the smearing), and denoted as Bronze/Steel samples 1 through 3 and Steel samples 1 through 3, respectively, within the context of this report. The Defense Ammunition Center (DAC) created this fragment during detonation of excess ordnance at the New Mexico Institute of Mining and Technology, Socorro, New Mexico. The ordnance was stacked in the shape of a pyramid, with a certain number of projectiles detonated (exact number unknown at the time of this writing). This detonation set off a chain reaction, exploding the remaining ordnance by a process known as "sympathetic detonation". It was unknown at the outset whether the fragment under investigation originated from a detonated projectile, or a projectile subjected to sympathetic detonation.

The HE projectile is used principally for fragmentation and blast effects, and the body is comprised of AISI 1045, 1046 or 1050 Steel, depending on the manufacturer. The engineering drawing material requirements for the projectile are listed as follows (Reference B.1):

Hot-forged carbon steel, hot-rolled, semi-finished forging quality, non-resulfurized, per ASTM A711. Steel quality shall be equal to or better than macrograph standards S3, R3, C3 or ASTM E381. The use of strand cast steel permitted in accordance with the requirements of MIL-S-70703, Class I, II; Type A: hot forge.



FIGURE B.1. Original Fragment from the Exploded M107 Ordnance. Reduced ~67%.



FIGURE B.2. Exterior Surface of Fragment Showing Smeard Bronze from the Rotating Band. Reduced ~67%.

The likely manufacturer of this projectile provided the following information regarding processing (Reference B.2); the AISI 1046 Steel is austenitized at 1550°F, quenched in slow/medium oil (internally and externally quenched) and tempered at 980°F. The expected microstructure from this process is mostly pearlitic/ferritic with occasional bands of martensite, especially towards the nose section. The part is forged from a billet, heated and extruded through mandrels and punched. Uniform grain flow can be expected from the base to the nose. The interior is left as forged, while the exterior is machined. The part should exhibit a final hardness in the lower 20's HRC.

RESULTS OF EXAMINATION

Metallographic Examination (Bronze/Steel Samples). Each of these three samples were metallographically prepared and subjected to subsequent examination. The bronze layer was

featureless in the as-polished condition. The samples were subsequently etched with 2% nital. Areas of “waviness” in the steel was noted, as well as shear bands within the steel which were consistent with the explosive force upon detonation. One of the samples exhibited a feature similar in appearance to solid-phase mixing, a condition whereby metal-to-metal contact has resulted in excessive adhesive wear and material transfer without melting (common in galling failures). These samples were subsequently immersed quickly in concentrated nitric acid (HNO_3) in order to examine the structure of the bronze surface layer. The bronze layer atop these specimens contained equiaxed grains, with evidence of recrystallization at the surface. Recrystallization generally occurs as a result of annealing this alloy between the temperatures of 800 – 1450°F. At higher magnification, there was evidence of what appeared to be the effect of shock on the structure of the bronze (distortion and twinning). The distortion took the form of a “feathery” structure within the bronze (Figure B.3). This structure was not consistent with the “needle-like” structure characteristic of dendrites, expected to be present had the bronze melted and re-solidified. As such, it was determined that the bronze most likely had not melted.



FIGURE B.3. Deformed Structure Noted Within the Bronze. Equiaxed grains were also noted. Etchant: Concentrated HNO_3 . Original mag. 500x.

Metallographic Examination (Bronze/Steel Samples). Steel samples away from the bronze layer were prepared in an effort to establish the temperature experienced by the fragment, and to be able to state with confidence that the bronze had not melted. These as-polished steel samples were immersed in a 5% picral etchant, showing seven distinct microstructural features. These included:

- A microstructure of pearlite and grain boundary ferrite (depicted as “original” structure herein),
- Elongated “original” grains,
- Shear banding,

- A layer of fine white grains along the exterior surface of each steel sample, most likely untempered martensite,
- A layer of decarburization (acicular to blocky ferrite) along the interior surface of the projectile body,
- Either the bainitic phase, or Widmanstätten structure,
- Forming flow lines more prominent towards the interior wall,
- A layer of tempered martensite on the highly deformed steel sample.

Figures B.4 through B.10 display these seven distinct microstructural features noted within the steel samples, respectively. These micrographs typify the representative features observed on each sample, and any features different than these are displayed along with the individual sample characterization. The pearlite and ferrite microstructure (Figure B.4) is the structure expected after the initial heat treatment of the projectile body, and was predominant throughout each of the steel samples examined. Regions of elongated grains (Figure B.5) were also observed on each of the samples mostly associated with shear bands, or highly deformed regions of the samples, where the original grains had been "work-hardened". Shear banding took the form of deformation bands (dark-etching), as shown in Figure B.6. These shear bands emanated from the exterior wall. White-etching grains were observed along the exterior surface of each sample (Figure B.7). These grains were most likely the result of aggressive machining during manufacturing that produced enough heat to transform many of the surface grains to untempered martensite. These grains were sporadic, i.e., they did not form a complete white layer. Another possibility is that the surface temperature was exposed to the re-austenitizing temperature (at least 1440°F) as a result of the explosion, forming austenite that subsequently transformed to untempered martensite. This was probably not the case, since retained austenite is not common to this alloy, as it is forced to transform to another phase (insufficient alloying elements are present to retain the austenite). Figure B.8 shows the ferrite layer noted on the interior surfaces of each of the steel samples examined, most likely the decarburized as-forged surface that was not as affected by the heat and energy of detonation. Figure B.9 contains evidence of the bainitic phase, or possibly even Widmanstätten structure, both of which have been noted by the manufacturer on projectile samples during normal processing operations. Figure B.10 shows an example of the original forming flow lines, emanating from, and following the interior surface. These flow lines were consistent with prior forging during manufacturing, since this region represented the center of the original billet where chemical segregation could be expected. One of the steel samples was highly twisted and deformed, and contained numerous shear bands, and regions of deformed grain structure. Figure B.11 schematically illustrates the typical features noted on the samples. A marked microstructural difference was noted on the highly deformed sample, in the outer layer of what used to be the exterior surface. It etched much darker than the previous two steel samples, and seemed to contain less untempered martensitic grains. Additionally, this layer transformed to what appeared to be tempered martensite toward the other end of the sample (Figure B.12).



FIGURE B.4. Microstructure of Pearlite with Ferrite Islands Along the Grain Boundaries, Which was Predominant on Each of the Steel Samples Examined. This structure was most likely formed during original processing. Original mag. 1000x.



FIGURE B.5. Microstructure of Elongated Pearlite with Ferrite Observed Mainly Closest to the Exterior Surface of the Projectile Body. Compare to Figure B.15. This structure was most likely formed as a result of the energy produced during detonation. Original mag. 1000x.



FIGURE B.6. Shear Bands Noted on the Edge of Steel Sample 3. Note the deformed grains adjacent to these bands. Etchant: 5% Picral. Original mag. 100x.

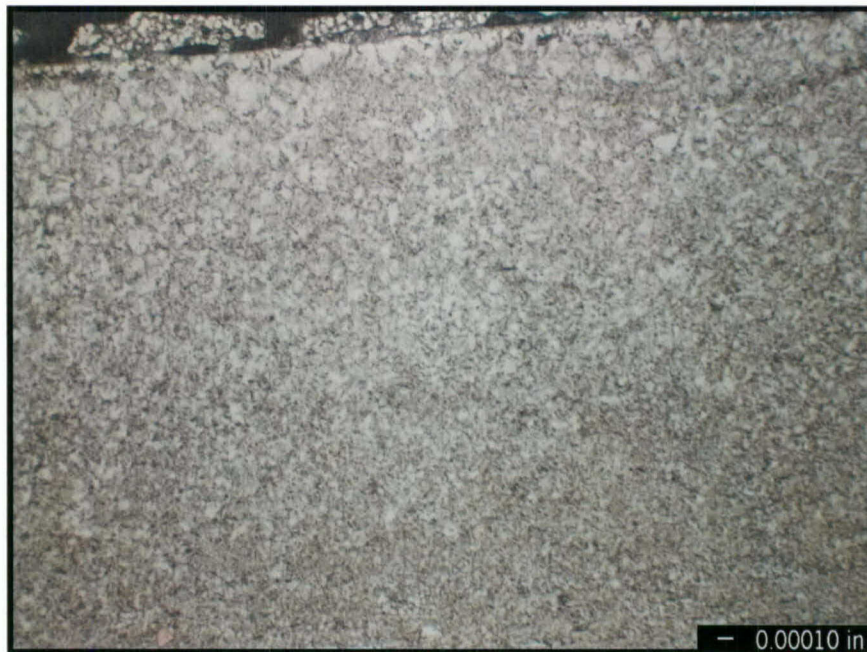


FIGURE B.7. Untempered Martensitic Grains (White) Observed Along the Exterior Surface of the Projectile Body. Original mag. 1000x.

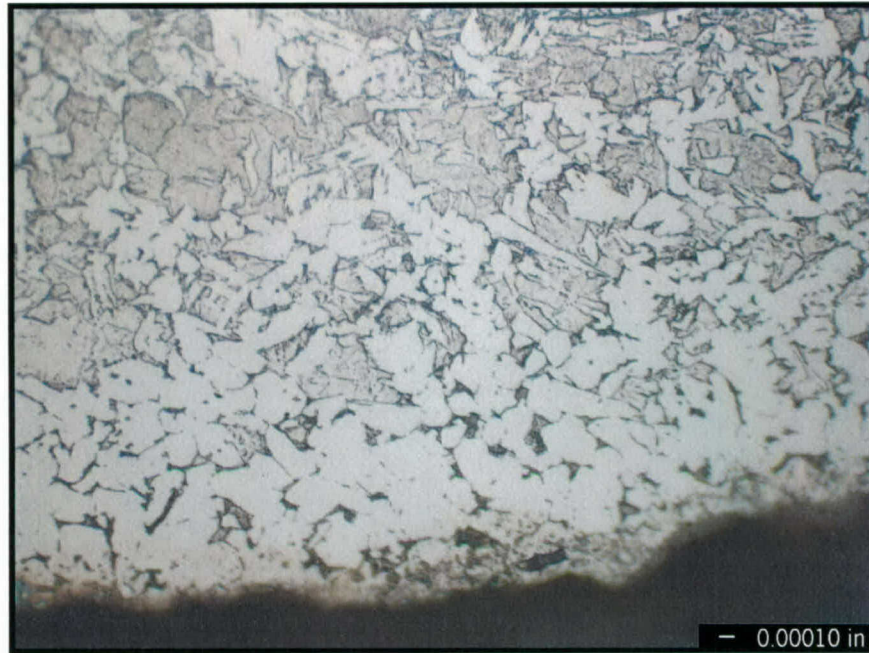


FIGURE B.8. Layer of Decarburization Consisting of Blocky and Acicular Ferrite Grains along the Interior Surface of the Projectile Body. Note the larger size (compared to those grains in Figure B.7). Original mag. 1000x.

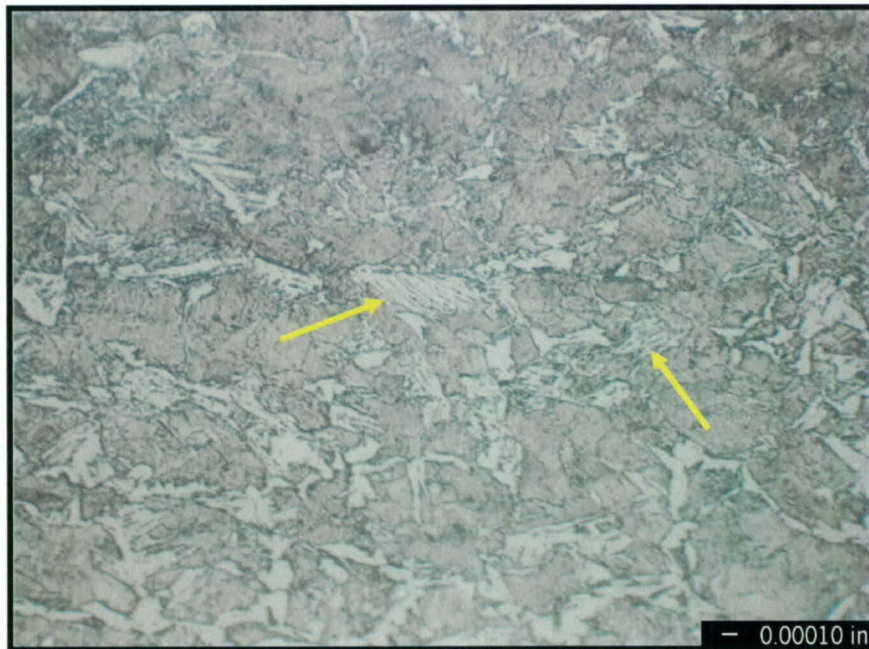


FIGURE B.9. Bainite or Widmanstätten Structure, Noted in Various Regions. Original mag. 1000x.



FIGURE B.10. Flow Lines Noted Emanating from the Interior Surface of the Projectile Body, the Result of Prior Forging. Original mag. 200x.

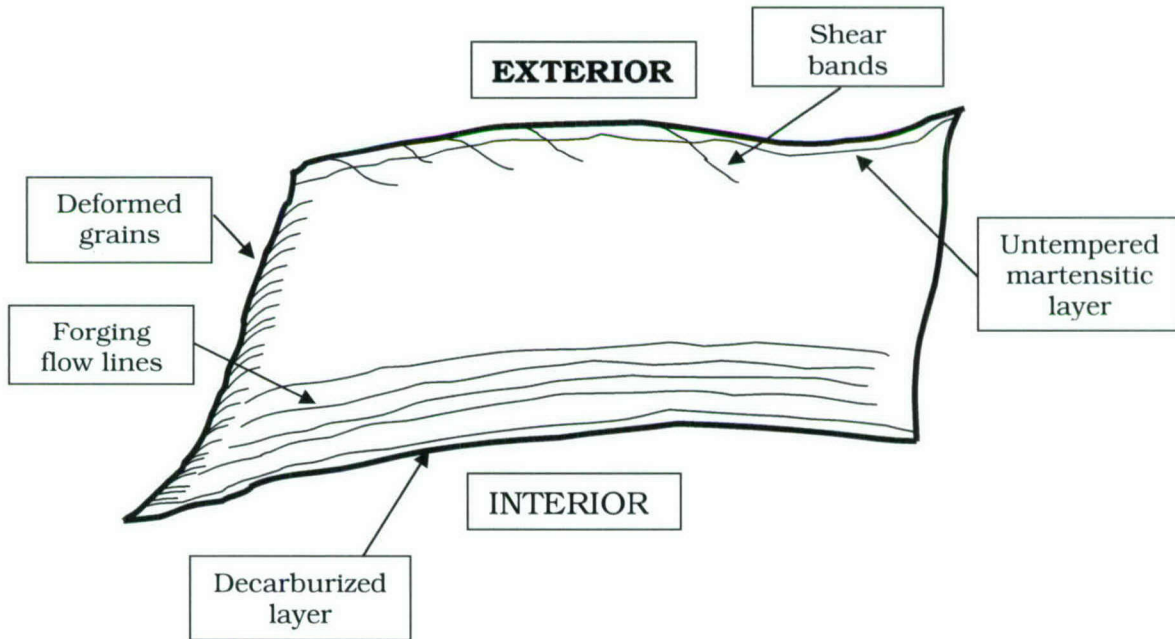


FIGURE B.11. Schematic Illustrating Representative Metallographic Findings (not drawn to scale).

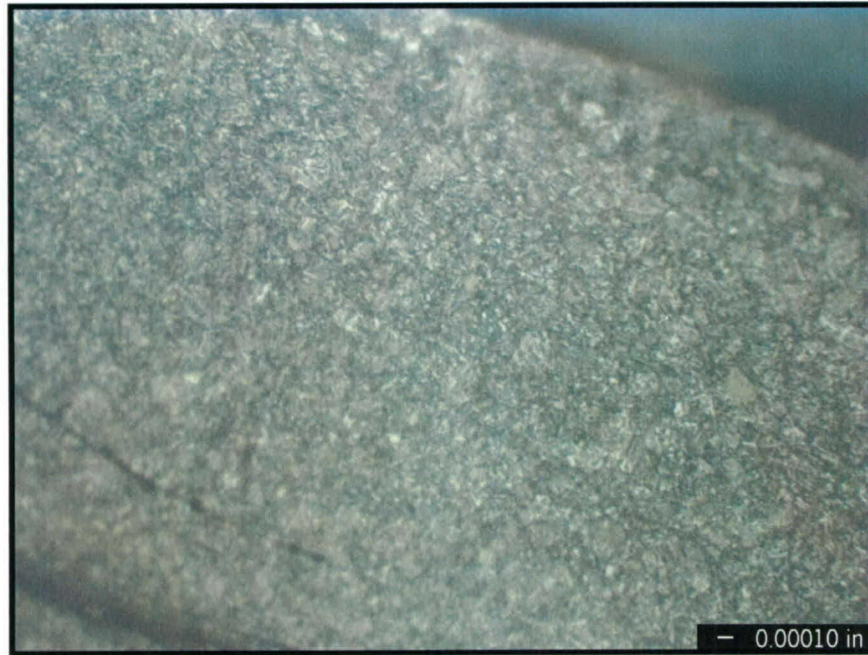


FIGURE B.12. Tempered Martensite Shown in the Outer Layer of the Highly Deformed Sample (compare to the surface layer shown in Figure B.7). Etchant: 5% Picral. Original mag. 1000x.

Chemical Analysis. A section of the steel fragment was analyzed for elemental composition in an effort to confirm the chemistry. As mentioned previously, this projectile can be fabricated from either AISI 1045, 1046 or 1050 Steel. Carbon and sulfur contents were determined through combustion, while the remaining elements were determined through inductively coupled plasma spectroscopy (ICP). As the results show (Table B.1), the composition compares favorably with either AISI 1045 or 1046 Steel. The likely manufacturer stated that the results compared favorably to the target values established at their plant for AISI 1046, but since AISI 1045 has an overlapping composition, there was still a measure of uncertainty.

TABLE B.1. Chemical Analysis, Weight Percent.

Element	Fragment	AISI 1045	AISI 1046	AISI 1050
Carbon	0.47	0.43 – 0.50	0.43 – 0.50	0.48 – 0.55
Manganese	0.86	0.60 – 0.90	0.70 – 1.00	0.60 – 0.90
Phosphorus	0.009	0.040 max. typ.	0.040 max. typ.	0.040 max. typ.
Sulfur	0.022	0.050 max. typ.	0.050 max. typ.	0.050 max. typ.
Chromium	0.01	N/A	N/A	N/A
Copper	0.02	N/A	N/A	N/A
Molybdenum	<0.01	N/A	N/A	N/A
Nickel	0.01	N/A	N/A	N/A
Silicon	0.25	N/A	N/A	N/A
Iron	balance	balance	balance	balance

Microhardness Testing. Microhardness testing was conducted within four of the different microstructures mentioned earlier (as well as the martensitic layer on the deformed sample). Each of these regions displayed varying hardness levels, as the data in Tables B.2 through B.4 show (for steel samples 1 through 3, respectively).

TABLE B.2. Steel Sample 1 Microhardness Results,
Knoop Indentor, 500gf load, Converted to HRC.

Reading	Exterior surface – untempered martensite	“Original” structure pearlite/ferrite	Deformed “original” structure	Interior surface – decarburized (ferrite)
1	448.8 (44)	345.0 (34)	402.7 (40)	328.3 (32)
2	443.8 (43)	330.5 (33)	415.2 (41)	297.6 (28)
3	440.3 (43)	337.9 (33)	411.4 (41)	267.4 (23)
4	441.0 (43)	340.2 (34)	443.1 (43)	280.7 (25)
5	456.0 (44)	340.7 (34)	409.5 (41)	303.9 (29)
6	422.9 (42)	348.8 (35)	430.1 (42)	282.1 (26)
7	405.8 (40)	345.0 (34)	428.1 (42)	276.5 (25)
8	373.0 (37)	355.8 (35)	422.9 (42)	262.5 (22)
9	393.8 (39)	341.6 (34)	424.2 (42)	270.7 (24)
10	415.2 (41)	340.2 (34)	432.8 (43)	274.4 (24)
11		340.7 (34)	432.8 (43)	
12		354.3 (35)	417.7 (41)	
13		355.8 (35)	410.7 (41)	
14		345.9 (34)	412.0 (41)	
15		347.4 (35)	413.9 (41)	
Average	424.1 (42)	344.7 (34.2)	420.5 (41.6)	284.4 (25.8)

TABLE B.3. Steel Sample 2 Microhardness Results
Knoop Indentor, 500gf load, Converted to HRC.

Reading	Exterior surface – untempered martensite	“Original” structure pearlite/ferrite	Deformed “original” structure	Interior surface – decarburized (ferrite)
1	422.9 (42)	374.1 (37)	376.8 (38)	296.1 (28)
2	382.9 (38)	362.4 (36)	368.2 (37)	298.4 (28)
3	450.2 (44)	359.3 (36)	378.4 (38)	290.1 (27)
4	421.6 (42)	356.8 (35)	381.8 (38)	277.9 (25)
5	417.7 (41)	360.4 (36)	407.0 (40)	286.7 (26)
6	412.6 (41)	370.3 (37)	384.0 (38)	297.2 (28)
7	429.5 (42)	365.5 (36)	388.0 (39)	319.1 (31)
8		375.2 (37)	379.6 (38)	
9		363.4 (36)	408.9 (40)	
10		360.4 (36)	379.0 (38)	
11		354.3 (35)	401.5 (40)	
12		357.3 (36)	396.8 (39)	
13		365.5 (36)	386.9 (38)	
14		374.1 (37)	415.2 (41)	
15		366.1 (37)	401.5 (40)	
16			390.9 (39)	
17			405.8 (40)	
18			377.9 (38)	
Average	419.6 (41.4)	364.3 (36.2)	390.5 (38.8)	295.1 (27.6)

TABLE B.4. Steel Sample 3 Microhardness Results,
Knoop Indentor, 500gf load, Converted to HRC.

Reading	Exterior surface – untempered martensite*	Exterior surface – tempered martensite*	“Original” structure pearlite/ferrite	Deformed “original” structure	Interior surface – decarb. (ferrite)
1	295.3 (28)	345.4 (34)	365.5 (37)	369.8 (37)	289.3 (27)
2	306.3 (29)	326.1 (32)	367.6 (37)	381.2 (38)	287.5 (27)
3	299.5 (28)	321.3 (31)	366.6 (37)	367.6 (37)	283.9 (26)
4	291.9 (27)	308.7 (30)	363.4 (36)	367.6 (37)	288.2 (27)
5	284.6 (26)	302.7 (29)	362.9 (36)	369.2 (37)	281.4 (26)
6	275.4 (25)		355.8 (36)		260.6 (22)
7	298.8 (28)		363.4 (36)		267.4 (23)
8	307.1 (29)		354.8 (35)		266.4 (23)
9	291.5 (27)		362.4 (36)		252.0 (20)
10	299.5 (28)		362.9 (36)		256.9 (21)
11			376.2 (38)		251.1 (20)
12			364.5 (36)		274.4 (24)
13			379.6 (38)		265.8 (23)
14			371.9 (37)		255.0 (21)
15			364.5 (36)		269.0 (22)
Average	295.0 (27.5)	320.8 (31.2)	365.5 (36.5)	370.7 (37.2)	269.9 (23.5)

* - Readings were measured closer to the edge than that recommended in ASTM E384, to fit within the desired region. Results may have an inherent error associated with this fact.

Since the hardness of these phases is paramount to understanding the temperatures that may have been attained during the explosion, a few of the areas on these steel samples were scrutinized. These areas included the region containing the untempered martensite, the decarburized layer and the tempered martensite region of Steel Sample 3. This was necessitated since it was noted that some of the readings performed in fulfilling Tables B.2 through B.4 were not exactly within the area of concern, based on thin layers, small grains, etc. Hence, a 50gf load was used with the Knoop microhardness test, to check the accuracy of the previous readings. Caution should be used when converting Knoop readings to Rockwell readings below 500gf loads, but it was believed the advantage to be gained highly outweighed this concern. Table B.5 includes the results of readings taken at 50gf.

The following describes the results of microhardness testing (incorporating the results of Table B.5):

- “Original” Structure of Pearlite/Ferrite. According to the likely manufacturer, this is the structure to be expected from the manufacturing of this projectile. The hardness range of 33 – 38 HRC exceeded the hardness to be expected from the prior tempering cycle at 980°F, which would yield a hardness range from 20 - 26 HRC. It is surmised that the shock wave may have played a role in this increase.
- Work Hardened Pearlite/Ferrite. This structure was most likely the result of the explosive force, since it was mainly associated with, and located adjacent to shear banding and highly deformed areas. It basically consisted of flattened “original” grains. The hardness range of 37 – 43 HRC was most likely achieved by the work hardening that took place.

- Untempered Martensitic Grains on the Exterior Surface. The microhardness within this layer of untempered martensitic grains along the exterior surface ranged from 37 to 44 HRC, using the 500-gf load. At 500gf load, the indent essentially took an average between the untempered martensite and underlying matrix. Readings performed at 50gf load (53 – 55 HRC) reveal a hardness more in line with the hardness expected of untempered martensite, since care was taken to attempt to place the indent close to within these individual grains. The actual readings were slightly lower than the ~61 HRC expected of untempered martensite at this carbon level. This was attributed to readings still not falling completely within the individual untempered martensitic grains.
- Tempered Martensitic Grains on the Exterior Surface (deformed sample only). The microhardness within this band of grains along the exterior surface ranged from 29 to 34 HRC (500gf load) and 35 to 36 HRC using the 50gf load. Again, it is believed that these 50gf load readings are more accurate, since they fit within the entire layer, unlike the previous readings taken at 500gf. The 35 – 36 HRC range is not unreasonable to expect from the tempering of untempered martensite.
- Decarburized Layer (Ferrite Grains) on the Interior Surface. The likely manufacturer indicated that the interior of the projectile is not machined subsequent to heat-treating, only the exterior. The layer of decarburization is common to this process, and is to be expected. The ferrite grains noted along the interior surface had a hardness range of 22 – 32 HRC using the 500gf load, and a range of 92HRB – 24 HRC using the 50gf load. Again, the 50gf load readings are most likely closer to actual, since these readings were fully contained within the decarburized layer, unlike the 500gf readings. The latter range is typical of that expected from a decarburized surface layer.

TABLE B.5. Region-Specific Microhardness Results
Knoop Indentor, 50gf load, Converted to HRC (or HRB where noted).

Reading	Exterior surface – untempered martensite (steel sample 2)	Exterior surface – tempered martensite (steel sample 3)	“Original” structure pearlite/ferrite (steel samples 2 and 3)*	Interior surface – decarb. (ferrite) (steel samples 2 and 3)
1	615.4 (54)	352.8 (35)	382.9 (38)	272.4 (24)
2	626.4 (55)	364.1 (36)	379.4 (38)	267.2 (23)
3	601.2 (53)	360.8 (36)	379.4 (38)	236.9 (97 HRB)
4	630.1 (55)	359.2 (36)	386.5 (39)	239.5 (98 HRB)
5	626.4 (55)	349.7 (35)		271.3 (24)
6				250.4 (20)
7				211.4 (92 HRB)
8				263.1 (22)
9				263.1 (22)
10				254.2 (21)
Average	619.9 (55)	357.3 (36)	382.1 (38)	N/A

* - Used for cross referencing earlier 500gf readings

Note: Caution should be used when converting to HRC from less than 500gf loads

Scanning Electron Microscopy. A representative section of the original fragment was analyzed using a scanning electron microscope (SEM). Of particular interest was the edge of the sample.

Bourne, et. al. (Reference B.3) reported the observation of rolled edges on fragments from combinations of different explosives and metals. These smooth, featureless edges are created by a melting and rolling over of sharp edges by the hot detonation gases. This characteristic signifies intense heating imparted to the edge of the steel. The edge of the sample examined under the SEM is shown in Figure B.13 (arrow). Upon closer examination, this rolled edge did not compare to the scanning electron micrograph included within Reference B.3. The most distinct difference, was the presence of morphology, i.e., the rolled edge was not featureless. Figure B.14 shows the edge at higher magnification.

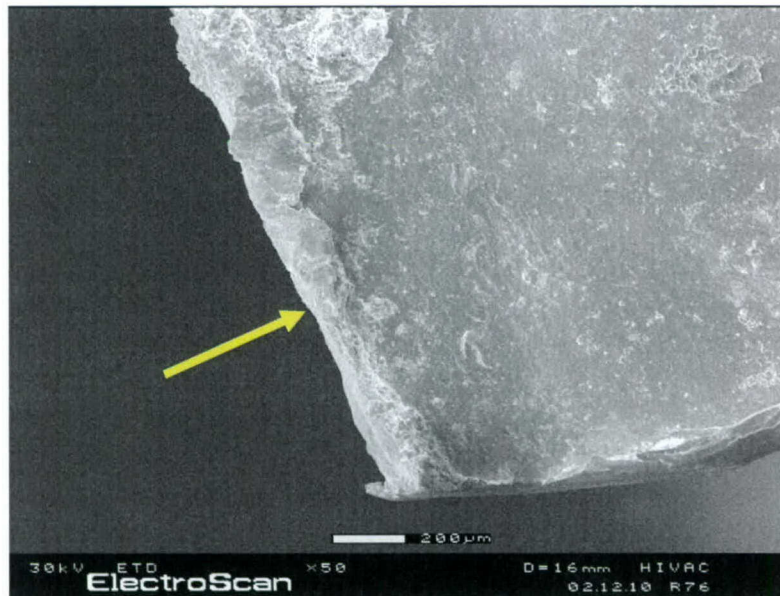


FIGURE B.13. Rolled Edge Noted on a Representative Section of the Fragment.



FIGURE B.14. Magnified View of the Rolled Edge Shown in Figure B.13. The morphology was not consistent with a featureless rolled edge created by intense heating.

As Figures B.15 and B.16 show, evidence of metal smearing was evident at higher magnification. These micrographs show that the edges of the fragment under investigation were deformed most likely by the force of detonation, rather than by intense heating.



FIGURE B.15. An Additional Region of the Rolled Edge Showing Metal Smearing, as Opposed to Melting.



FIGURE B.16. Another Example of Metal Smearing on the Rolled Edge Shown in Figure B.13.

DISCUSSION: Three distinct metallographic effects are produced as a result of dynamic deformation. These include shear banding, twinning and recrystallization. Although evidence of shear banding was irrefutable, there is very low probability that twinning and recrystallization occurred. Twinning has not been observed in steels with higher than 0.2% carbon (Reference B.4), and evidence of recrystallization was not found. If the untempered martensite was present on the exterior of the projectile as a result of prior machining operations (a feature noted previously by the likely manufacturer), recrystallization did not occur.

Typically, shear bands are characterized as either "deformation" bands, or "transformation" bands (Reference B.5) and are usually precursors to crack formation. Transformation bands are usually associated with localized melting, and etch white metallographically. It is believed that the bands noted on these steel samples were predominantly "deformation" bands, based on the dark-etching characteristics. On the steel samples, the banding was noted emanating from the exterior surfaces inward only (where the fragment was not twisted and highly deformed), which was consistent with the findings of J. Pearson et. al. (Reference B.6) and Qingdong et. al. (Reference B.7) who found that for plain wall cylinders, shear fractures initiate at the outer surface and propagate inward.

The bronze rotating band, in conjunction with the rifling of the gun tube imparts spin to the moving projectile (Reference B.8). The rotating band associated with the M107 projectile is fabricated from C22000 bronze (commonly referred to as 220 bronze, or commercial bronze). The nominal composition of this alloy is as follows: 89 – 91% Cu, 0.05% Pb max., 0.05 Fe max., balance zinc. The melting point of this alloy is reported to be 1910°F (Reference B.9), but the alloy softens considerably above 800°F (annealing temperatures = 800 – 1450°F) (Reference B.10). At these elevated temperatures (combined with the pressure or force of the detonation), mechanical smearing of the alloy could have occurred, leaving the bronze-colored remnants noted on the steel fragment. The evidence of solid-phase mixing, grain distortion and twinning, and recrystallization indicated that the bronze might have been severely deformed as a result of the shock, without melting.

Transmission electron microscopy (TEM) and X-ray analysis were beyond the scope of this investigation, therefore, the presence of shock-induced changes in the microstructure (i.e., dislocation densities, etc.) could not be confirmed. Furthermore, there was not a "before explosion" projectile to analyze to make these analyses worthwhile. Based on what was revealed metallographically (accompanied by the background information provided by the likely manufacturer), it appeared as if the shear bands and accompanying deformed grains were the only effect of the shock wave.

The hardness of the steel casing as a result of processing is nominally in the low 20's HRC. The hardness of this phase after detonation was between 33 – 38 HRC. This was a significant increase, accompanied by no apparent change in structure. However, David Lahrman, LSP Technologies (Reference B.11) indicated that oftentimes, and for the alloy under investigation, shock-induced microstructural changes are subtle, and therefore, at least a portion of the hardness increase (if not all) could be attributed to the shock wave. It has been reported (Reference B.12) that for steels having a carbon level of 0.46%, a hardness increase of up to 100HV points could be achieved after being subjected to an explosive force. This difference is

consistent with a "before" hardness of 23 HRC (~255 HV) - which is in the realm of the hardness level of the as-produced projectile - and 36 HRC (~355 HV) - the average of the "original" grains measured herein. TEM and X-Ray studies may be the only way to determine the dislocation density increase in the fragment, but with no "original", undetonated piece of steel to compare the results to, the analysis becomes a moot point.

It was interesting to note that the tempered martensitic layer was observed on the very outer edge of the highly deformed fragment, not connected or subjected to the "heat sink" of the main projectile body. This fact made it clearer that this region may have retained the heat from the explosion longer, thereby providing a "tempering" environment on the untempered martensitic layer.

The theoretical temperature achieved in steel when TNT is detonated behind it is approximately 1225°F (Reference B.13). Although the M107 is loaded with TNT, the correlation between theory and "real-life" is unknown. If this is relatively accurate, it is one more piece of evidence that melting of the bronze rotating band did not occur.

SUMMARY AND CONCLUSIONS: Metallographically, not much evidence was observed showing that the bronze rotating band or steel case was subjected to extremely high temperatures. Based on the overall evidence, including the results of bronze and steel metallography, hardness, SEM, the background information provided by the likely manufacturer and the theoretical temperature achieved in steel in contact with TNT, it seems unlikely that melting of the bronze could have occurred.

SEQUENCE OF EVENTS: The layer of untempered martensite noted on each of the steel samples was formed during exterior machining of the projectile. On a section of the fragment subjected to extreme distortion, the untempered martensite became tempered as a result of the temperature attained during the detonation, and the small cross-section of the fragment (no adjacent heat sink). This temperature would not have melted the bronze rotating band, but may well have been greater than the annealing or "softening" temperature of the alloy (800°F) to produce recrystallization. This temperature is below the austenitizing temperature of the AISI 1046 Steel (1440°F).

REFERENCES

- B.1. Electronic correspondence from Don Carlucci, Picatinny Arsenal, dated 25 November 2002.
- B.2. Conversation with Ken Anderson, Technical Director, Drake Damerau, Chief Metallurgist and Heat Treatment Engineer, Jim Flaherty, Executive Vice President and Jeff Brunoizzi, Vice President of Operations, Chamberlain Manufacturing Corporation, 4 December 2002.
- B.3. B. Bourne, P. N. Jones, and J. A. Markham. "Microstructural Features of Shock-Loaded Metals," Inst. Phys. Conf. Ser. No. 70, Paper presented at 3rd Conf. Mech. Prop. High Rates of Strain, Oxford, 1984, pp. 115-116.

B.4. J. Palczewski and J. Gronostajski. "Steel-18G2A and Steel-14HNMBCu Strengthened by Explosive and Cold-Rolled Deformation," *Journal De Physique III*, Volume 1, October 1991, pp. C3-511 – C3-518.

B.5. T. Z. Blazynski. Explosive Welding, Forming and Compaction, Applied Science Publishers, New York, 1983, p. 37.

B.6. J. Pearson and S. A. Finnegan. "A Study of the Material Failure Mechanisms in the Shear-Control Process," Shock Waves and High-Strain-Rate Phenomena in Metals, Concepts and Applications, Edited by Meyers, M.A and Murr, L.E., Proceedings of International Conference on Metallurgical Effects of High Strain Rate Deformations and Fabrications, 1980, p. 250.

B.7. D. Qingdong, H. Bayi, H. Changsheng, and H. Haibo. "Expansion and Fracture of AISI 1045 Steel Explosive-Filled Cylinders," *Journal de Physique IV*, Number III, Volume 4, September 1994, p. C8-417.

B.8. Weapons Manual FM 6-50, MCWP 3-1.6.23, Chapter 10, "Ammunition," p. 10-1, no date listed, <http://www.adtdl.army.mil/cgi-bin/atd1.d11/fm/6-50/ch10.pdf>, referenced 2 December 2002.

B.9. ASM Metals Handbook, Volume 2, Tenth Edition, "Properties and Selection: Nonferrous Alloys and Special-Purpose Materials," Metals Park, OH, 1990, p. 297.

B.10. Electronic correspondence with Mark Tur, Managing Director, Cole Tubes Limited, Berkshire, UK, dated 11 December 2002.

B.11. Telephone conversation with David Lahrman, LSP Technologies, 10 December 2002.

B.12. T. Arvidsson and L. Eriksson. "Fragmentation, Structure and Mechanical Properties of Some Steels and Pure Aluminum After Shock Loading," Metallurgical Effects at High Strain Rates, edited by Rohde, R.W. et. al., Plenum Press, New York, 1973, p. 611.

B.13. Electronic correspondence from Don Carlucci, Picatinny Arsenal, dated 20 December 2002.

ACKNOWLEDGMENT

The authors would like to thank Ken Anderson, Technical Director; Drake Damerau, Chief Metallurgist and Heat Treatment Engineer; Jim Flaherty, Executive Vice President and Jeff Brunozzi, Vice President of Operations Chamberlain Manufacturing Corp.; Don Carlucci, US Army, Picatinny Arsenal; and David Lahrman, LSP Technologies for their assistance. In addition, thanks are extended to Bob Gerber and Thom Boggs of the Engineering Sciences Division, China Lake, CA, for helpful comments.

Appendix C
CCS METAL EMISSIONS REPORT

PARTICULATE MATTER AND METAL
EMISSIONS FACTORS RECOMMENDED FOR USE IN
HEALTH RISK ASSESSMENT FOR
BURRO CANYON OB AND OD ACTIVITIES

Prepared by
Chemical Compliance Systems, Inc.
Lake Hopatcong, NJ
and
Bill Mitchell and Associates, LLC
Durham, NC

for

Naval Air Warfare Center Weapons Division (NAVAIR)
China Lake, CA

October 1, 2003

1.0 INTRODUCTION

One of the missions of the Naval Air Warfare Center Weapons Division (Center) at China Lake, CA is designing, developing, characterizing and qualifying weapons systems. Because this program involves a wide variety of munition items (e.g., ammunition, bombs, warheads, bomblets, and large rocket motors), the Center generates substantial quantities of wastes containing energetic materials. In addition, for safety reasons, most of these wastes must be destroyed or otherwise rendered harmless (treated) on the Center. For cost and safety reasons, the preferred method of treatment is open detonation (OD) of the waste materials at the Center's Burro Canyon OB/OD facility and the alternative treatment is open burning (OB) in steel pans at the same location.

Historically, the OB and OD activities conducted at Burro Canyon have been conducted in conformance with the terms and conditions of a RCRA Interim Subpart X permit. However, some of the activities recently became regulated under Title V of the Clean Air Act (CAA) and EPA has mandated that the CAA requirements shall replace any identical requirement in RCRA. The Center now wishes to replace this interim permit with a permanent one and to also obtain the required Title V permit. To obtain both permits, the Center must demonstrate through a Health Risk Assessment (HRA) that the disposal of energetic wastes by OB and OD in Burro Canyon will not endanger either human health or the environment.

Many of the energetic wastes treated by the Center contain metals, some of which can be toxic. The predominant exposure pathway for these metals is entrainment within and

transportation off-site by the detonation or burn plume. Therefore, one of the critical inputs the Center needed for the HRA is a credible, representative estimate of the quantities (percentage) of the metals that could possibly be transported off-site in these plumes.

To obtain this data, the Center contacted Chemical Compliance Systems Inc. (CCS), Lake Hopatcong, NJ which had recently reviewed and compiled the available (air) emissions data on OB and OD processes into two databases and then validated the databases in accordance with the procedures specified in the USEPA guidance document entitled: "Procedures for Preparing Emission Factor Documents" (Reference C.1). One of these databases, the OD - Chemical Release Database (OD - CRD), contains emissions factors (EFs) derived from the open detonation of 28 energetic materials and the other, the OB-Chemical Release Database (OB-CRD), contains EFs derived from the open burning of 19 energetic materials. The EFs in the two databases were obtained from DOD-sponsored studies conducted in detonation chambers and on the open range with active USEPA oversight and review. The original EFs were reported either in concentration units or in the traditional EF units, i.e., mass of emission product (analyte) released per mass of explosive material (NEW) detonated or burned. When CCS compiled the emissions data into databases, it converted all concentration unit data into the traditional EF units.

Unfortunately, this traditional unit for reporting OB and OD emission factors does not show the relationship between the mass of the emission product and that of the substance(s) in the energetic material treated which produced the emission product. But this latter relationship is much more appropriate when the emissions factors are to be used as input in a HRA and in preparing many environmental reports, such as Toxic Release Inventory (TRI) reports. To overcome this limitation and to expand the applications of the two EF databases, CCS included an alternate set of emissions factors in the databases. This alternate set of emissions factors, termed Environmental Fate Factors (EFFs), was derived by multiplying the average EF (e.g., kg Pb/kg NEW) by the average NEW detonated or burned and then dividing the product by the mass of the relevant species (e.g., kg Pb) in the material treated. (The primary source of information for the mass of the metals in the materials covered by the two databases was the Munitions Inventory Disposal Action System (MIDAS) database maintained by the Defense Ammunition Center, McAlester, OK. If the material was not listed in MIDAS, then the information was taken from the test report, if it was available.)

In March 2003, the Center contracted with CCS to review the emissions data in the OB-CRD and OD-CRD databases to identify emissions factors the Center could use in the HRA to estimate the quantities of the metals that could be transported off-site in the OB and OD plumes. The contract also required CCS to recommend some emission factors for particulate matter for use in the HRA and to provide a written report containing the following information: the experimental conditions (test conditions) under which the emissions data were obtained, the composition of the materials detonated and burned, and the number of detonation and burn events (trials) used to obtain the emissions data. CCS in turn contracted with Bill Mitchell and Associates, LLC, Durham, NC to assist them in obtaining the emissions data the Center had requested.

This report and its three appendices describe the results of our effort to fulfill the terms of the contract.

2.0 DERIVATION OF RECOMMENDED METAL EFF VALUES FOR THE HRA

Our review of the two databases determined that there were only 36 EFF values in both databases that would be suitable for use in a HRA. Six of these were in the OB-CRD database (three for Al and three for Pb) and the remaining 30 were in the OD-CRD database. In addition, nine of the 30 EFF values in the OD-CRD database had been derived by substituting a value of 1/2 of the emissions test method's minimum detection limit (MDL) for non-detect values. The metals represented by these 30 EFFs were: Al (10), Ba (2, both = to 1/2 MDL), Cd (1), Cu (3), Pb (8, with 4 = to 1/2MDL) and Zn (6, with 3 = 1/2MDL). This limited number of values occurred for several reasons. First, the mass of metals in many of the materials detonated and burned was too small to produce concentrations in the plumes that were measurably greater than the background. Second, many of the descriptions in the test reports reported only the mass(es) of the energetic material(s) in the items treated, the information needed to calculate and report the emissions data using the traditional units.

Brief descriptions of the materials for which metal EFF values were available and the test conditions under which the emissions from these materials were obtained are presented in Tables C.1 (OB) and C.2 (OD). Nineteen of the materials were characterized in 930 m³ hemispherical detonation chambers called BangBoxes (References C.2 and C.3) and the remaining two were characterized in a 4,600 m³ detonation chamber at the Nevada Test Site (References C.4, through C.7). In these tables materials characterized in BangBoxes have identification numbers containing the letters BB and those characterized in the Nevada Test Site chamber have identification numbers containing the letters NTS. (The chemical composition of the test materials and the test conditions under which their emissions were characterized can be found in Appendix C-1 and the procedure used to convert the original emissions data to metal EFF values can be found in Appendix C-2.)

It is well documented that the actual location of the metal in an material detonated or burned plays an important role in determining the quantity of the metal that is released into the plume (References C.2 and C.8 through C.11). Therefore, the EFF emissions data (expressed as the equivalent percentage value) were placed into the following categories which encompass all the matrices in which metals are found in the materials disposed of by OB and OD at the Center (Reference C.11): (a) thick-wall casings, rotating bands and bulky interior metal components (e.g., warheads, projectiles, bombs, rocket motors); (b) thin-walled casings (e.g., small ammunition, bomblets, flares, impulse fuses); (c) protective coatings (e.g., paints, metal plating); (d) metal compound within energetic (e.g., lead azide); and (e) elemental metal in energetic (e.g., aluminum powder). The percentages in each category were then tabulated by treatment process, matrix and metal. The results of this tabulation for the OB EFFs are presented in Table C.3 and those for the OD EFFs are presented in Tables C.4 (Casings and Rotating Bands), C.5 (Coatings) and C.6 (Energetics)

The data in Tables C.3 through C.6 were then used to calculate the arithmetic mean and median values by treatment process (OB, OD) and matrix (i.e., location of the metal) shown in

Table C.7. These values were derived based on the assumption that all the EFF values in a matrix represented an estimate of the percentage of the metal that would be released into the detonation or burn plume. For example, in Table C.4 there are nine values for the thin wall casing category and the mean and median values associated with these nine values are 1.7% and 1.6%, respectively.

Although the number of metal EFF values is small, the values in Table C.7 conform to detonation theory and every day experience. For example, a greater percentage of the metal is released into the detonation plume when the metal is an integral part of an energetic material than when the metal is contained in coating. Similarly, a greater percentage of a metal is released into the detonation plume when the metal is in a thin-wall casing than when the metal is in a thick-wall casing.

TABLE C.1. Description of Items Burned and Test Conditions

Material (see Appendix D)	No. of trials	Test conditions
BB-OB1 (Aluminized Ammonium Perchlorate)	2	A 1.2kg block of propellant was placed in a stainless steel burn pan. Then a flap was cut in the top of the block and an 81-mm propellant bag containing 4g of smokeless powder was placed in the hole along with two electric squibs. The flap was then placed back over the hole and the burn was initiated.
BB-OB2 (MK-6 Composite Propellant)	1	448g of MK-6 propellant chips were placed in a stainless steel burn pan and the burn was initiated using two electric matches that had been inserted into the mix.
BB-OB3 (Double Base Propellant)	2	2.2kg of pelletized propellant was placed in a stainless steel burn pan along with an 81-mm propellant bag containing 4g of smokeless powder and the burn was initiated using an electric squib that had been inserted into the smokeless powder.
BB-OB4 (AA2 Double Base Propellant)	1	454g of AA2 propellant chips and 26.6g of ethyl cellulose were placed in a stainless steel burn pan and the burn was initiated using an electric match that had been inserted into the mix.
NTS-OB1 (Hawk Rocket Motor)	1	Two rocket motors (605kg propellant total mass) were burned simultaneously. The rocket motors burned for approximately 20 seconds. Copper linear-shaped charges and explosive cutting tape were used to split the steel rocket motor cases longitudinally and at both ends and to initiate the burn.
NTS-OB2 (NIKE Rocket Motor)	2	Two NIKE rocket motors were burned in the first trial and four in the second. Each burn lasted approximately 20 seconds. Copper linear-shaped charges and explosive cutting tape were used in each burn to split the steel rocket motor case longitudinally and at both ends and to initiate the burn. The total masses of energetic material burned in the first and second trials were 683kg and 1365kg, respectively.

TABLE C.2. Description of Items Detonated and Test Conditions.

Material (see Appendix D)	No. of trials	Test conditions
BB-OD1 (20 mm HEI Cartridge)	3	3, 20 mm brass (70% Cu/30% Zn) cartridges were placed on a 57g C-4 brick, tied in place with wire and the assembly detonated using an electric blasting cap (EBC).
BB-OD2 (40mm HEI Cartridge)	3	2, 40 mm Cu/Zn clad aluminum-alloy cartridges were placed on a 57g C-4 brick, tied in place with det cord and the suspended assembly was detonated using an EBC.
BB-OD3 (Impulse Cartridge, BBU-36)	3	42 aluminum-alloy cartridges were clustered around a 57g C-4 brick and down with det cord. 18 cartridges were tied to the sides of a 0.5 m length of det cord that had been folded into a 0.25 m length. The two assemblies were detonated simultaneously using EBCs.
BB-OD4 (Impulse Cartridge, M187, ARD-446)	3	10 aluminum alloy cartridges were placed wrapped around a 57g C-4 brick and tied to the brick using det cord. The assembly was detonated using an EBC.
BB-OD5 (Impulse Cartridge, MK-107)	3	5 steel cartridges were placed on 57g brick of C-4 and tied in place with det cord and the assembly was detonated using an EBC.
BB-OD6 (Fuse, FMU-139A/B)	3	One steel-encased fuse was placed between two 28-g, C-4 bricks and the assembly detonated using an EBC.
BB-OD7 (Fuse, FMU-54)	3	One steel-encased fuse was sandwiched between two 28-g, C-4 bricks and the assembly detonated using an EBC.
BB-OD8 (M18A1 Claymore Mine)	3	The steel pellets and 2/3 of the RDX explosive charge were removed from the polystyrene/fiberglass encased mine and the mine was detonated using an EBC.
BB-OD9 (Flare, Red Star, M43A2)	3	3 aluminum alloy-encased flares were tied to a 57g C-4 brick using wire and the assembly was detonated using an EBC.
BB-OD10 (Flare, Red Star, M158)	3	4 aluminum alloy-encased flares were tied to a 57g C-4 brick using det cord and the assembly was detonated using an EBC.
BB-OD11 (Adapter Booster, T45E7)	3	A 10g piece of C-4 was inserted into the steel barrel of the booster cartridge and the assembly was detonated using an EBC.
BB-OD12 (HBX Surrogate)	3	227g of HBX surrogate was placed in a polyethylene bag and the suspended bag was detonated using an EBC and 8g of C-4.
BB-OD13 (Tritonal Surrogate)	1	227g of tritonal surrogate was placed in a polyethylene bag and the suspended bag was detonated using an EBC and 8g of C-4. Three detonation trials were conducted, but only the last detonation went high order. Therefore, only the results from this last detonation were placed in the OD-CRD emissions factor database.
BB-OD14 (Tritonal Surrogate with Ca Stearate)	3	227g of tritonal surrogate containing 2% Ca stearate was placed in a polyethylene bag and the suspended bag was detonated using an EBC and 8g of C-4.
NTS-OD1 (155mm Projectile, M-107)	3	C-4 bricks were placed on each projectile, the bricks were then connected with detonation cord and the assembly was detonated. Three detonation trials were conducted. The first two detonations involved 24 projectiles (27kg C-4) lying in two parallel rows of 12 each. The third detonation involved 60 projectiles (38kg C-4) in which the projectiles were placed in rows containing 15 projectiles with two of the four rows stacked on top of the other two rows.

TABLE C.3. EFFs (Expressed as Percentages) for the Metals in Energetics
Derived from BB and NTS Burn Tests.

Material	Present as element	Present as compound
	Al	Pb
Aluminized Ammonium Perchlorate	5.4%	-
MK-6 Composite Propellant	29%	-
Double Base Propellant	-	63%
NOSIH-AA2 Double Base Propellant	-	136%
Hawk Rocket Motor	33%	-
NIKE Rocket Motor	-	28%

TABLE C.4. EFFs (Expressed as Percentages) for Metals in Casings
and Rotating Bands Derived from BB and NTS Detonation Tests

Material	Donor/ energetic	Thin-wall casing (a)			Thick-wall casing (b)		Rotating band	
		% Al	% Cu	% Zn	% Mn	% Fe	% Cu	% Zn
20mm HEI Cartridge	1:2	-	1.8%	3%	-	-	-	-
40mm HEI Cartridge	1:3	1.6%	-	-	-	-	-	-
Impulse Cartridge, BBU-36	2:1	0.69%	1.3%	3.6%(c)	-	-	-	-
Impulse Cartridge, ARD-446	3:4	0.43%	-	0.56%(c)	-	-	-	-
Flare, Red Star, M43A2	1:2	2.1%	-	-	-	-	-	-
155 mm Projectile, M-107	1:9	-	-	-	0.0067%	0.0026%	0.015%	0.061%

(a) Casing wall less than or equal to 2.3 mm thick.

(b) Casing wall greater than 2.3 mm thick.

(c) ½ MDL value used in calculating percentage.

TABLE C.5. EFFs (Expressed as Percentages) for Metals in Coatings Derived from BB Detonation Tests.

Material	Donor/energetic	% Cu	% Zn	% Cd	Comments
40mm HEI Cartridge	1:3	91%	25%	-	Aluminum casing clad with Cu/Zn coating. Cartridges lying on C-4 brick.
Adapter Booster, T45E7	1:8	8.0%	10%	10%	Steel casing clad with Cu/Zn coating. Donor charge detonated inside barrel.

TABLE C.6. EFFs (Expressed as Percentages) for Metals in Energetics Derived from BB and NTS Detonation Tests.

Material	Donor/energetic	Present as element	Present as compound		Comments
		% Al	% Pb	% Ba	
20mm HEI Cartridge	1:2	1.5%	4.9%	5.2% (a)	Al powder in detonator cup, Ba compound in primer
Impulse Cartridge, MK-107	3:4	-	-	0.23%(a)	Ba compound in primer
Impulse Cartridge, BBU-36A	2:1	-	20%(a)	-	
Impulse Cartridge, ARD-446	3:4	-	0.31%(a)	-	
Fuse, FMU-139AB	1:3	-	107%	-	
Fuse, FMU-54A/B	2:7	-	1.1%(a)	-	
HBX Surrogate	1:28	4.8%	-	-	
M18A1 Claymore Mine	1:50	-	0.19%(a)	-	
Flare, Red Star, M-43A2	1:2	-	6.1%	-	
Flare, Red Star, M-158	2:3	-	0.77(a)	-	
Adapter Booster, T45E7	1:8	0.081%	-	-	Al liner
Tritonal Surrogate	1:28	8.9%	-	-	
Tritonal Surrogate with Ca Stearate	1:27	9.5%	-	-	
155mm Projectile, M-107	1:9	-	0.58%	-	Al liner

(a) ½ MDL value used in calculating percentage.

The last column in Table C.7 presents the metal EFF values we recommend using in the HRA. Considering the small size of the data sets, the median and mean values agree surprisingly well, so either value could be used in the HRA for each treatment/matrix combination. However, in small data sets, the mean value is much more strongly influenced by the distribution of the individual values than is the median value, so the median usually provides the better estimate of

the center of the statistical distribution for the data set (Reference C.12). Therefore, we recommend using the median EFF values for the HRA. Also, because OB events are essentially a series of small scale detonation events occurring on the surface of the energetic material and they produce the same mix of emission products as OD events, we recommend using the corresponding OD median value as the default value in the HRA for those OB matrices in Table C.7 for which there are no data.

TABLE C.7. Arithmetic Mean and Median EFFs for Metals
(Expressed as Percentages) for Each Treatment/Matrix.

Treatment	Location of metal (matrix)	No. of values	Average %	Median %	EFF recommended for HRA
OD	In thin -wall Al, Cu, brass or steel casing	9	1.7%	1.6%	Median value
	In thick-wall steel casing or projectile rotating band	4	0.021%	0.011%	Median value
	On plated, coated or painted surface	5	29%	10%	Median value
	In energetic as compound	11	13%	1.1%	Median value
	In energetic as element	5	5.0%	4.8%	Median value
OB	In thin-wall casing (all types)	None	No data	No data	Use corresponding OD mean as default value
	In thick-wall casing or rotating band	None	No data	No data	Use corresponding OD median as default value
	On plated, coated or painted surfaces	None	No data	No data	Use corresponding OD median as default value
	In energetic as compound	3	75%	63%	Median value
	In energetic as element	3	22%	29%	Median value

3.0 RECOMMENDED PARTICULATE MATTER EMISSION FACTORS FOR THE HRA

The OB-CRD and OD-CRD databases contained PM-10 emissions factors for 29 energetic materials and PM-2.5 emission factors for 9 energetic materials. The PM-10 values were derived in studies conducted in BangBoxes in which 0.2kg quantities of 20 different energetic materials were detonated and 2.2kg of 9 different energetic materials were burned. For all 29 energetic materials, the particulate concentrations were measured using Hi-Vol samplers located in the detonation chamber (Reference C.2).

The PM-2.5 values were derived in studies conducted on the open range at Dugway Proving Grounds (DPG), UT in which 900kg quantities of the four explosives shown in Table C.8 were

detonated at ground level and 2,000 to 3,100kg quantities of the five propellants shown in Table C.9 were open burned in steel pans. An airplane equipped with Hi-Vol sampler filters was used to measure the particulate concentrations in the plumes released by these nine materials (Reference C13). (A detailed description of the energetic materials detonated and burned in the DPG tests, the conditions under which the tests were conducted and the method used to derive the PM-2.5 EFs can be found in Appendix E.)

Table C.10 presents summary statistics for the set of PM-10 and PM-2.5 EFs obtained from the BangBox and ground level detonation DPG tests. Inspection of the data in this table shows that the OD PM-2.5 EFs are greater than the corresponding PM-10 particles. This would be expected because the majority of particles in detonation plumes are soil particles and therefore, particulate EFs derived from detonations conducted on soil would be greater than EFs derived by detonating materials suspended above a steel pit in the concrete floor of the BangBox. In contrast, the mean and median PM-2.5 EFs for the propellant burns are smaller than the PM-10 EFs from the BangBox. But, this is also expected because PM-2.5 is a subset of PM-10 and soil particles were not a significant portion of the particulate matter in either the DPG or the BangBox burn plumes.

For the following reasons, we recommend using the median OD and OB PM-2.5 EFs from the DPG tests in the HRA. First, the soil at the Center has physical and chemical properties very similar to that at DPG and the quantities detonated and burned in the DPG studies are much closer to those used at the Center than are those used in the BangBox studies. Second, particles in the PM-2.5 aerodynamic size range are of higher regulatory concern than those in the PM-10 size range and the percentage of PM-2.5 particles transported off-site would be greater than that for PM-10 particles.

TABLE C.8. Items Burned and Number of Plumes Sampled
During Each Phase of the DPG Field Tests.

Material ID number (see Appendix F)	Overview of test conditions	No. of burn plumes sampled
DPG-OB1	3,175kg quantities of M-30 triple base propellant burned in steel pans (2 3-burn trials)	6
DPG-OB2	3,000kg quantities of a propellant manufacturing residue - A. (A mixture of one aluminized ammonium perchlorate and four double base propellants) burned in steel pans. (1, 2-burn trial)	2
DPG-OB3	2,200kg quantities of propellant manufacturing residue - B. (A mixture of two double base propellants) burned in steel pans. (2, 2-burn trials).	4
DPG-OB4	3,300kg quantities of M-6 single base propellant burned in steel pans. (4, 3-burn trials).	12
DPG-OB5	3,160kg quantities of M-1 single base propellant burned in steel pans. (2, 3-burn trials).	6

TABLE C.9. Items Detonated and Number of Plumes Sampled During Each Phase of the DPG Field Test.

Material ID number (see Appendix F)	Overview of test conditions	No. of detonation plumes sampled
DPG-OD1	900kg quantities of reclaimed TNT were detonated in steel barrels sitting on the ground. (1, 5-detonation trial and 2, 3-detonation trials).	11
DPG-OD2	900kg quantities of reclaimed TNT were detonated in steel barrels suspended 12 m above the ground. (1, 3-detonation trial)	3
DPG-OD3	916kg quantities of bulk Explosive D (picric acid) were detonated in steel barrels sitting on the ground. (2, 3-detonation trials)	6
DPG-OD4	890kg quantities of bulk RDX were detonated in steel barrels sitting on the ground. (2, 3-detonation trials).	6
DPG-OD5	907kg quantities of bulk Composition B (TNT/RDX) were detonated sitting on the ground. (1,2-detonation trial and 2, 3-detonation trials).	8

TABLE C.10. Selected Summary Statistics for the BangBox and DPG Particulate Matter EFs (kg / kg NEW).

Treatment	EF	No. of materials tested	No of plumes sampled	Max. EF	Min. EF	Mean EF	Median EF	EF recommended for HRA
OB	PM-10	9	21	0.91	0.001	0.21	0.019	Median PM-2.5 EF
	PM-2.5	5	28	0.002	0.009	0.012	0.011	
OD	PM-10	20	60	0.60	0.012	0.22	0.18	Median PM-2.5 EF
	PM-2.5	4	34	11.0	7.2	9.2	9.3	

4.0 REFERENCES

C.1. Procedures for Preparing: Emissions Factor Documents. U.S. Environmental Protection Agency, Office of Air Quality Planning and Standards, Durham, NC. EPA Report - EPA 454/R-95-015 (Revised), September 1997.

C.2. Mitchell, W. J. and J. C. Suggs. "Emission Factors for the Disposal of Energetic Materials by Open Burning and Open Detonation (OB/OD)," EPA Report Number EPA/600/R-98/103, August 1998. 130p.

C.3. M. Johnson. "Development of Methodology and Techniques for Identifying and Quantifying Products from Open Burning and Open Detonation Thermal Treatment Methods -

Bang Box Test Series, Volume 1 (Test Summary)," U.S. Army, AMMCOM, Rock Island, IL 61299-6000, January 1992.

C.4. Executive Summary of Phase I Demonstrations - Detonation of Conventional Weapons: 155-mm High Explosive M107 Projectiles. Lawrence Livermore National Laboratory Report Number UCRL-ID-131252 prepared for US Army Defense Ammunition Center, McAlester, OK. July 1998, 38 pp.

C.5. Individual Test Reports, Appendix B, Draft Detonation Summary Report for the Nevada Test Site. Report prepared by Radian International LLC, Oak Ridge, TN, for Lockheed Martin Energy Systems, Inc., Oak Ridge, TN. August 1997.

C.6. Executive Summary of Phase II Demonstrations: The Low-Pressure Rocket Motor Burns in X-Tunnel. Sandia Report Number SAND2000-8202, January 2000. Report prepared for US Army Defense Ammunition Center, McAlester, OK. 34 pp.

C.7. Individual Test Reports, Appendix B, Draft Rocket Motor Summary Report for the Nevada Test Site. Report prepared by Radian International LLC, Oak Ridge, TN, for Lockheed Martin Energy Systems, Inc., Oak Ridge, TN. October 1997.

C.8. M. A. Cook and G. Thompson. "Chemical Explosives - Rocket Propellants," Chapter 19 in Riegel's Handbook of Industrial Chemistry, Seventh Edition. J.A. Kent, Editor. Van Nostrand Reinhold Co., NY, NY. 1974 (pp 570-595).

C.9. D.L. Ornellas. "Calorimetric Determinations of the Heat and Products of Detonation for Explosives; October 1961 to April 1982," Lawrence Livermore Laboratory Publication No. UCRL-52821, University of California, Livermore, CA 94550 (April 1982). Available from the National Technical Information Service, U.S. Department of Commerce, 5285 Port Royal Road, Springfield VA 22161.

C.10. R. R. McGuire and D. L. Ornellas. "Detonation Chemistry: Diffusion Control in Non-Ideal Explosions," Propellants and Explosives, 4, 23-26, 1979.

C.11. T. M. AtienzaMoore, T. L. Boggs, O.E. Heimdahl, D Wooldridge, B. Gerber, L. A. Zellmer and B. M. Mohn. "Preliminary Report - Metals Emissions from the Open Detonation Treatment of Energetic Wastes," Naval Air Warfare Center Weapons Division, China Lake, CA 93555. May 2002.

C.12. J. K. Taylor. "Statistical Techniques for Data Analysis," Lewis Publishers, Inc., Boca Raton, Florida, 1990. pp. 23-28.

C.13. M. Johnson. "Development of Methodology and Techniques for Identifying and Quantifying Products from Open Burning and Open Detonation Thermal Treatment Methods - Field Test Series A, B and C, Volume 1 (Test Summary)," U.S. Army, AMMCOM, Rock Island, IL 61299-6000, January 1992.

Appendix C-1
DESCRIPTION OF THE TEST CONDITIONS AND
MATERIALS USED TO DERIVE METAL EFF VALUES

TEST CONDITIONS USED IN BANGBOX OB AND OD TESTS

Tests OB-1 thru OB-BB4 and OD-BB-1 thru OD-BB-13 were conducted in an inflatable, 930 m³, 16.5 m diameter hemispherical test chamber (BangBox) made from a flexible polyvinyl-coated polyester fabric (Reference C-1.1). Six fans spaced 60° apart located in the BangBox were used to maintain a homogeneous pollutant mix in the chamber while the plume samples were collected. The particulate concentrations in the chamber were measured using two and sometimes three Hi-Vol samplers equipped with Teflon or Teflon-coated quartz fiber filters located in the BangBox. These filter samples were then analyzed for metals, the Teflon filters were analyzed by X-ray Fluorescence and the quartz fiber filters were acid extracted and then analyzed by Inductively Coupled Argon Plasma Emission Spectroscopy (ICP). Sulfur hexafluoride (w SF₆) was used to determine the volume of the detonation and burn plumes generated, so that emissions factors could be calculated. This was accomplished by releasing a known mass of SF₆ into the chamber when the burn or detonation was initiated and determining the average concentration of this gas in the chamber while the samples were being collected.

All burn tests were conducted by placing the propellant material (test material) on a bed of pea gravel in a stainless steel pan at the center of the BangBox. The burns were initiated using one or more electric squibs placed in the test material. In the 13 detonation tests, the material detonated was suspended either 1m above the opening of a 1m³ steel-lined pit or suspended 0.5 m above the floor of the pit. The test chamber was purged with air for at least 60 minutes (two air volume exchanges) between detonation trials for the same material and for at least 8 hours between detonations of different materials.

TEST CONDITIONS USED IN NTS OB AND OD TESTS

One set of detonation tests and two sets of rocket motor burn tests were conducted in the detonation chamber located at the end of a 130m long tunnel in a mountain at the Nevada Test Site (Reference C-1.2 through C-1.5). The chamber, which is entered through a sealable steel door, is approximately 11m high by 15m wide by 30m long. The chamber has a gravel floor and its walls and the door are coated to a depth of 4 to 10 cm with a concrete - like material called shot-crete. It has a nominal volume of 4,600m³.

Samples of the emission products released by each detonation test were collected from the sealed chamber by means of probes inserted through four sampling ports in the chamber door (containment plug). Hi-Vol filters equipped with quartz-fiber filters were used to measure the concentration of particulate matter in the plume. These filters were subsequently acid extracted and analyzed for (solid or particulate) metals using ICP. Because there was a possibility that gaseous metal compounds might be emitted, samples of the plumes were also collected using EPA Test Method 29 (Multiple Metals). In the Method 29 sampler the gas is pulled through a high efficiency quartz fiber filter and then through a set of impingers containing solutions of

iodine monochloride and potassium permanganate where the gaseous metal species are collected. Only the impinger portion of the Method 29 sampler was analyzed for metals. The results from the impinger analyses were combined with the corresponding results from the Hi-Vol filter analyses to produce a total concentration for each metal. (Pb was the only metal detected in the impingers.)

A mixture of He and Ne was used to determine the volume of the plumes generated by the detonations and burns. The procedure was similar to the SF₆ release procedure used in the BangBox tests.

DESCRIPTION OF MATERIALS USED IN BURN TESTS

Test BB-OB1 (Aluminized Ammonium Perchlorate (AP) Propellant)

The AP propellant used in this test was delivered to the BangBox as kg blocks where it was divided into pieces weighing approximately 1.2kg each for the testing. One 1.2kg block was burned in each trial. The block was prepared for the test as follows. First, the block was placed in a 30.5 by 50.8 by 15.2cm deep burn pan. Then a flap was cut in the top of the block and a 81mm propellant bag containing 4g of Hercules unique smokeless powder was placed in the hole along with two electric squibs. The flap was then placed back over the hole and the burn was initiated on the command of the test coordinator. Other than the following elemental composition, no information is available for this propellant: 19% Al, 20.8% Cl, 10.09% C, 3.7% H, 8.3% N, 38.1% O and 0.008% P. This formulation implies that the propellant contained 69% AP by weight. Two, single-burn trials were conducted. The NEW's (including 4g of smokeless powder) for the first and second trials were 1,216g and 1,159g, respectively for an average NEW of 1192g. This average mass would contain: 3.8g NC, 0.2g NG, 821g AP, 226g Al, and 141g of a material with an elemental composition of C₂₀H₃₄O.

Test BB-OB2 (Composite Propellant MK-6, 88 P-217)

448g of MK-6 propellant chips were placed in a stainless steel burn pan and the burn was initiated using two electric matches that had been inserted into the mix. The NEW burned was 448g. The major energetic constituents of the propellant were: 381g AP, 35.9g hydroxy-terminated polybutadiene, 20.2g dioctyl sebacate and 4.5g aluminum. One, single-burn trial was conducted.

Test BB-OB2 (Double-Based Propellant)

2,223g of pelletized propellant was placed in a stainless steel burn pan along with a 81mm propellant bag containing 4g of smokeless powder and the burn was initiated using an electric squib that had been inserted into the smokeless powder. Two, single-burn trials were conducted. The propellant contained NC, NG and diphenylamine. Its elemental composition was 20.36% C, 2.97% H, 28.73% N, 46.14% O, 0.89% Pb, 0.89% Zr and 0.02% Sn which corresponds to 454.4g C, 66.1g H, 639.8g N, 1027.5g O, 19.8g Pb, 19.8g Zr and 0.5g Sn.

Test BB-OB4 (Double-base Propellant-NOSIH-AA2)

454g of propellant chips and 26.6g of ethyl cellulose were placed in a stainless steel burn pan and the burn was initiated using an electric match that had been inserted into the mix. One, single-burn trial was conducted. The major constituents of the propellant were: 240g NC, 184g NG, 26.6g ethyl cellulose, 12.3g triacetin, 9.1g of di-propyl adipate and 4.5g lead.

Test NTS-OB1 (Improved HAWK Rocket Motor, DODIC PC08)

Two rocket motors (605kg propellant total mass) were burned simultaneously in the single trial conducted. The mass of propellant would contain approximately 352kg AP, 74kg NG, 44kg Al and 118kg polyurethane foam. Copper linear-shaped charges and explosive cutting tape were used to split the steel rocket motor cases longitudinally and at both ends and to initiate the burn. These explosive charges added 1.1kg of RDX to the total energetic mass burned. The exact composition of the propellant is classified, however, from the Executive Summary (Reference C-1.4) and the test report(11) it was possible to determine that the total masses of C, N and Cl in the material burned were 85.6kg, 71.1kg and 116.2kg, respectively. The rocket motors burned for approximately 20 seconds, but elevated temperatures and pressures and severe plume stratification existed in the chamber over most of the plume sampling effort. The peak temperature was reached about 50 sec after the burn was initiated, but the average peak temperature is uncertain because the temperatures measured by the five thermocouples in the chamber ranged from 330 to 540°C at the time. This substantial temperature difference continued for quite some time after the burn ended. For example, the approximate temperature range measured in the chamber at 2, 3, 4 and 5 minutes after the burn was initiated were: 250-450°C, 180-350°C, 120-280°C and 90-220°C. The maximum pressure measured in the chamber during the burn was 40 psia.

Test NTS-OB2 (NIKE Rocket Motor)

Two, single-burn trials were conducted. The first trial involved the simultaneous burn of two NIKE rocket motors and the second trial involved the simultaneous burn of four NIKE rocket motors. Each NIKE rocket motor contained approximately 341kg of a double base propellant comprised primarily of nitrocellulose (203kg) and nitroglycerin (88kg). The propellant also contained 36kg of glycerol triacetate (triacetin); 7kg of 2-nitrodiphenylamine; 1.7kg of lead (as lead stearate); 9kg of dimethylphthalate; 9kg of diethylphthalate; and a chlorinated rubber liner. The total masses of energetic material burned in the first and second trials were 683kg and 1365kg, respectively. Copper linear-shaped charges and explosive cutting tape were used in each burn to split the steel rocket motor case longitudinally and at both ends and to initiate the burn. These explosive charges added approximately 0.6 to 1.01kg of RDX to the total energetic mass burned. Each burn lasted approximately 20 seconds, but elevated temperatures and pressures and severe plume stratification existed in the chamber over most of the plume sampling effort. For both burns the peak temperature (800°C) was reached about 1-minute after the burn was initiated and the differences between the thermocouples was approximately 50-90°C. The approximate temperatures in the chamber at 2, 3, 4 and 5 minutes after the burns were initiated were: 550°C, 425°C, 350°C, and 280°C, respectively. The maximum pressures measured in the chamber during the two and four rocket motor burns were 56 and 85 psia, respectively.

DESCRIPTION OF MATERIALS USED IN DETONATION TESTS**Test BB-OD1 (20mm HEI Cartridge, M56A4, NSN 1305000094255)**

Three, single-detonation trials were conducted. The NEW detonated in each trial was 189g, including 60g of C-4 with an EBC. Three, 20mm brass cartridges were placed on the C-4 strip and tied in place with 16-gauge iron wire for each detonation. Each cartridge contained 8.8g RDX (explosive charge), 39.2g of WC870 propellant (major energetic constituents: 33g NC and 3.3g NG), 0.9g of lead, 0.53g chromium, 89.4g copper, 33.3g zinc, 4.1g aluminum, 67.3g iron, and 0.07g of barium.

Test BB-OD2 (40mm HEI Cartridge, M384, DODIC B574)

Three, single-detonation trials were conducted. The NEW detonated in each trial was 158g, including 40g of C-4 with an EBC. Two 40mm aluminum alloy cartridges were placed on the C-4 strip and tied in place with 16-gauge iron wire for each detonation. Each cartridge contained 54.4g of composition A5 explosive (comprised of 53.3g RDX, and 1.1g stearic acid); 4.6g of M-2 propellant (major energetic constituents: 3.5g NC, 0.9g NG), 74g aluminum, 0.8g copper, 0.8g manganese, 0.35g zinc and small, but undefined, quantities of barium, lead and tin. The overall composition of the projectile is classified.

Test BB-OD3 (Cartridge, Impulse, BBU 36B, DODIC MG11)

This item deploys chaff from aircraft and contains a pyrotechnic filler that readily burns when initiated. Each aluminum alloy cartridge has a NEW of 875mg. Three, single-detonation trials were conducted. Sixty cartridges were used in each of the three detonations. In each detonation, 42 cartridges were clustered around a 57g block of C-4 and 18 cartridges were placed on the sides of a 0.5 m length of detonation cord that had been folded into a 0.25 m length. In trial 1, the two assemblies were hung separately with one end of the detonation cord inserted in the block of C-4. An EBC was used to detonate the C-4. In trials 2 and 3, the C-4 and detonation cord assemblies were bound together using 16-gauge iron wire. The NEW of the assemblies detonated was 144g, including 91g from the detonation train. The energetic composition of the cartridge is not fully known; it did contain approximately 1g of smokeless powder. Each cartridge also contained 3.7g aluminum, 1.0g chromium, 0.21g copper, 0.015g lead and 0.012g zinc.

Test BB-OD4 (Cartridge, Impulse, Mod O, ARD446-1, DODIC M187)

This item has a NEW of 12.5g. Three, single-detonation trials were conducted. For each trial, ten aluminum alloy cartridges were tied to a 57g C-4 brick using detonation cord and the suspended assembly was detonated using an EBC. The NEW of the assembly was 216g, including 91g from the detonation train. Each cartridge was stated to contain 20g of aluminum, 0.63g of copper, 0.29g of zinc, 0.214g lead and approximately 8g of smokeless powder.

Test BB-OD5 (Cartridge, Impulse, MK107, Mod 01, DODIC M943)

This cartridge has a NEW of 24.5g. Three, single-detonation trials were conducted for each detonation, five steel cartridges were placed around a 57g block of C-4. They were parallel to each other, but alternated tip to base. This assembly was wrapped with 3 m of detonation cord and detonated over the detonation pit using an EBC. The NEW of each assembly was 208g, including 91g for the detonation train. The energetic composition of the MK107 cartridge was 17.4g NC, 5.0g NG, 1g barium nitrate and 1.2g of potassium nitrate. The item also contained some aluminum pellets and a small quantity of lead, but the amounts are not known. In addition, the steel casing contained small quantities of chromium, nickel, zinc, and aluminum.

Test BB-OD6 (Fuze, Tail Bomb, Fuze Mechanical Unit, 139B, DODIC F762)

This fuze, which has a stainless steel housing, contains 126g of TETRYL. It is used to initiate the longitudinal detonation cast into GP air-dropped bombs. Three, single detonation, single fuze trials were conducted. Each fuze was prepared for detonation as follows. A 28.5g block of C-4 was taped to the side of the fuze near its main explosive charge and the assembly wrapped in polyethylene sheeting. 1.5m of detonation cord was then wrapped around the fuze and the fuze was screwed onto a threaded shaft. (The opposite end of the shaft was attached to a 1.9cm thick by 30.5cm diameter steel plate. The purpose of the steel plate was to break up any focused blast effect resulting from the detonation.) The fuze was detonated 0.5m above the floor of the detonation pit using an EBC. The NEW of the fuze is 126g. The total NEW of the each assembly detonated was 172g, including 46g from the detonation train. Each fuze also contained 0.4g lead and small, but undefined, quantities of aluminum, copper, chromium and tin.

Test OD-OD7 (Fuze, Tail Bomb, Fuze Mechanical Unit FMU-54A/B, DODIC F841)

This fuze, which contains 163g of TETRYL, initiates the longitudinal detonator cast into general purpose (GP) air-dropped bombs such as the M117 and MK82. The NEW of the fuze is 163.3g. Three, single detonation, single fuze trials were conducted. Each fuze was prepared for detonation as follows. A 28.5g block of C-4 was taped to the side of the fuze near its main explosive charge and the assembly wrapped in polyethylene sheeting. 1.5 m of detonation cord was then wrapped around the fuze and the fuze was screwed onto a threaded shaft. (The opposite end of the shaft was attached to a 1.9cm thick by 30.5cm diameter steel plate. The purpose of the steel plate was to break up any focused blast effect resulting from the detonation.) The fuze was detonated 0.5m above the floor of the detonation pit using an EBC. The NEW was 209g, including 46g from the detonation train. Each fuze also contained 0.6g lead and small, but undefined, quantities of aluminum, chromium, copper, iron and zinc.

Test OD-OD8 (M18A1 Antipersonnel Mine (Claymore), DODIC K143)

Three, single-detonation, single-mine trials were conducted. The NEW detonated in each trial was 227g. Because the mine contained 681g of C-4, it was necessary to remove 454g of the C-4 before detonating it in the BangBox, which has a detonation NEW limit of approximately 230g. The mine was opened and the 700, 22-caliber steel balls and 454g of C-4 were removed from the 360g of fiberglass resin casing. The case was a 50:50 composite of fiberglass and a

polystyrene/polybutadiene resin. The mine was suspended in the detonation pit, an EBC inserted in the 227g of C-4 remaining and the mine was detonated. The mine also contained 0.36g of lead and small, but undefined, quantities of aluminum, copper, chromium, and zinc.

Test BB-OD9 (Signal, Illumination, Aircraft, Red Star M43A2, DODIC L231)

This aluminum alloy-encased flare has a NEW of 56.8g with 56.6g of this NEW in the illuminating charge. The illuminating charge contains 10.2g magnesium powder, 13.6g potassium perchlorate, 24.9g strontium nitrate, 3.4g hexachlorobenzene, 4g asphaltum, 0.02g barium, 0.1g lead, and small, but undefined, quantities of cadmium, copper and zinc and the aluminum tube contains 78g of Al. Three, single detonation trials using three flares (and there bandoliers) per detonation were conducted. The three flares were tied to a 57g block of C-4 and detonated employing a procedure similar to that used for the M158 flares. The NEW of each assembly detonated was 260g, including 91g from the detonation train.

Test BB-OD10 (Signal, Illumination, Ground, Red Star, M158, DODIC L306)

This flare is housed in an cylindrical, aluminum alloy casing (weight not specified in MIDAS) with a steel liner. It has a NEW of 36.8g. Three, single detonation trials using four flares (and their bandoliers) per detonation were conducted. Two flares were placed on one side of a 57g block of C-4 and two were placed on the opposite side. This assembly was wrapped in polyethylene sheeting; 3 m of detonation cord was then wrapped around the assembly and secured with 16-gauge iron wire. This final assembly was detonated with the flare-releasing end pointed down into the pit. An EBC was used to initiate each detonation. The NEW of each assembly was 239g, including 91g from the detonation train. The complete energetic composition of the item is unknown. It did contain 2.5g of black powder, 5.2g of strontium nitrate, 2.5g magnesium, 11g potassium nitrate, 2.5g charcoal, 0.23g lead and small but undefined quantities of cadmium and zinc.

Test BB-OD11 (Adapter-booster, T45E7, DODIC F372)

The NEW detonated was 83g, which included 10g of C4 with an EBC. (NOTE- the 1995 test report indicated that this item had a NEW of 183g, but the latest MIDAS data indicate that the NEW is 73g. Some small changes in the masses of Al and Pb were also found between the test report and MIDAS. Therefore, the originally reported EFs were adjusted to reflect the current MIDAS data on this item.) Three, single-detonation, single-adapter-booster trials were conducted. The adapter-booster contained 73g of tetryl, a booster pellet and a hollow bursted well which was closed with a 980g steel plug and housed in a 440g steel cylinder 17.3cm long and 7.2cm in diameter. It also contained two 7.5g pressed wool wafers (to protect the booster casing), 2.9g chromium, 1.2g copper, 412g aluminum, 2.0g cadmium, 1.1g zinc, and approximately 2g of lead (in lead chromate). To reduce the chance for the blast pulse to become focused, a steel wool plug was placed in the large end of the bursted well and the end was closed with a 31g plastic plug. A 1.6cm diameter by 25cm long steel rod was screwed into the fuze well and a 2.5cm thick by 23cm diameter steel disk was fastened to the other end of the rod. This assembly was suspended horizontally in the detonation pit. A 10g charge of C-4 with an EBC initiated the detonation. However, significant focusing of the blast still occurred as noted by:

(1) the hole punched through the 1.25cm steel plate lining the pit and the charred paper on the fiberglass insulation behind the steel plate; and (2) the charred wood on the "witness shield" approximately 3 meters above the pit (1m above the top of the metal, shrapnel-containment cage (suppressive shield) covering the pit.

Test BB-OD12 (HBX Surrogate)

HBX is an aluminized form of Composition B; it is used in a variety of bombs, depth charges and torpedoes. The HBX surrogate was prepared by mixing aluminum powder with granular Composition B. The energetic composition of the HBX surrogate detonated was: 109g RDX, 72g TNT, 7.8g mineral oil/polyisobutylene and 38.5g Al. Three, 227g portions of this mix were placed in thin polyethylene bags and the bags closed with cotton string. One bag was used in each detonation; the detonations were done with the bags suspended approximately 1 m above the concrete floor of the Bang Box. Three, single-detonation trials were done. The material was detonated using an EBC inserted into a 6.5g block of C-4. The NEW of the material detonated was 235g, including 8g from the C-4/EBC.

Test BB-OD13 (Tritonal Surrogate)

Low density tritonal is used in 750 lb. air-dropped bombs. It is comprised of 80% TNT and 20% finely powdered aluminum by weight. A tritonal surrogate was prepared using crushed TNT block and aluminum powder. These components were placed in a jar and mixed until the mixture appeared to be homogeneous. This mix contained 1274g TNT and 431g Al. Three, 227g portions of this mix were placed in thin polyethylene bags and the bags closed with cotton string. One bag was used in each detonation; the detonations were done with the bags suspended approximately 1 m above the concrete floor of the Bang Box. Three, single-detonation trials were done. In the first two trials, a single M-6 EBC was used to initiate the detonation. It was apparent from the noise of the blast and the residues on the floor that the two detonations did not go high order. To ensure that the third detonation went high order, the EBC was inserted into a 6.5g block of C-4 for this detonation. The NEW of the material detonated in the three detonations was 229g for the first two detonations and 235g for the last detonation. Because they were not high order detonations, the results from the first two detonations are not included in the database.

Test BB-OD14 (Tritonal Surrogate with 2.5% Calcium Stearate)

The calcium stearate served as a surrogate for the organic materials associated with tritonal when it is steamed out of 750 lb. bombs. Three, single-detonation trials were done. A 6.4g block of C-4 and an EBC were used to initiate each detonation. The tritonal/calcium stearate mixes detonated were contained in thin polyethylene bags in a manner identical to the tritonal surrogate detonations. Each bag contained 216g of the tritonal surrogate mix prepared earlier and 11g of calcium stearate. The NEW of the material detonated was 226g, including 8g from the C-4/EBC.

Test NTS-OD1 (155mm Projectile HEI, M-107, DODIC D544)

This test was conducted in the X-tunnel at the Nevada Test site (References C-1.2 and C-1.3). Each projectile contained 6.98kg of Composition B (60% RDX, 39% TNT and 1% wax by weight) and 0.13kg of a supplementary charge (98.5% Composition B, 1.5% barium stearate by

weight). The projectile has a steel casing and weighs approximately 34.5kg, approximately 0.61kg of this is attributable to a 90% copper/10% zinc rotating ring on the exterior of the projectile. Each projectile is also coated with 2.4g of zinc phosphate and 5.6g of zinc chromate (0.067kg zinc/projectile). Four, single-detonation trials were done. The results from the first trial were excluded from the emission factor database because it was an operational readiness test (ORI). The second and third trials involved the detonation of 24 projectiles and the fourth involved the detonation of 60 projectiles. The second trial was done with the projectiles lying on top of a steel plate and the third and fourth trials were done with the projectiles lying on gravel. For the 24 projectile trials, the projectiles were placed in two rows of twelve projectiles each with the lifting plugs in one row pointing in the opposite direction from those in the other row. For the 60-projectile detonation trial, they were placed in rows containing 15 projectiles each; two of the rows were stacked on top of the other two rows. The rows were oriented in the same manners as the 24 projectile detonation trials. The donor charge was Composition C4 (91% RDX, 5.3% di(2-ethylhexyl)sebacate, 2.1% polyisobutylene, and 1.6% motor oil by weight) initiated with PETN-based slip on boosters (one per projectile) and 10m of primacord. Approximately, 27.2kg of C-4 was used in the 24-projectile detonations and 38.5kg were used in the 60-projectile detonation. Including the PETN boosters and primacord cord, the net mass of energetic material (NEW) detonated in each of the 24-projectile trials was 199kg and in the 60-projectile trial was 468kg. The results from the second, third and fourth trials were averaged for inclusion in the CRD which results in the following masses: 288.7kg NEW, 173.3kg RDX, 112.5kg TNT, 1221kg iron, 21.1kg copper, 2.23kg zinc, 1.1E-02kg lead, 90kg nitrogen, 71kg carbon and 2.1kg aluminum.

REFERENCES

- C-1.1. W. J. Mitchell and J. C. Suggs. "Emission Factors for the Disposal of Energetic Materials by Open Burning and Open Detonation (OB/OD)," EPA Report Number EPA/600/R-98/103, August 1998. 130 pp.
- C-1.2. Executive Summary of Phase I Demonstrations - Detonation of Conventional Weapons: 155-mm High Explosive M107 Projectiles. Lawrence Livermore National Laboratory Report Number UCRL-ID-131252 prepared for US Army Defense Ammunition Center, McAlester, OK. July 1998, 38 pp.
- C-1.3. Individual Test Reports, Appendix B, Draft Detonation Summary Report for the Nevada Test Site. Report prepared by Radian International LLC, Oak Ridge, TN, for Lockheed Martin Energy Systems, Inc., Oak Ridge, TN. August 1997.
- C-1.4. Executive Summary of Phase II Demonstrations: The Low-Pressure Rocket Motor Burns in X-Tunnel. Sandia Report Number SAND2000-8202, January 2000. Report prepared for US Army Defense Ammunition Center, McAlester, OK. 34 pp.
- C-1.5. Individual Test Reports, Appendix B, Draft Rocket Motor Summary Report for the Nevada Test Site. Report prepared by Radian International LLC, Oak Ridge, TN, for Lockheed Martin Energy Systems, Inc., Oak Ridge, TN. October 1997.

Appendix C-2
PROCEDURE USED TO DERIVE METAL
EFF VALUES RECOMMENDED FOR THE HRA

METAL EFF VALUES DERIVED FROM BANGBOX TESTS

When EPA compiled this set of background corrected EFs in 1998, it used information in the individual test reports to determine the composition of the materials detonated and burned (Reference C-2.1). For the most part, these descriptions did not identify the trace metal content of the items detonated and burned, so EPA was not aware that some of the materials contained very small quantities of metals. Based on a comparison between the EPA report and the MIDAS database, it became apparent that for some of the energetic materials EPA assigned a value of 0.0E+00 (metal not present in material) rather than the more appropriate ND or ½ the MDL value (metal present but not detected in plume). In those cases, the 0.0E+00 value was replaced by a value equal to ½ of the method Minimum Detection Limit (MDL) expressed as mass of metal emitted/mass of NEW detonated or burned. The MDL values were obtained by dividing the Method Quantitation Limits (MQL) provided in the EPA report by three. (EPA had derived the MQL values by multiplying the MDL by three.)

METAL EFF VALUES DERIVED FROM NTS CHAMBER TESTS

The Army reported the emissions from the projectile detonations and rocket motor burns only as concentration (either ppbv or mg/m³) corrected to one atmosphere pressure and 20°C and did not correct the concentrations for the metals released into the plume by the shot-crete on the walls and door of the chamber (References C-2.2 and C-2.3). So, it was necessary to convert these concentrations to the corresponding EFs by multiplying the average concentration values for each analyte/material by the average plume volume for that material (References C-2.4 and C-2.5) and then dividing the product by the average mass of the material detonated or burned.

For the following reasons, correcting the resulting metal EFs for the contribution from metals in the shot-crete on the chamber surfaces was not a simple process. First, the Army had only collected six background air samples across all of the detonation and burns and the samples had been collected in quiescent air rather than under the turbulent conditions that existed in the chamber when the detonation and burn samples were collected. Second, the shot-crete contained significant quantities of all of the target metal analytes. Third, examination of the metal content in the samples collected from the surfaces of the chamber over the duration of the tests showed that the actual and relative concentrations of most of the metals were sometimes noticeably different from one location to another. Fourth, the lead emission factor derived from the HAWK rocket motor burn was a 1000 fold greater than the mass of Pb in the HAWK rocket motor which indicated that the HAWK burn plume had been contaminated by lead released into the chamber during the two NIKE burns which had occurred several months before the HAWK Burn. (The NIKE contained 1.7kg of lead stearate.)

The following procedure was used to obtain corrected emission factors for the metals from the projectile detonations. (This procedure is based on the observation that three alkaline earth metals (Ca, Mg and K) were the predominate metals in the shot-crete and these metals were not

present in the materials detonated and burned.) First, the average mass of each element found in all samples collected from the walls of the chamber during the detonation tests and the ratios of the target analyte metals with respect to Ca, Mg and K were determined. (Columns 3, 4, and 5 of Table C-2.1). Second, the average Ca, Mg and K EFs (column 2) were multiplied by the appropriate factor from column 3, 4 and 5 to obtain an estimate of the emissions factors which would have been produced just from the shot-crete (columns 6, 7 and 8), e.g., the values in column 6 were obtained by multiplying the values in column 2 by 7.9E-04. Third, these shotcrete-derived emissions factors were then combined to produce an estimated average background emission factor for each target metal analyte (column 9). Fourth, the average background emission factor was then subtracted from the appropriate uncorrected emission factor (column 2) to produce an adjusted emission factor (column 10). Fifth, each adjusted emissions factor was compared to the theoretical emission factors to determine if it was reasonable (based on the mass of the metal in the projectile). All of the emissions factors were determined to be reasonable and were therefore included in the OD-CRD database in the traditional EF units and, where possible, in the alternate EFF units.

The procedure used to obtain corrected emission factors for the metals from the rocket motor burns was similar to the one described above for the projectile detonations. The adjusted emission factors for the HAWK burn are presented in Table C-2.2 and those for the NIKE burns are presented in Table C-2.3. All of the adjusted emissions factors in these two tables, with the exception of the emission factor for Pb for the HAWK burn, were considered reasonable based on the limited amount of information available for the two rocket motors. (The HAWK did not contain lead and the source of the lead was likely the two NIKE rocket motor burns, which preceded the HAWK burn.) Because much of the information on the composition of these rocket motors is classified, it was possible to calculate EFF values only for Pb for the NIKE rocket motor and for Al for the HAWK rocket motor.

TABLE C-2.1. Adjusted Metal Emissions Factors for Projectile Detonation.

Metal	Uncorrected EF	Ratio of target metal to Ca, Mg and K in surface materials			Target metal EF due to chamber surface materials (based on Ca, Mg and K EFs)				Adjusted EF
		Ca	Mg	K	Ca	Mg	K	Average	
Al	2.1E-04	6.5E-02	2.5E+00	3.4E+00	5.2E-5	9.1E-05	3.2E-04	1.55E-04	5.0E-05
Ba	3.7E-06	1.2E-03	4.5E-02	6.2E-02	9.3E-07	1.6E-06	5.7E-06	2.76E-06	1.0E-06
Cd	2.2E-08	3.2E-06	1.2E-04	1.7E-04	4.4E-09	4.4E-09	1.6E-08	7.46E-09	1.5E-08
Ca	7.9E-04	-	-	-	-	-	-	-	-
Cr	5.0E-07	2.2E-04	8.5E-03	1.2E-02	1.8E-07	3.1E-07	1.1E-06	5.22E-07	0.0E+00
Cu	1.1E-05	2.8E-04	1.1E-02	1.5E-02	2.2E-07	3.8E-07	1.4E-06	6.5E-07	1.1E-05
Fe	3.1E-04	8.7E-02	3.4E+00	4.6E+00	6.9E-05	1.2E-04	4.2E-04	2.05E-04	1.1E-04
Pb	3.5E-07	5.6E-05	2.1E-03	2.9E-03	4.4E-08	7.7E-08	2.7E-07	1.30E-07	2.2E-07
Mg	3.6E-05	-	-	-	-	-	1.3E-04	-	-
Mn	3.8E-06	1.4E-03	5.3E-02	7.2E-02	1.1E-06	1.9E-06	6.7E-06	3.22E-06	6.0E-07
K	9.3E-05	-	-	-	-	-	-	-	-
Zn	5.1E-06	2.9E-04	1.1E-02	1.5E-02	2.3E-07	4.0E-07	6.7E-07	6.71E-07	4.4E-06

TABLE C-2.2. Adjusted Metal Emissions Factors for the HAWK Rocket Motor Burn.

Metal	Uncorrected EF	Ratio of target metal to Ca, Mg and K in surface materials			Target metal EF due to chamber surface materials (based on Ca, Mg and K EFs)				Adjusted EF
		Ca	Mg	K	Ca	Mg	K	Average	
Al	2.5E-03	6.5E-02	2.5E+00	3.4E+00	4.5E-07	5.8E-08	4.1E-05	1.50E-05	2.5E-03
Ba	1.9E-06	1.2E-03	4.5E-02	6.2E-02	8.0E-09	7.4E-07	7.4E-07	2.68E-07	1.6E-06
Cd	5.2E-09	3.2E-06	1.2E-04	1.7E-04	2.2E-11	1.6E-10	2.0E-09	7.25E-10	4.5E-09
Ca	6.8E-06	-	-	-	-	-	-	-	-
Cr	8.4E-06	2.2E-04	8.5E-03	1.2E-02	1.5E-09	1.1E-08	1.4E-07	5.08E-08	8.4E-06
Cu	5.9E-05	2.8E-04	1.1E-02	1.5E-02	1.9E-09	1.4E-08	1.8E-07	6.35E-08	5.9E-05
Fe	8.3E-05	8.7E-02	3.4E+00	4.6E+00	4.4E-06	4.4E-06	5.5E-05	1.99E-05	6.3E-05
Pb	2.3E-03	5.6E-05	2.1E-03	2.9E-03	3.8E-10	2.8E-09	3.5E-08	1.27E-08	2.3E-03
Mg	1.3E-06	-	-	-	-	-	-	-	-
Mn	1.0E-06	1.4E-03	5.3E-02	7.2E-02	9.3E-09	6.9E-08	8.6E-07	3.14E-07	7E-07
K	1.2E-05	-	-	-	-	-	-	-	-
Zn	4.9E-06	2.9E-04	1.1E-02	1.5E-02	1.9E-09	1.4E-08	1.8E-07	6.53E-08	4.9E-06

TABLE C-2.3. Adjusted Metal Emissions Factors for the NIKE Rocket Motor Burn.

Metal	Uncorrected EF	Ratio of target metal to Ca, Mg and K in surface materials			Target metal EF due to chamber surface materials (based on Ca, Mg and K EFs)				Adjusted EF
		Ca	Mg	K	Ca	Mg	K	Average	
Al	2.5E-05	6.5E-02	2.5E+00	3.4E+00	6.8E-06	2.0E-06	2.4E-04	1.07E-04	0.0E+00
Ba	7.6E-07	1.2E-03	4.5E-02	6.2E-02	1.1E-07	3.6E-08	4.4E-06	1.91E-06	0.0E+00
Cd	3.4E-05	3.2E-06	1.2E-04	1.7E-04	3.1E-10	9.8E-11	1.2E-08	5.16E-09	3.4E-05
Ca	6.8E-06	-	-	-	-	-	-	-	-
Cr	1.1E-06	2.2E-04	8.5E-03	1.2E-02	2.2E-08	6.8E-09	8.3E-07	3.61E-07	7E-07
Cu	1.9E-05	2.8E-04	1.1E-02	1.5E-02	2.7E-08	8.5E-09	1.0E-06	4.51E-07	1.9E-05
Fe	7.6E-05	8.7E-02	3.4E+00	4.6E+00	8.5E-06	2.7E-06	3.2E-04	1.42E-04	9.2E-08
Pb	1.4E-03	5.6E-05	2.1E-03	2.9E-03	5.4E-09	1.7E-09	2.1E-07	9.03E-08	1.4E-03
Mg	1.4E-05	-	-	-	-	-	-	-	-
Mn	8.0E-07	1.4E-03	5.3E-02	7.2E-02	1.3E-07	4.2E-08	5.1E-06	2.23E-06	0.0E+00
K	-	-	-	-	-	-	-	-	-
Zn	2.2E-05	2.9E-04	1.1E-02	1.5E-02	2.8E-08	8.8E-09	1.1E-06	4.64E-07	2.2E-05

REFERENCES

C-2.1. W. J. Mitchell and J. C. Suggs. "Emission Factors for the Disposal of Energetic Materials by Open Burning and Open Detonation (OB/OD)," EPA Report Number EPA/600/R-98/103, August 1998. 130p.

C-2.2. Executive Summary of Phase I Demonstrations - Detonation of Conventional Weapons: 155-mm High Explosive M107 Projectiles. Lawrence Livermore National Laboratory Report Number UCRL-ID-131252 prepared for US Army Defense Ammunition Center, McAlester, OK. July 1998, 38 pp.

C-2.3. Executive Summary of Phase II Demonstrations: The Low-Pressure Rocket Motor Burns in X-Tunnel. Sandia Report Number SAND2000-8202, January 2000. Report prepared for US Army Defense Ammunition Center, McAlester, OK. 34 pp.

C-2.4. Individual Test Reports, Appendix B, Draft Detonation Summary Report for the Nevada Test Site. Report prepared by Radian International LLC, Oak Ridge, TN, for Lockheed Martin Energy Systems, Inc., Oak Ridge, TN. August 1997.

C-2.5. Individual Test Reports, Appendix B, Draft Rocket Motor Summary Report for the Nevada Test Site. Report prepared by Radian International LLC, Oak Ridge, TN, for Lockheed Martin Energy Systems, Inc., Oak Ridge, TN. October 1997.

Appendix C-3
DESCRIPTION OF TEST CONDITIONS AND MATERIALS
USED TO DERIVE THE PARTICULATE MATTER EMISSION
FACTORS RECOMMENDED FOR THE HRA

TEST CONDITIONS USED IN DPG OB AND OD OPEN RANGE EMISSIONS TESTS

These emission tests were conducted in 1989 and 1990 (Reference C-3.1). The testing was done in three phases. Samples of the emission products were collected from the plumes using a twin engine, turboprop airplane that traversed the plume at 90 knots (46m/second) and an altitude of 300m.

The OD tests involved detonating 900-kg quantities of four explosives in topless, steel barrels approximately 1.2m high and 1.1m in diameter. The detonations were initiated using 0.5kg of C-4 and an electric blasting cap. All four explosives were detonated with the barrel sitting on the ground (surface OD) and one of the explosives (TNT) was detonated with the barrel suspended approximately 12m above the ground. This latter test was conducted to determine if the efficiency of the detonation could be substantially improved and the particulate emissions substantially reduced by increasing the ease with which air could enter the detonation fireball and by decreasing the amount of detonation energy entering the soil. The identities and compositions of these four explosives can be found in the section below entitled "Detailed Description of Test Materials Used in DPG OB Tests."

The OB tests involved burning 2,000 to 3,200kg quantities of five propellant materials in three steel pans approximately 1.2m wide, 11.0m long and 0.25m high. The propellants were placed in the pans to a depth of 6 to 9cm and the burns initiated using black powder trains placed at opposite ends of each pan. The identities and compositions of these five propellant materials can be found in the section below entitled "Detailed Description of Test Materials Used in DPG OB Tests."

For the detonation plumes, the airplane made 3 passes through the plume over a 5-minute period and for the burn plumes it made two passes over a 3-minute period. Each pass lasted between 3 to 7 seconds. Plume samples were collected at an approximate isokinetic sampling rate through an externally mounted, 3m long, 8cm I.D. aluminum probe which exited into a sampling manifold inside the airplane. A sliding valve located at the union of the probe and sampling manifold directed the plume gases into either the manifold (sampling mode) or back into the atmosphere (bypass mode) during these tests.

The particulate samples were collected at a rate of 3 to 4m³/min using three high volume samplers equipped with Teflon-coated quartz fiber filters that sampled. As the airplane approached the plume for its initial pass, the high volume sampler motors were started, but the manifold sampling valve was left in the bypass mode. When the nephelometer mounted in the front of the airplane indicated that the airplane was entering the plume (sharp increase in nephelometer reading), the manifold sliding valve was moved to the sampling mode and then returned to the bypass mode when the nephelometer indicated that the airplane was exiting the

plume After the final pass through the plume, the high volume sampler motors were turned off. At the conclusion of each trial or background sample collection effort, the aircraft returned to the airfield where the high volume filters were recovered, placed in an ice-cooled container and transported to a laboratory where the mass of the particulate collected was determined for each filter. Each set of detonations and burns was comprised of two to three events spaced 15 to 20 minutes apart. To ensure that sufficient particulate would be collected, the same high volume filters were used for all detonations comprising a trial. This approach produced total sampling volumes from 4 to 10m^3 .

At least once each day, the airplane collected a background air sample by sampling for 20 minutes at an altitude of 300m above the test range using the same sampling procedures and equipment used to collect plume samples. The concentrations of particulate matter found in these background samples were subtracted from the concentrations measured in the plume samples.

The Army converted the average particulate concentrations for each propellant material to the corresponding EF using a carbon mass balance procedure. This procedure is based on the fact that 98% of the C in the energetic material detonated and burned ends up as either CO, CO₂ or CH₄. Thus, the average plume volume during the time the particulate sample was collected can be determined by determining the total concentration (as C) of these gases in a plume sample collected at the same time as the particulate sample and then dividing this concentration into the total mass of C in the material burned or detonated. For example, if the material burned contained 10^{+3} kg of C and the concentration of C in the plume sample was $10^{-3}\text{kg}/\text{m}^3$, then the plume volume at the time the particulate sample was collected was approximately 10^6m^3 .

For unknown reasons, the Army did not convert the detonation plume particulate concentrations to EFs. Nor did it provide the plume volumes required to convert these average concentrations into the equivalent EFs. However, it did provide the following information that made it possible to estimate the average plume volumes. First, the initial pass of the airplane through the plume occurred approximately 85 seconds after the detonation was initiated, the second pass occurred approximately 250 seconds after the detonation was initiated and the last one occurred approximately 380 seconds after the detonation was initiated. Second, the airplane traversed the plume in 5 to 7 second at an altitude of 300m. Inputting these sampling and plume traverse times and a nominal mass of 900kg NEW detonated into BlazeTech Corporation's ADORA fate and transport model produced the following estimated plume volumes for the three passes through the plume: first pass ($6,000,000\text{m}^3$), second pass ($40,000,000\text{m}^3$) and third pass ($75,000,000\text{m}^3$).

The average concentrations for the four materials detonated at ground level were: RDX ($200 \text{mg}/\text{m}^3$); Composition B ($200 \text{mg}/\text{m}^3$); Explosive D ($250 \text{mg}/\text{m}^3$) and TNT (Phase A - $45\text{mg}/\text{m}^3$, Phase C - $258\text{mg}/\text{m}^3$). Multiplying the average concentrations by the average estimated plume volume ($40,000,000 \text{m}^3$) and dividing the product by the average mass (NEW) of the material detonated produced the following emission factors (kg particulate/kg NEW detonated): RDX (9.6); Explosive D (10.9); Composition B (9.0); and TNT (7.2).

Although the Army had designated the particulate sampling results as Total Suspended Particulate (TSP), the test report had noted that some of the particulate was lost in the sampling

probe (due to particle deposition). Therefore, the following calculation was done using the procedure of Liu and Agarwal (Reference C-3.2) to determine how this deposition affected the measurement. This calculation was conducted based on the following assumptions: (a) the vast majority of the particulate matter was comprised of DPG soil particles which had a density of 2.5g/cc; (b) the internal diameter of the sampling probe was 8cm; (c.) the length of the probe was 3m; and (d) the sampling rate was equal to the velocity of the aircraft which was 46 m/sec. It produced the following predictions as to the possibility for particles of various aerodynamic diameters to be lost in the probe: particles with aerodynamic diameters equal to or larger than 3.5 microns (100% deposition); 3.0 micron particles (85% deposition); 2.5 micron (58% deposition); 2.0 micron (35% deposition); 1.5 micron (15% deposition); 1.0 micron (1% deposition); and 0.5 micron (0% deposition). This particle penetration efficiency curve is very similar to that of the PM-2.5 inlet used in ambient sampling equipment that indicates that the particulate emissions factors for the detonations should be designated as PM-2.5 and not TSP. Since carbon-based particles and not soil particles were the major particulate species in the burn plumes, the density of the particulate matter in these plumes cannot be determined. However, particle deposition in the probe also occurred when the burn plumes were sampled, so it is likely that the particulate matter EF for these plumes cannot be designated as TSP. The most reasonable designation based on the information available would be to designate them as PM-2.5.

DETAILED DESCRIPTION OF TEST MATERIALS USED IN DPG OPEN RANGE OB TESTS

Test DPG-OB1 (M-30 Propellant Burn)

This triple base propellant was burned as perforated pellets during the Phase A test series. The material burned contained approximately 890kg nitrocellulose (NC), 715kg of nitroglycerine (NG), 1510kg nitroguanidine (NQ), and 50kg of ethyl centralite (N,N-diethyl-N,N-diphenylurea). Two, three-burn trials were conducted. The NEW of the first burn was 3,144kg and the NEW of the second burn was 3,193kg. The two burns were initiated 14 minutes apart. The burn time for each burn was approximately 20 seconds. The ash left in the burn pan contained milligram quantities of phenol, ethyl centralite, NC, NG and 2,4 DNT. The total mass of the ash was not determined.

Test DPG-OB2 (Propellant Manufacturing Residue A Burn)

This material, which was comprised of four, double-base propellants and one ammonium perchlorate (AP) or composite propellant, was burned during the Phase B test series. Some of the propellants were in pellet form, others were in sheet form and one was in the form of chunks, but, the form of each propellant was not given in the report. The AP propellant was placed in the center pan and the double base propellants were placed in the outer pans. This propellant mixture served as a surrogate for the residues that result from propellant manufacturing processes when the final product does not meet the product performance/quality specifications and is destroyed by open burning in steel pans. The material burned contained 1135kg NC, 865kg NG, 45kg diphenylamine (DPA), 606kg AP, 85kg triacetin, 70kg of Pb, and 35kg Al. A single trial comprised of two, 3,000kg burns spaced approximately 11minutes apart, was conducted. One

burn required 180 seconds to complete and the other required 240 seconds. The average mass of ash recovered from the burn pan for the two burns was 5.4kg, which is equal to 0.2% of the energetic mass burned. The ash contained 2.9 mg of phenol; no other SVOC or energetic target analytes were found.

Test DPG-OB3 (Propellant Manufacturing Residue B Burn)

This material was comprised of two, double base propellants in sheet form. The propellants were open burned while rolled out flat in the burn pans during the Phase C test series. The two propellants together contained 1115kg NC, 793kg NG, 43kg DPA, 13kg triacetin, 55kg Pb and 184kg dibutylphthalate. Two, two-burn trials were conducted. The first trial consisted of one open burn with an NEW of 2,253kg and a second burn with an NEW of 2,184kg. In the second trial, two 2,218kg quantities of the propellant were burned. The two burns in the first trial were initiated approximately 12 minutes apart and the two burns in the second trial were initiated approximately 15 minutes apart. The burn times for the four burns ranged from 63 to 68 seconds. The average mass of ash recovered from the burn pan for the four burns was 0.6kg, which is equal to 0.1% of the energetic mass burned. The ash contained low nanogram quantities of 2,4-DNT; no other SVOC or energetic target analytes were found.

Test DPG-OB4 (M-6 Propellant Burn)

This single base propellant was burned as multi-perforated pellets approximately 1.7cm long and 0.8cm in diameter during the Phase C test series. The material burned contained 2,793kg NC, 28kg DPA, 309kg 2,4-dinitrotoluene (2,4-DNT), and 80kg dibutylphthalate. Four, three-burn trials were conducted. In the first three trials, the burns were initiated approximately 12 minutes apart and in the fourth they were initiated approximately 15 minutes apart. The NEW in each of the first nine burns was 3,184kg and in the last three burns the NEW was 3,320kg. The burn times for the 12 burns ranged from 12 to 21 seconds. The average mass of ash recovered from the burn pan for the four trials was 2.6kg, which is equal to 0.026% of the energetic mass burned. The ash contained 30mg of 2,4-DNT and 91mg of dibenzofuran; no other SVOC or energetic target analytes were found.

Test DPG-OB5 (M-1 Propellant Burn)

This single base propellant was burned as multi-perforated propellants approximately 1cm long and 0.4cm in diameter during the Phase C test series. The material burned contained 2,729kg NC, 16kg DPA, 321kg 2,4-DNT, and 160kg dibutylphthalate. Two, three-burn trials were conducted. Each trial involved the open burning of three 3,159kg quantities of propellant. In the first trial, the second burn was initiated approximately 14 minutes after the first and the third burn was initiated approximately 21 minutes after the second. In the second trial, the three burns were initiated approximately 13 minutes apart. The burn times for the six burns ranged from 16 to 19 seconds. The average mass of ash recovered from the burn pan for the six burns was 4.0kg, which is equal to 0.1% of the energetic mass burned. The ash contained 76mg of 2,4-DNT and 3mg of 2,6-DNT; no other SVOC or energetic target analytes were found.

DETAILED DESCRIPTION OF TEST MATERIALS USED IN DPG OPEN RANGE OD TESTS**Test DPG-OD1 (Bulk Reclaimed TNT Ground Level Detonation)**

The TNT detonated was reclaimed material. TNT detonations were conducted during all three phases of the test series. The emissions data from Phase A (one trial comprised of five, 898kg detonations) and Phase C (two trials comprised of three, 900kg detonations each) were averaged to produce the emissions factors in the CRD. The Phase A detonations were initiated 10-20 minutes apart. During the first trial in Phase C, the second detonation was initiated approximately 20 minutes after the first and the third was initiated approximately 28 minutes after the second detonation. During the second Phase C trial, the second detonation was initiated approximately 18 minutes after the first and the third was initiated approximately 15 minutes after the second detonation. (The Phase B TNT detonations were excluded because the TNT was severely contaminated with asphaltum and gum residues, was not homogeneous in physical properties and suffered from other defects that caused it not to meet the test specifications.)

Test DPG-OD2 (Bulk Reclaimed TNT Detonated 12 Meters Above Ground Level)

The TNT detonated was reclaimed material. Above ground TNT detonations were conducted during Phase B and Phase C of the test series, but only the emissions results from the Phase C tests (one trial comprised of three, 900kg detonations spaced approximately 13 minutes apart) were included in the CRD. The TNT was detonated in a barrel suspended approximately 12m above the ground by a wire running between two telephone poles. (The Phase B TNT detonations were subsequently determined to be invalid because the TNT was severely contaminated with asphaltum and gum residues, was not homogeneous in physical properties and suffered from other defects that caused it not to meet the test specifications.)

Test DPG-OD3 (Bulk Explosive D Detonation)

The Explosive D was in granular form and may have been recycled material. The material contained 915kg of picric acid. Two, three detonation trials were conducted during Phase C of the test series. The NEW of each of the six detonations was 916kg. During the first trial, the second detonation was initiated approximately 10 minutes after the first and the third was initiated approximately 21 minutes after the second detonation. In the second trial, the three detonations were spaced approximately 20 minutes apart.

Test DPG-OD4 (Bulk RDX Detonation)

The RDX was received in pasteboard boxes and was detonated without removing it from the boxes. The two, three-detonation trials were conducted during the Phase C test series. The material detonated contained 835kg of RDX and 45kg of Viton A rubber. The NEW for the first, second and third detonations in the first trial were 871kg, 875kg and 880kg, respectively. The NEW for the same detonations in the second trials were 899kg, 880kg and 880kg, respectively. The three detonations in the first trial and the first two in the second trial were spaced

approximately 15 minutes apart. The third detonation in the second trial was initiated approximately 20 minutes after the second detonation.

Test DPG-OD5 (Bulk Composition B Detonation)

The composition B was reclaimed material in flake form. The detonated material contained approximately 360kg TNT, 525kg RDX and 10kg wax. Three detonation trials were conducted. The first trial involved two 907kg detonations approximately 15 minutes apart. The second and third trials each involved three detonations spaced approximately 15 minutes apart. In the second trial, the first and third detonations were 907kg detonations and the second was a 916kg detonation. The third trial involved three, 907kg detonations.

REFERENCES

C-3.1. M. Johnson. "Development of Methodology and Techniques for Identifying and Quantifying Products from Open Burning and Open Detonation Thermal Treatment Methods - Field Test Series A, B and C, Volume 1 (Test Summary)," U.S. Army, AMMCOM, Rock Island, IL 61299-6000, January 1992.

C-3.2. B. Y. H. Liu and J. K. Agarwal. "A Criterion for Accurate Aerosol Sampling in Calm Air," J. American Industrial Hygiene Association 41, 1980. pp. 191-197.

INITIAL DISTRIBUTION

- 1 Naval Surface Warfare Center, Crane, IN (Code 4073, D. Burch)
- 1 Naval Surface Warfare Center, Indian Head Division, Indian Head, MD (M. Hancock)
- 1 Naval Surface Warfare Center, Indian Head Division, Yorktown Detachment, Yorktown, MD (Code 240B, J. Johnston)
- 1 Navy Region Southwest, San Diego, CA (N45, P. Dyck)
- 1 Naval War College, Newport, RI (1E22, President)
- 1 Army Aberdeen Test Center, Aberdeen Proving Ground, MD (CSTE-DTC-AT-SL-ME, P. Klara)
- 4 Army Defense Ammunition Center, McAlester, OK
 - SJMAC-DEM
 - P. Cummins (1)
 - S. Kwak (1)
 - T. Nordquist (1)
 - L. Nortunen (1)
- 2 Army Environmental Command, Aberdeen Proving Ground, MD 21911
 - Janet Martin (1)
 - Tamara Rush (1)
- 1 US Army Engineer Research and Development Center, Vicksburg, MS (J. Pennington)
- 1 National Aeronautics and Space Administration, Washington, DC (Code QS, J. Mullin)
- 1 Headquarters, 497 INOT, Falls Church (IOG Representative)
- 2 AFRL/PROF, Edwards AFB, CA (D. Schwartz)
- 2 Defense Technical Information Center, Fort Belvoir, VA
- 2 DOD Explosive Safety Board, Alexandria, VA
 - J. Covino (1)
 - L. Sanchez (1)
- 1 Center for Naval Analyses, Alexandria, VA (Technical Library)
- 1 Cold Regions Research & Engineering Laboratory, Hanover, NH (T. Jenkins)
- 1 Ordnance Environmental Support Office, Indian Head, MD (L. Bohne)
- 1 Alliant Techsystems, Magna, UT (B. Price)
- 1 AOT-Maryland, Inc., Indian Head, MD (E. Baroody)
- 1 Bill Mitchell and Associates, LLC, Durham, NC (B. Mitchell)
- 1 CH2M Hill, Salt Lake City, UT (M. Lindsay)
- 2 Chemical Compliance Systems, Inc., Lake Hopatcong, NJ (G. Thompson)
- 1 Concurrent Technologies Corporation, San Diego, CA (T. Bernitt)
- 2 Defense Research and Development Canada, Canada
 - G. Ampleman (1)
 - S. Thiboutot (1)
- 1 Federal Facilities Environmental Journal, Centreville, VA (M. West)
- 1 FR Countermeasures, Milan, TN (C. McKnight)
- 1 Honeywell Technology Solutions, Inc., Las Cruces, NM (B. Greene)
- 3 Lawrence Livermore National Laboratory, Livermore, CA
 - D. Fergenson (1)
 - P. Hsu (1)
 - B. Watkins (1)
- 1 Los Alamos National Laboratory, Los Alamos, NM (J. Sanchez)
- 1 MSE Technology Applications, Inc., Butte, MT (T. Rivers)
- 1 National Defence Headquarters, Ottawa, Canada (R. Boulay)
- 1 Sandia National Laboratories, Livermore, CA (B. Horn)
- 1 Sverdrup Inc., Ridgecrest, CA (R. Gerber)
- 1 Swedish Defense Research Agency, Tumba, Sweden (J. Hägvall)
- 1 Tetra Tech FW, Inc., Boston, MA (B. Corbett)
- 1 Tybrin Corporation, Edwards Air Force Base, CA (H. Beutelman)

ON-SITE DISTRIBUTION

- 2 Code 4TL000D (1 plus Archive copy)
- 2 Code 4T4200D
 - Eric Erickson (1)
 - Andrew Chafin (1)
- 12 Code 4T4300D
 - T. AtienzaMoore (5)
 - T. Boggs (5)
 - O. Heimdahl (1)
 - K. Wells (1)
- 1 Code 470000D, L. Lusk
- 1 Code 474330D, D. Wooldridge
- 4 Code 476500D
 - J. Hibbs (1)
 - M. Martyn (1)
 - M. Pepi (2)
- i Code 521500D, B. Oldroyd
- 1 Code 5297001, M. Austin
- 6 Code N45NCW
 - B. Abernathy (1)
 - L. Zellmer (5)